National Aeronautics and Space Administration

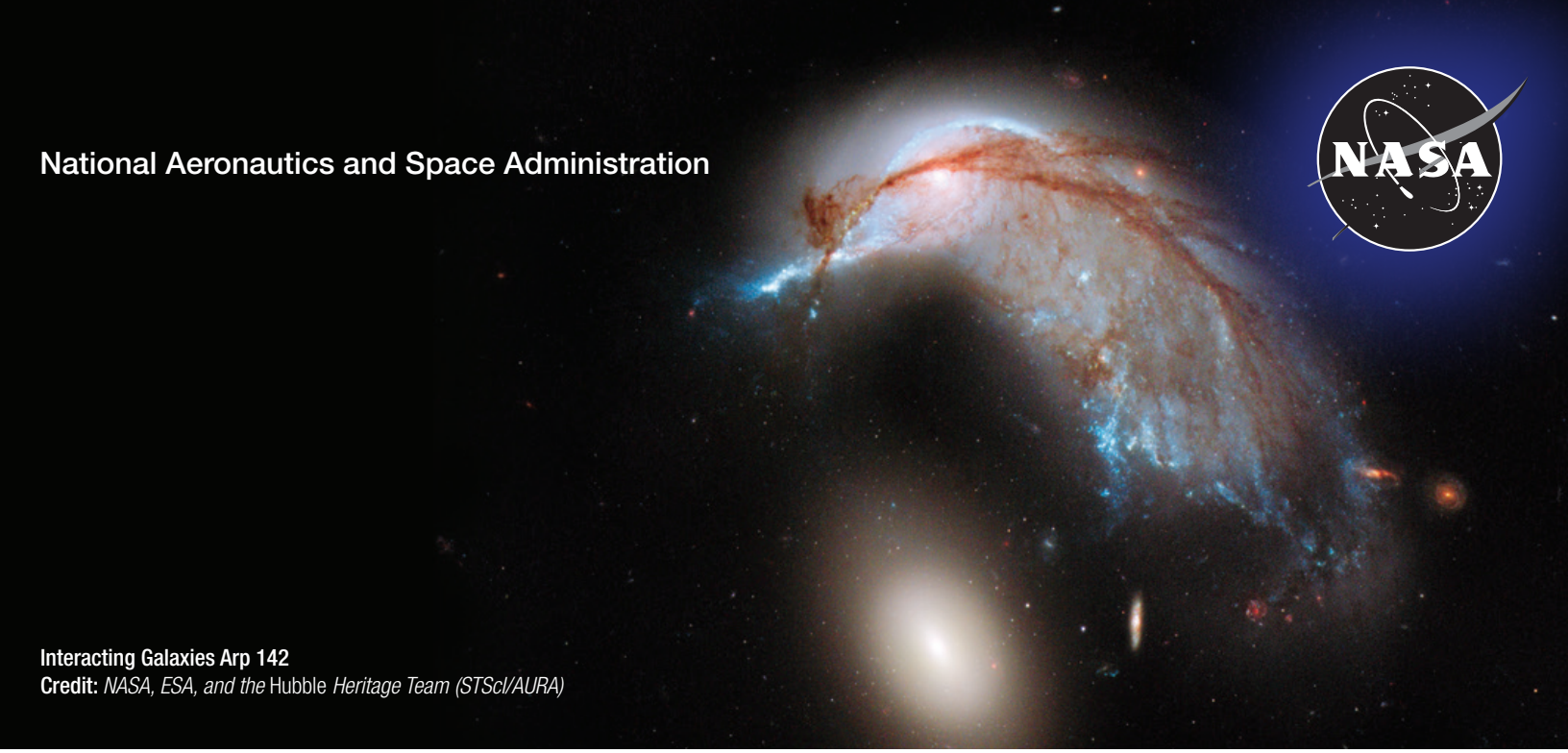

Interacting Galaxies Arp 142
Credit: *NASA, ESA, and the* Hubble *Heritage Team (STScI/AURA)*

[2013] VOL [30] ISSUE [02]

NEWSLETTER
Space Telescope Science Institute

Hubble Cycle 21 Proposal Selection

Andrew Fox, *afox@stsci.edu*, **Claus Leitherer,** *leitherer@stsci.edu*,
Brett Blacker, *blacker@stsci.edu,* **Neill Reid** *inr@stsci.edu*

The annual *Hubble* proposal selection process is one of the key community activities of the Institute. Each summer, around 140 members of the international astronomical community travel to Baltimore to participate in this peer review process and make their recommendations on *Hubble* observing time to the Director. Through careful consideration and lively discussion, the reviewers identify those proposals deemed to be of the highest scientific quality and most worthy of approval. Given the high over-subscription of *Hubble* time, and the uniformly high standard of submissions, the selection process entails many difficult decisions and depends critically on the scientific expertise of the reviewers. In this article we give an overview of the construction and outcome of the Cycle 21 review.

The *Cycle 21 Call for Proposals* was released in December 2012, and the Phase I deadline was 1 March 2013. We received a total of 1,094 proposals, similar to the Cycle 20 number of 1,090, and the second-highest ever (after Cycle 7). The total number of orbits requested, 19,742, marked a considerable increase from last year's total of 16,767, in part reflecting the introduction of medium-sized proposals and the Ultraviolet (UV) Initiative (discussed below).

The Review Panels

The process of selecting the panelists begins with the selection of the Time Allocation Committee (TAC) chair about six months prior to the proposal deadline. The Cycle 21 TAC chair was Debra Elmegreen (Vassar College). Next, we select the chairs of the panels, the at-large TAC members, and finally the panel members. The recruitment of panelists is usually completed about four months prior to the proposal deadline, although we occasionally recruit panelists later in the process as the need arises. The primary consideration when constructing panels is to ensure they contain an appropriate range of scientific expertise to cover the relevant astronomical topics. Other considerations include ensuring a healthy mix of experienced senior panelists and younger postdoctoral panelists, gender balance, and appropriate representation of European Space Agency (ESA) member states and other countries. To aid our search for panelists, we consider who has been a successful principal investigator (PI) or co-investigator (Co-I) in the last few cycles, who has served as a panelist before, and who is well known in their field. The final Cycle 21 review involved a total of 135 panelists and TAC members, including 44 first-time panelists.

The reviewers are grouped into 14 panels organized by science category. Each panel has one or more "mirrors," which allow proposals to be transferred when needed to avoid conflicts of interest. In Cycle 21, there were two panels on Planets (including Solar System and Exoplanets), three on Stars (including Star Formation and Interstellar Medium), two on Stellar Populations, three on Galaxies, two on Active Galactic Nuclei (AGM) and Intergalactic Medium (IGM), and two on Cosmology. Regular General Observer (GO), Medium GO, Archival, Theory, and Snapshot SNAP proposals were reviewed by these panels. Large, Treasury, Pure Parallel, and Archival Legacy proposals were reviewed by the TAC, which consists of the chairs of the 14 panels, three at-large TAC members, and the TAC chair. The at-large members have broad expertise and advise panels when additional perspective is needed to review a particular proposal.

The Review Process

The Cycle 21 proposal review took place from 14–18 May 2013 at the Institute, the Physics and Astronomy Department of the Johns Hopkins University (JHU), and the nearby *Inn at the Colonnade* hotel. The panels met for the first two-and-a-half days of the review; then the TAC met for the final two days.

All panels are of similar size (9–10 members, including the chair) and are typically assigned between 60 and 90 proposals. Each proposal is assigned a primary and secondary reviewer, based on matching the scientific keywords provided by the proposers and the reviewers. Reviewers read all proposals in their panel before

TAC
from page 1

arriving at the review meeting, and provide preliminary grades through a web-review system. These grades are used to construct a triage list, which is made up of the lower 40% of the proposals in each panel. At the beginning of the review meeting, panelists have the opportunity to resurrect triaged proposals (if a scientific case is made), but otherwise, triaged proposals are discarded and not discussed further. This system is designed to make the best use of the available resources at the meeting by ensuring the panelists focus their discussion on proposals that have a reasonable chance of being approved.

The number of orbits given to each panel for allocation to Small GO programs is determined by both the number of proposals and the number of orbits requested in that panel (giving equal weight to each). This ensures that the over-subscription in each panel is approximately equal, and that proposals in areas that tend to request fewer orbits (like Planets) have an equal chance of success as proposals in areas that tend to make larger orbit requests (like Cosmology and AGN/IGM).

For each proposal, panel operations begin with a discussion led by the primary and secondary reviewers, who after debating the proposal's merits and weaknesses, then open the discussion to the full panel. After the discussion's conclusion, all panelists (except those conflicted) give final votes on the proposal, determining its final grade. After all proposals are graded and ranked, the panel is then able to see which proposals lie above the "cutoff line," the point where their orbit allocation has been reached. Under the direction of the panel chair, they then consider the balance of the proposals above the cutoff line, paying particular attention to where any SNAP, Archival, Medium GO, and UV Initiative proposals lie, making adjustments to the final ranked list as necessary. Note that all proposal types are ranked together on the same scale based on the science—without quotas for each category.

Ensuring Impartiality

Conflicts of interest are closely monitored during the review process. Striking a balance between minimizing conflicts and maximizing the expertise of a panel is challenging because expert reviewers are often conflicted on many proposals in their panel. To handle this, we transfer proposals to mirror panels whenever possible, and we distinguish between major and minor conflicts. A major conflict arises when a panel member is a PI or Co-I on the proposal, or a family member, current student, recent student, current advisor, or recent advisor of a PI or Co-I. In this case, the panelist must leave the room during the discussion of the proposal and may not vote on it. A minor conflict arises when one of the panel members is a close collaborator of a Co-I, or is at the same institution as a Co-I. In this case, the panelist may, at the chair's discretion, participate in the proposal discussion—but may not cast a vote. We find the ability of reviewers with minor conflicts to partake in the discussion leads to a healthier debate on the proposals.

The panels are observed by roving astronomers of the Science Policies Group at the Institute, NASA representatives from Goddard Space Flight Center, and the at-large members from the TAC. These observers ensure that all rules are followed and answer policy-related questions that arise during the review, but do not provide any scientific or technical opinions.

A TAC Ombudsperson

Time allocation on *Hubble* is highly competitive. As a result, it is not uncommon for the TAC results to generate some controversy. The Institute makes every effort to ensure that the TAC process is both fair and seen to be fair by the astronomical community. Controversies also arise in government and in the business world, and a mechanism often used for their resolution is to employ an ombudsperson, an independent third party who can provide an impartial assessment of the situation. Following that example, the Director decided to ask a prominent member of the community to serve as a TAC ombudsperson in Cycle 21.

Formally, the TAC ombudpersons is charged with investigating issues and complaints brought forward by members of the astronomical community with regard to the allocation of telescope time, and with providing an independent assessment of the fairness of the current TAC process. The ombudsperson is encouraged to make direct contact with community members to obtain additional information on specific issues as the need arises. Those interactions remain confidential. The ombudsperson provides a report to the Director on the overall process, as well as an assessment of the utility of role of ombudsperson, and that report will be made public.

Dr. Fred Lo, the former Director of the National Radio Astronomy Observatory, agreed to serve as the inaugural TAC ombudsperson. His remit was to follow up on issues raised in Cycle 20 and to attend the Cycle 21 TAC meeting as an observer. Prior to the meeting, he discussed time allocation with other observatories and contacted individuals in the community who had raised specific concerns in the past cycle. Dr Lo's report has been submitted, completing his charge. His report makes a number of recommendations for potential improvements that will be discussed with the Space Telescope Users Committee (STUC) at their next meeting, where we will also invite the STUC's input on the potential future role of an ombudsperson. Dr. Lo's report will be published in full in the next *Institute Newsletter*.

Medium-sized Proposals

Proposals that request more than 30 orbits have had a somewhat checkered history at the TAC (see figure *Proposal Success rate as a function of Orbit Request, Cycle 17–21* and the article "The Evolution of the TAC Process" in Vol. 31, Issue 1 of the Institute Newsletter). Faced with a fixed orbit budget, panel members can find it difficult to sink a substantial fraction of those resources into a single program, effectively leading to a higher threshold for acceptance of medium-sized proposals. In past cycles, a central orbit pool has been maintained as a subsidy to panels to offset this effect, and this has had some success. For example, in Cycle 19, the panels approved 13 proposals requesting between 31 and 55 orbits for a total of 405 orbits. However, in Cycle 20, only two medium-sized proposals, for 31 and 39 orbits respectively, were accepted by the panels (two additional proposals for 60 orbits each were approved by the TAC). Feedback from TAC members indicated that this deficit stemmed partly from ineffectiveness of the subsidy pool, and partly from the community tailoring proposals to smaller resource requests.

One of the strengths of a general-purpose observatory, like *Hubble*, is that the proposal process allows for different types of science program from focused, single-target experiments to broad surveys, requiring a range of resources. The Cycle 20 results therefore raised concerns that the allocation process might be militating against specific types of investigation. Following discussions to the Space Telescope Users Committee and with TAC members, the decision was taken to adopt a new strategy in Cycle 21, introducing the category of "Medium" proposals, requesting between 35 and 74 orbits. Small proposals request between 1 and 34 orbits, while the lower boundary for Large programs was reduced to 75 orbits. A fixed number of orbits was allocated to each of the three categories for approval.

The new category attracted significant community interest, with 109 Medium proposals submitted in response to the Cycle 21 call. Twenty proposals were sent forward from the panels to the TAC and 13 proposals (requiring between 35 and 60 orbits) were approved for a total of 558 orbits. Discussions with TAC members indicate that those proposals were well matched to the requested resources and rated as scientifically comparable with both Large and Small approved programs. The new system will likely continue in future cycles, although we will take steps to mitigate the workload imposed on TAC members, who are faced with reviewing a shortlist of 15–20 Medium proposals at short notice.

Ultraviolet Initiative

A UV Initiative was introduced in Cycle 21 to maximize the scientific impact from *Hubble*'s UV capabilities in the final phase of the mission, given the lack of planned future UV facilities. This initiative took the form of orbit allocation targets for UV observations (wavelengths <3,200 Angstroms). Each panel was asked to dedicate at least 40% of its orbits to UV-specific observations, and the TAC was asked to dedicate at least 50% of its orbits to UV-specific observations (see article in the *Institute Newsletter* Vol. 29 Issue 2 by N. Reid & K. Sembach; **https://blogs.stsci.edu/newsletter/2013/01/07/an-ultraviolet-initiative-for-hubble-in-cycle-21/**). These numbers were treated as guidelines, not quotas, and all proposals recommended for acceptance had to meet the usual requirement of high scientific quality. The UV Initiative also extended to Archival and Theory proposals, provided they led to UV high-level data products and tools for the *Hubble* archive or provided new models or theories to aid in the interpretation of UV *Hubble* data.

Summary of Cycle 21 Results

Proposals	Requested	Approved	% Accepted	ESA Accepted	ESA % Total
General Observer	822	192	23.4%	44	22.9%
... Small	663	171	25.8%	41	24.0%
... Medium	109	13	11.9%	2	15.4%
... Large	50	8[1]	16.0%	1	12.5%
Snapshot	55	9	16.4%	2	22.2%
Regular AR	142	35	24.6%	0	
Legacy AR	13	2[2]	15.4%	0	
Theory	63	11[2]	17.5%	1	9.1%
Total	1,094	249	22.8%	47	22.9%[4]
Primary Orbits	19,742	3,308[3]	16.8%	587	17.7%

[1] *8 Large approved includes 1 Pure-Parallel and 4 Treasury proposals*
[2] *1 Legacy AR proposal is also a Theory proposal*
[3] *3,308 approved orbits does not include 8 Prime Calibration orbits*
[4] *Excluding Archival proposals*

UV proposals fared extremely well under the initiative, with 60% of the primary GO observing time and 43% of the approved proposals dedicated to UV observations. Twelve of the 30 Archival and Theory UV programs submitted were approved.

Frontier Fields

The Institute Director has devoted a significant fraction of his discretionary time in Cycles 21–23 to a Frontier Fields program (see article in *STScI Newsletter* Vol. 30 Issue 1 by J. Lotz et al.; **https://blogs.stsci.edu/newsletter/2013/04/12/hubble-boldly-goes-the-frontier-fields-program/**). This involves deep imaging observations of six galaxy clusters and offset blank fields using the Advanced Camera for Surveys (ACS) and Wide Field Camera 3 (WFC3) operating in parallel. The lensing power of these clusters will reveal hitherto inaccessible populations of $z = 5–10$ galaxies. In Cycle 21, proposers were encouraged to submit supplemental observing proposals and archival proposals in support of the Frontier Fields; three GO programs and seven AR programs were accepted in response.

Cycle 21 Statistics

The Cycle 21 TAC and panels nominally had 3,200 orbits available for allocation, 400 orbits higher than the number available in Cycle 20, largely due to the completion of the three Multi-Cycle Treasury (MCT) Programs. The 3,200 available orbits were broken down into 1,000 orbits for Large and Treasury proposals, 500 orbits for Medium proposals, and 1,700 orbits for Small proposals. The TAC was also able to recommend approval of up to 1,000 Snapshot observations.

Of the 1,094 proposals submitted, 249 proposals were approved, including eight Large and Treasury Programs (one of which was a Pure Parallel Program), thirteen Medium Programs, two Archival Legacy Programs, and nine Snapshot Programs. In addition, one joint *Hubble/Chandra* program, three joint *Hubble/Spitzer* programs, and four joint *Hubble/XMM-Newton* programs were awarded time. Further breakdown of the submitted and approved programs into proposal categories is given in the table *Summary of Cycle 21 Results*.

The over-subscription ratio for GO programs was approximately 6:1 by orbits, similar to last year, and 4.3:1 by proposals, slightly lower than last year. The over-subscription for Archival and Theory proposals was 5:1, representing a significant increase over previous cycles. This appears to reflect, at least partially, the community's increasing awareness of the growing holdings of the *Hubble* archive, particularly in an age where Large and Treasury programs typically have no proprietary period.

WFC3 was once again the most widely used prime instrument, with an approved Cycle 21 usage of 41.8%, followed by the Cosmic Origins Spectrograph (COS) with 28.5%, Space Telescope Imaging Spectrograph (STIS) with 16.3%, ACS with 13.1%, and Fine Guidance Sensors (FGS) with 0.2% (see *Cycle 21 Instrument Statistics*). Accounting for parallel and Snapshot observations, WFC3 accounts for 53.6% of all usage. Among the approved GO prime orbits, 38.0% were allocated for spectroscopy and 62.0% for imaging, compared to 26.9% for spectroscopy and 73.1% for imaging in Cycle 20. The significant increase in the spectroscopy percentage between Cycles 20 and 21 is clearly a direct result of the UV Initiative.

Proposal Breakdown by PI Country

Country	Submitted	Approved	Country	Submitted	Approved
Australia	14	3	Japan	9	2
Austria	1	0	Korea	4	0
Belgium	3	1	Mexico	2	1
Brazil	2	0	Norway	1	0
Canada	8	1	Russia	3	0
Chile	14	2	South Africa	2	0
China	4	1	Spain	11	4
Denmark	3	0	Sweden	5	2
France	22	7	Switzerland	8	0
Germany	44	10	The Netherlands	17	5
Iceland	1	0	United Kingdom	59	13
India	1	0	United States	835	193
Israel	5	1			
Italy	16	3	ESA Proposals	203	47

Proposal Acceptance Ratio: Over-subscription by Cycle

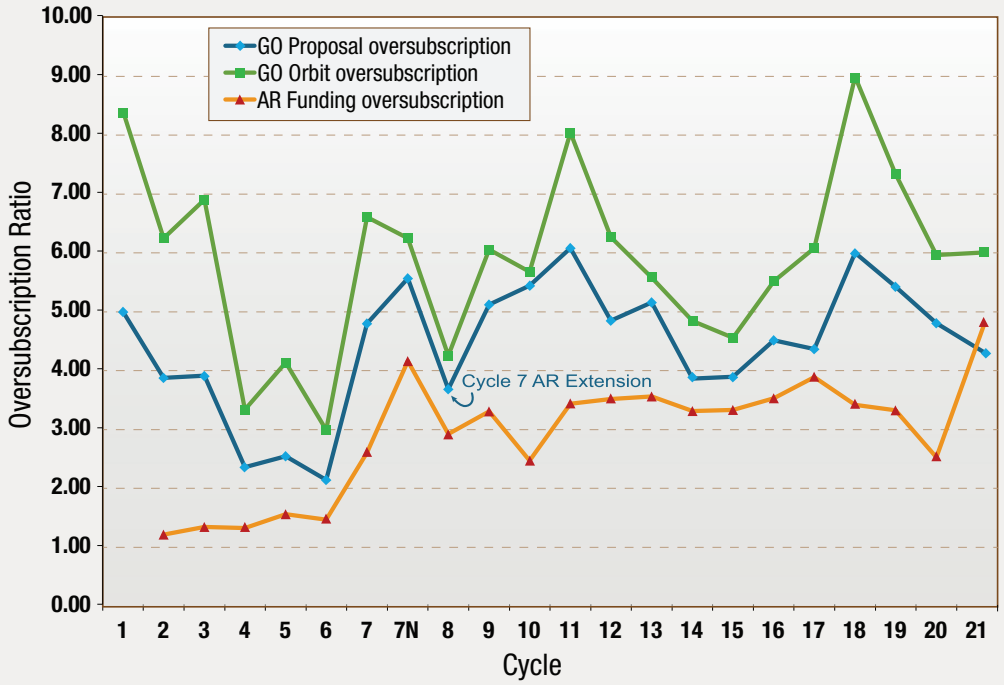

Proposal Success Rate as a Function of Orbit Request, Cycles 17–21

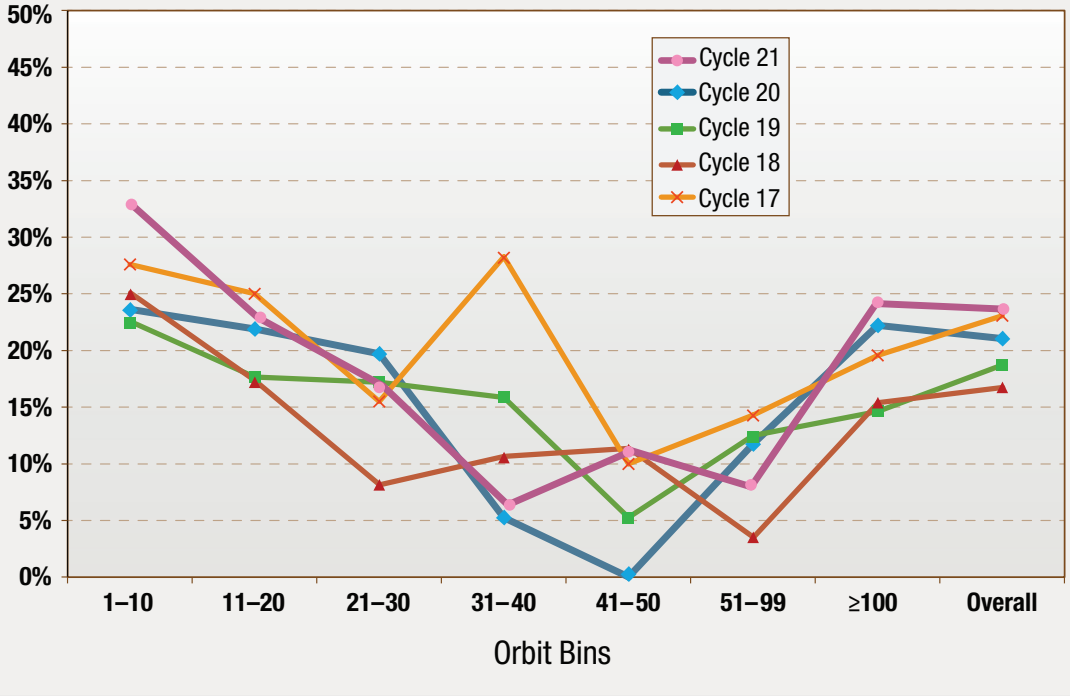

TAC
from page 5

Hubble is a joint NASA–ESA mission. ESA scientists were PIs on 22.9% of the accepted GO and SNAP proposals and 17.7% of the primary orbits allocated. Since its launch, ESA scientists have been PIs on 21.7% of *Hubble* proposals utilizing 17.3% of its orbits, consistent with the lifetime requirement that ESA scientists account for at least 15% of *Hubble* observations. The total number of ESA investigators (PIs and Co-Is) involved in *Hubble* proposals has risen for the fifth year in a row, and now stands at almost 500, indicating the continuing strength of European involvement in *Hubble*. The total number of approved proposals with ESA PIs has also risen consistently since Cycle 16, reaching 47 this year.

Scientists from 40 of the 50 states proposed to use *Hubble* in Cycle 21. The five states with the highest number of submissions (based on PI location) are California, Maryland, Arizona, Massachusetts, and Texas. Internationally, *Hubble* attracted proposals from 26 countries across 6 continents, with the USA being followed by the United Kingdom, Germany, France, and the Netherlands in terms of number of proposals submitted (and by proposals approved). Outside Europe and North America, the countries submitting the highest number of proposals are Australia, Chile, and Japan.

Science Program

As always, the TAC and the panels recommended a set of proposals that span a broad range of science areas. The accepted Treasury, Large, Archival Legacy, and Pure Parallel Programs are now briefly described.

In *Follow The Water: The Ultimate WFC3 Exoplanet Atmosphere Survey,* PI Jacob Bean (University of Chicago) and his collaborators will conduct a comprehensive exoplanet atmosphere survey using the unrivaled capabilities of the WFC3 infrared IR channel. They will measure high-precision transmission, dayside emission, and phase-resolved emission spectra over a broad wavelength range for several exoplanet systems. These data will yield unprecedented constraints on the abundances of water, elemental abundance ratios, thermal profiles, chemistries, presence of clouds and hazes, and dynamics of exoplanet atmospheres.

Cycle 21 Instrument Statistics

Config-uration	Mode	Prime %	Coordinated Parallel %	Total	Instrument Prime Usage	Instrument Prime + Coordinated Parallel Usage	Pure Parallel Usage	SNAP Usage
ACS/SBC	Imaging	1.6%	0.0%	1.2%			0.0%	0.0%
ACS/SBC	Spectroscopy	0.029%	0.0%	0.0%			0.0%	0.0%
ACS/WFC	Imaging	10.4%	29.3%	14.7%			0.0%	37.5%
ACS/WFC	Ramp Filter	1.1%	0.0%	0.9%	13.1%	16.8%	0.0%	0.0%
ACS/WFC	Spectroscopy	0.0%	0.0%	0.0%			0.0%	0.0%
COS/FUV	Spectroscopy	23.7%	0.0%	18.3%			0.0%	4.6%
COS/NUV	Imaging	1.4%	0.0%	1.1%	28.5%	22.0%	0.0%	0.0%
COS/NUV	Spectroscopy	3.4%	0.0%	2.6%			0.0%	0.0%
FGS	POS	0.2%	0.0%	0.2%	0.2%	0.2%	0.0%	0.0%
FGS	TRANS	0.0%	0.0%	0.0%			0.0%	0.0%
STIS/CCD	Imaging	0.9%	1.6%	1.0%			0.0%	0.0%
STIS/CCD	Spectroscopy	2.8%	0.0%	2.2%			0.0%	0.0%
STIS/FUV	Imaging	0.5%	0.0%	0.4%	16.3%	13.3%	0.0%	0.0%
STIS/FUV	Spectroscopy	5.2%	1.6%	4.4%			0.0%	10.9%
STIS/NUV	Imaging	6.9%	0.0%	5.3%			0.0%	0.0%
STIS/NUV	Spectroscopy	0.0%	0.0%	0.0%			0.0%	10.6%
WFC3/IR	Imaging	10.6%	13.7%	11.3%			0.0%	6.8%
WFC3/IR	Spectroscopy	10.4%	9.5%	10.2%	41.8%	47.7%	60.0%	0.0%
WFC3/UVIS	Imaging	20.8%	44.2%	26.2%			40.0%	29.6%
WFC3/UVIS	Spectroscopy	0.0%	0.0%	0.0%			0.0%	0.0%
		100.0%	100.0%	100.0%	100.0%	100.0%	100.0%	100.0%

In *LEGUS: Legacy ExtraGalactic UV Survey*, PI Daniela Calzetti (University of Massachusetts) and her collaborators will build the first *Hubble* UV Atlas of 51 nearby star-forming galaxies, carefully selected to span the full range of morphology, star-formation rate, mass, metallicity, internal structure, and interaction state found in the local universe. In combination with archival and new optical WFC3/ACS data, the requested WFC3/UV images will be used to derive accurate recent (<50 Myr) star formation histories from resolved massive stars and extinction-free ages and masses of star clusters and associations. LEGUS will generate the most homogeneous high-resolution, wide-field UV dataset to date, building and expanding on the *Galaxy Evolution Explorer (GALEX)* legacy.

In *Advanced Spectral Library II: Hot Stars*, PI Thomas Ayres (University of Colorado) and his collaborators will obtain STIS UV echelle spectra—comparable in signal-to-noise ratio and resolution to the best ground-based spectra—for a diverse sample of representative hot stars, to build an Advanced Spectral Library, a foundation for astrophysical exploration: stellar, interstellar, and beyond. The team's first effort, in Cycle 18, involved cool stars. Now they are turning their attention to the hot side of the Hertzsprung-Russell diagram. The group will study the dynamics of O-star mass loss, the detection of rare species in sharp-lined B stars, and the properties and kinematics of local interstellar clouds. They will also release the spectra to the public, enabling other community investigations for decades to come.

In *The HST Legacy Survey of Galactic Globular Clusters: Shedding UV Light on Their Populations and Formation*, PI Giampaolo Piotto (University of Padua) and his team will build on the ACS Globular Cluster Treasury Program by imaging most of its clusters through three UV/blue filters on WFC3/UVIS (F275W, F336W, and F438W). This "magic trio" of filters has shown an uncanny ability to disentangle and characterize multiple-population patterns, in a way that is sensitive to carbon, nitrogen, and oxygen abundance variations. The combination of these passbands with optical filters gives the best leverage for measuring helium enrichment. So far, the dozen clusters observed in these bands exhibit a bewildering variety of multiple-population patterns, and only a wide survey can map the full variance of the phenomenon.

In *The Grism Lens-Amplified Survey from Space* (*GLASS*), PI Tommaso Treu (University of California, Santa Barbara) and his team will conduct a WFC3 grism survey to address key questions in galaxy evolution including: How did galaxies reionize the universe? Why is galaxy evolution environment dependent? How do gas and metals cycle in and out of galaxies? GLASS will address these fundamental questions by taking WFC3 near-infrared integral field spectroscopy of 10 clusters with extensive *Hubble* imaging from the Cluster Lensing And Supernova survey with Hubble (CLASH) and the Frontier Field initiative. Assisted by lensing magnification, their carefully designed strategy will improve line sensitivity by an order of magnitude over current *Hubble* near-infrared spectroscopic surveys.

In *A Breakaway from Incremental Science: Full Characterization of the $z < 1$ CGM and Testing Galaxy Evolution Theory*, PI Chris Churchill (New Mexico State University) and his collaborators will study the circumgalactic medium (CGM), the massive, metal-enriched, extended gaseous reservoir surrounding galaxies. The CGM is the environment through which the large-scale physics of galaxy formation and evolution is controlled and regulated. Using high-resolution COS quasar spectra, the group will measure absorption in H I, O VI, C IV, and other metals in the CGM of 39 $z = 0.08–0.97$ galaxies that have existing *Hubble* images. With such a sample, the team plans to change focus from the "atmospheric conditions" to the overall "meteorological character" of the CGM.

In *Mapping the AGN Broad-Line Region by Reverberation*, PI Brad Peterson (the Ohio State University) and his team will produce the first reverberation map of time-variable broad UV emission from the Seyfert 1 galaxy NGC 5548, crucial to studies of the evolution of black hole masses across cosmic time. Reverberation mapping is the only direct method for measuring black hole masses beyond the local universe, using time resolution as a substitute for spatial resolution. Obtaining unique velocity-delay maps for strong emission will clarify the nature of the broad-line region, its role in the apparently complicated accretion/outflow process, and determine the accuracy of the AGN black hole masses that are now a key component of any study of black hole growth and evolution.

In *Proper Motions of Distant Halo Stars: New Clues to Milky Way Structure, Evolution and Mass*, PI Roeland van der Marel (STScI) and his team will conduct an Archival Legacy Program to study proper motions of Galactic halo stars from multi-epoch *Hubble* data, using distant background galaxies as an absolute reference frame. They will create Legacy catalogs and extract proper motions for ~710 distant Galactic halo stars, including 100 beyond 50 kpc. This will yield a spectacular improvement in our understanding of the halo, and of the structure, past evolution, and mass of the Milky Way.

In *High-level science products from deep ACS and WFC3/IR imaging over the CDF-S/GOODS-S region*, PI Garth Illingworth (University of California, Santa Cruz) and his group will conduct an Archival Legacy Program to study the *Chandra* Deep Field-South. The Chandra Deep Field South is a unique region in the sky with an astonishing 6 Msec of *Hubble* data (nearly 2,600 orbits of WFC3 and ACS data alone), 6 Msec of *Spitzer* images, and 4 Msec of *Chandra* data, plus ground-based spectra and imaging, and Atacama Large Millimeter Array (ALMA) observations. The team will use their extensive experience processing and delivering ACS and WFC3/IR datasets to the Barbara A. Mikulski Archive

Continued page 8

TAC
from page 7

for Space Telescopes (MAST) archive to deliver a complete, processed, and aligned dataset of all deep fields and the deeper, but as-yet-unused, supernovae follow-up and parallel datasets across the CDF-S.

In *WFC3 Infrared Spectroscopic Parallel Survey WISP: A Survey of Star Formation Across Cosmic Time*, PI Matthew Malkan (University of California, Los Angeles) and his team will continue their Pure Parallel Program using slitless spectroscopy to probe galaxy evolution in the redshift range $0.5 < z < 2.5$. WISP is particularly sensitive to low-mass, metal-poor galaxies with extreme star-formation rates that are missed by conventional continuum-selected surveys. This program will use 375 pure parallel orbits for grism spectroscopy in 50 deep (4–5 orbit) and 50 shallow (3-orbit) fields and will derive the extinction-corrected Hα luminosity function and the resulting cosmic history of star formation. The WISP value-added public data release is likely to be one of *Hubble*'s major legacies of 0.8–1.7 micron spectroscopy.

Acknowledgments

Numerous STScI personnel contributed to the Cycle 21 review process. Science Policies Group (SPG) astronomers Claus Leitherer, Neill Reid, Bob Williams, Andy Fruchter, and Andrew Fox were responsible for selecting the panelists, assigning the proposals to panels and panelists, coordinating policy, and providing oversight during the review. Technical Manager Brett Blacker received, organized, and distributed the proposals, oversaw the proposal database, released the results, and prepared the statistical summaries and figures presented here. The TAC logistics were coordinated by Sherita Hanna, with ESA support provided by Loretta Willers, and administrative support from Robin Auer, Roz Baxter, Martha Devaud, Flory Hill, Linda Kaiser, Karyn Keidel, Alisa Meizlish, Karen Petro, Dixie Shipley, Darlene Spencer, Rolanda Taylor, and Annie Valenzuela. Craig Hollinshead was responsible for developing and implementing the web-based review system. Romeo Gourgue, Craig Levy, Jessica Lynch, Greg Masci, Glenn Miller, Corey Richardson, and Patrick Taylor provided support from the Information Technology Services Division.The panel support scientists were Justin Ely, Jo Taylor, Susana Deustua, Andrew Colson, Aparna Maybhate, Paul Goudfrooij, Leonardo Ubeda, Tony Roman, David Golimowski, Stephen Holland, Charles-Philippe Lajoie, Chris Moriarty, Karla Peterson, and Tatjana Tomovic, with support from Lisa Frattare. Ray Beaser, Vickie Bowersox, Margie Cook, Karen Debelius, Lisa Kleinwort, Terry McCormac, Val Schnader, and Paula Sessa provided support from the Business Resource Center. John Eisenhamer and Pam Jeffries provided support from the Office of Pubic Outreach, and Zak Concannon provided assistance from the Copy Center. Facilities support was provided by Laura Bucklew, Andre Deshazo, Jay Diggs, Rob Franklin, Rob Levine, Glenn Martin, Jeff Nesbitt, Greg Pabst, Frankie Schultz, Mike Sharpe, and Mike Venturella. We thank Professor Dan Reich and Bloomberg facilities for providing the use of meeting rooms in the JHU Bloomberg building. Many members of the Instruments Division and the *Hubble* Mission Office also provided technical support.

Key for Orbits by Science Category Charts

AGN/Q:	AGN/Quasars
CS:	Cool Stars
COS:	Cosmology
DD:	Debris Disks
ESP:	Extra-Solar Planets
HS:	Hot Stars
ISM:	ISM and Circumstellar Matter
IEG:	ISM in External Galaxies
QAL:	Quasar Absorptions Lines and IGM
RSF:	Resolved Star Formation
RSP:	Resolved Stellar Populations
SS:	Solar System
USF:	Unresolved Star Formation
USP:	Unresolved Stellar Populations and Galaxy Structures

Submitted Orbits by Science Category

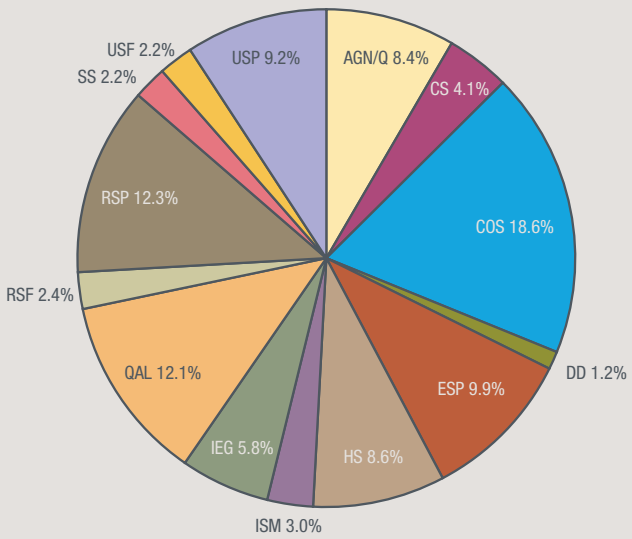

Approved Orbits by Science Category

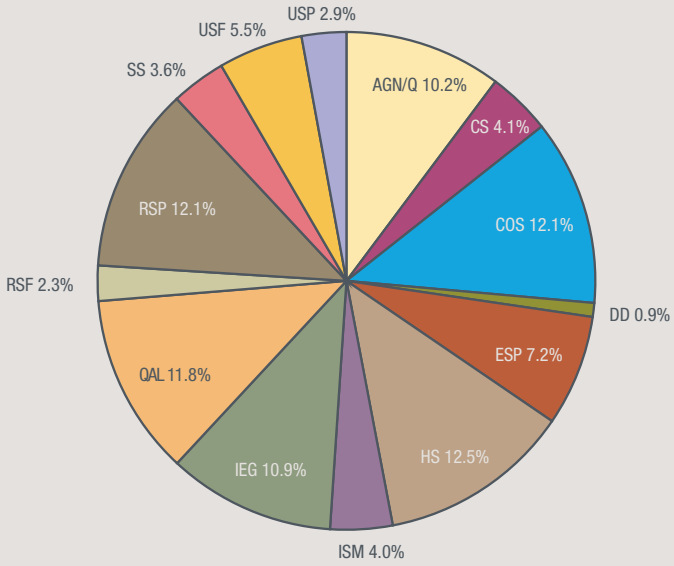

Cycle 21 TAC and Panel Members

Name	Institution
Debra Elmegreen, TAC Chair	Vassar College
Edward Jenkins, At Large	Princeton University
Bob O'Connell, At Large	University of Virginia
Rachel Somerville, At Large	Rutgers University
Extragalactic Panel Members	
Greg Aldering	Lawrence Berkeley National Laboratory
Nahum Arav	Virginia Institute of Technology
Lee Armus, Chair	California Institute of Technology
Daniel Batcheldor	Florida Institute of Technology
Greg Bothun	University of Oregon
Andrew Bunker	University of Oxford
Marcella Carollo	Swiss Federal Institute of Technology – Zurich
Jane Charlton, Chair	Pennsylvania State University
Chris Conselice	University of Nottingham
Kathy Cooksey	Massachusetts Institute of Technology
Elena Dalla Bontà	Università degli Studi di Padova
Romeel Dave, Chair	University of Arizona
Gisella de Rosa	The Ohio State University
Vandana Desai	Spitzer Science Center/Infrared Processing and Analysis Center
Tiziana di Matteo	Carnegie Mellon University
Aleks Diamond-Stanic	University of California, San Diego
Sara Ellison	University of Victoria
Dawn Erb	University of Wisconsin – Milwaukee
Brenda Frye	University of Arizona
Michael Gladders, Chair	University of Chicago
Oleg Gnedin	University of Michigan
Jenny Greene	Princeton University
Raja Guhathakurta	University of California, Lick Observatory
Chris Howk	Notre Dame University
Kelsey Johnson	University of Virginia
Jeyhan Kartaltepe	National Optical Astronomy Observatory
Brian Keeney	University of Colorado
Tae-Sun Kim	University of Wisconsin
Jean-Paul Kneib	Observatoire de Sauverny
Mark Lacy	National Radio Astronomy Observatory
David Law	University of Toronto
Kyoung-Soo Lee	Purdue University

Name	Institution
Andrew Levan	University of Warwick
Paul Martini	The Ohio State University
Steve McCandliss	The Johns Hopkins University
Iva Momcheva	Yale University
Julio Navarro	University of Victoria
John O'Meara	St. Michael's College
Pascal Oesch	University of California, Lick Observatory
Reynier Peletier	University of Groningen
Bryan Penprase	Pomona College
Elena Pian	Osservatorio Astronomico di Trieste
Annalisa Pillepich	University of California, Lick Observatory
Alexandra Pope	University of Massachusetts
Elena Rasia	University of Michigan
Naveen Reddy, Chair	University of California, Riverside
Beth Reid	Lawrence Livermore National Laboratory
Philipp Richter	University of Potsdam
David Schiminovich	Columbia University
Ralph Schoenrich	The Ohio State University
Brian Siana	University of California, Riverside
Daniel Stark	University of Arizona
Alan Stockton	University of Hawaii
Curtis Struck	Iowa State University
Yoshiaki Taniguchi	Tohoku University of Japan
David Thilker	The Johns Hopkins University
Scott Trager, Chair	University of Groningen
Kim-Vy Tran	Texas A&M University
Michele Trenti	Institute of Astronomy, University of Cambridge
Tommaso Treu	University of California, Santa Barbara
David Wake	University of Wisconsin
Martin Ward, Chair	Durham University
Gary Wegner	Dartmouth College
Jessica Werk	University of California, Lick Observatory
Lilya Williams	University of Minnesota
Lin Yan	California Institute of Technology
Planetary Panel Members	
Beth Biller	Max Planck Institute for Astronomy
Marc Buie, Chair	Southwest Research Institute
Nuria Calvet	Michigan University

Cycle 21 TAC and Panel Members (continued)

Name	Institution
Catherine Espaillat	Harvard-Smithsonian Center for Astrophysics
Jean-Claude Gérard	Université de Liège
Denis Grodent	Université de Liège
Paul Kalas	University of California, Berkeley
Alain Lecavelier des Etangs	Astrophysics Institute of Paris
Carey Lisse	The Johns Hopkins University Applied Physics Lab
Avi Mandell	NASA Goddard Space Flight Center
Katie Morzinski	University of Arizona
Jonathan Nichols	University of Leicester
Alex Parker	Harvard-Smithsonian Center for Astrophysics
Ilaria Pascucci	University of Arizona
John Spencer	Southwest Research Institute
Giovanna Tinetti, Chair	University College London
Hal Weaver	The Johns Hopkins University Applied Physics Lab
Galactic Panel Members	
Katelyn Allers	Bucknell University
John Bally	University of Colorado
Beatriz Barbuy	Universidade de São Paulo
Bob Blum	National Optical Astronomy Observatory
John Bochanski	Haverford College
Jo Bovy	Princeton University
Daniela Calzetti	University of Massachusetts
John Cannon	Macalester College
Gisella Clementini	Osservatorio Astronomico di Bologna
Arlin Crotts	Columbia University
Chris Evans	The Royal Observatory, Edinburgh
Steve Federman	The University of Toledo
Francesco Ferraro, Chair	University of Bologna
Ryan Foley	Harvard-Smithsonian Center for Astrophysics
Cynthia Froning	University of Colorado
Peter Garnavich, Chair	University of Notre Dame
Patrick Godon	Villanova University
Edward Guinan	Villanova University

Name	Institution
Patrick Hartigan, Chair	Rice University
Sally Heap	NASA Goddard Space Flight Center
Jon Holtzman	New Mexico State University
Christian Johnson	University of California, Los Angeles
David Kaplan	University of Wisconsin – Milwaukee
Oleg Kargaltsev	University of Florida
Matthew Kerr	Stanford University
Laura Lopez	Massachusetts Institute of Technology
Barbara MacArthur	University of Texas, at Austin
Justyn Maund	Queen's University Belfast
Alan McConnachie	National Research Council of Canada
Jennifer Patience	Arizona State University
Veronique Petit	University of Delaware
Slawomir Piatek	Rutgers University
Caty Pilachowski, Chair	Indiana University
Abi Saha	National Optical Astronomy Observatory
Ravi Sankrit	SOFIA/NASA Ames Research Center
Dick Shaw	National Optical Astronomy Observatory
Ulysses Sofia	American University
Peter Stetson	National Research Council of Canada
Toshiya Ueta	Denver University
Schuyler Van Dyk	IPAC/California Institute of Technology
Eva Villaver	Universidad Autónoma de Madrid
Serena Viti	University College London
Saeqa Vrtilek, Chair	Center for Astrophysics
Lucianne Walkowicz	Princeton University
Frederick Walter	State University of New York – Stony Brook University
Daniel Weisz	University of Washington
Klaus Werner	Universität Tübingen
Andrew West	Boston University

Cycle 21 Approved Programs

Name	Institution	Type	Title
Extragalactic Programs			
Nahum Arav	Virginia Polytechnic Institute and State University	AR	The COS Revolution of AGN Outflow Science
Guillermo Barro	University of California, Santa Cruz	GO	The Progenitors of Quiescent Galaxies at $z \sim 2$: Precision Ages and Star-formation Histories from WFC3/IR Spectroscopy
Danielle Berg	University of Minnesota – Twin Cities	GO	The Evolution of C/O in Low-metallicity Dwarf Galaxies
William Blair	The Johns Hopkins University	GO	Discovering and Characterizing the Young Supernova Remnant Population in M101
Joshua Bloom	University of California, Berkeley	GO	Absolute Calibration of the Extragalactic Mira Period–Luminosity Relation
Nicholas Bond	NASA Goddard Space Flight Center	AR	Rest-Optical Morphology of $2 < z < 3$ Lyman-alpha Emitters: Comparison with Rest-UV and Other High-redshift Galaxies
Médéric Boquien	Laboratoire d'Astrophysique de Marseille	GO	Determining Attenuation Laws Down to the Lyman Break in $z \sim 0.3$ Galaxies
Sanchayeeta Borthakur	The Johns Hopkins University	GO	Characterizing the Elusive Intragroup Medium and Its Role in Galaxy Evolution
Maruša Bradač	University of California, Davis	AR	Breaking Cosmic Dawn: Focusing Cosmic Telescopes to Observe the $z \gtrsim 7$ Universe
Larry Bradley	Space Telescope Science Institute	AR	Galaxy Evolution at the Frontier: The Rate of Galaxy Buildup between $z \sim 11$ and $z \sim 8$
Joel Bregman	University of Michigan	GO	The Missing Baryons around Nearby Dwarf Galaxies
Michael Brotherton	University of Wyoming	AR	Rehabilitating Ultraviolet-based Quasar Black Hole Mass Estimation
Howard Bushouse	Space Telescope Science Institute	GO	The Awakening of the Supermassive Black Hole at the Center of Our Galaxy
Benjamin Cain	University of California, Davis	AR	Resolving Galaxy Cluster Substructure with Gravitational Lensing Flexion
Rebecca Canning	Stanford University	GO	Riding the Wake of a Cluster Merger: Star Formation, Filaments and Turbulence
Sebastiano Cantalupo	University of California, Santa Cruz	GO	Illuminating the Dark Phases of Galaxy Formation with the Help of a $z = 2.4$ Quasar
John Chisholm	University of Wisconsin – Madison	AR	An Archival COS Study of Multi-phase Galactic Outflows and Their Dependence on Host Galaxy Properties
Francesca Civano	Dartmouth College	AR	A Dedicated Search for Gravitational Wave Recoiling Supermassive Black Holes in COSMOS
Dan Coe	Space Telescope Science Institute	GO	Infrared Grism Confirmation of a Strongly Lensed $z \sim 11$ Candidate: MACS0647–JD
Ryan Cooke	University of California, Santa Cruz	GO	Primordial Lithium in $z \sim 0$, Metal-poor, Damped Lyman-alpha Systems
Michael Cooper	University of California, Irvine	AR	The Role of Environment in the Growth of Compact Ellipticals
Asantha Cooray	University of California, Irvine	GO	Spatially Resolved WFC3/Grism Spectral Line Imaging of Gravitational Lensed *Herschel*-selected Luminous Dusty Starbursts
Xinyu Dai	University of Oklahoma	GO	Testing ISM Evolution Models with Gravitational Lenses
Megan Donahue	Michigan State University	GO	UV Line Emission from Million Degree Gas in a Galaxy Cluster Core
Rick Edelson	University of Maryland	GO	WFC3 Imaging and Galaxy Subtraction for the Kepler BL Lac W2R1926+42
Dawn Erb	University of Wisconsin – Milwaukee	AR	Galactic Outflows and the Growth of Disks at $1 < z < 2$
Xiaohui Fan	University of Arizona	GO	Escaping Lyman Continuum in Strongly Lensed Galaxies at $z = 2.0$–2.5

Cycle 21 Approved Programs

Name	Institution	Type	Title
Gary Ferland	University of Kentucky	AR	Reading the Message in the Light: Understanding STIS and COS Spectra, Preparing for the *Webb* Era
Wendy Freedman	Carnegie Institution of Washington	SNAP	The Hubble Constant to 1%? STAGE 4: Calibrating the RR Lyrae PL Relation at *H*-band using *HST* and *Gaia* Parallax Stars
Amy Furniss	University of California, Santa Cruz	GO	PG 1424+240: Too Distant to Be Seen?
Iskren Georgiev	European Space Agency – European Space Research and Technology Centre	GO	The Formation History of UGC 12591—The Most Massive Known Field S0 Galaxy
Suvi Gezari	University of Maryland	GO	*HST*/WFC3 UVIS Imaging of Tidal Disruption Event PS1–10jh
Margherita Giustini	European Space Agency – European Space Research and Technology Centre	GO	Unveiling the X–ray/UV Connection in AGN Winds: the PG 1126–041 Case Study
Jenny Greene	Princeton University	AR	AGN Fueling: Alignments Between Circumnuclear Structures and Radio Jets?
Pierre Guillard	Institut d'Astrophysique Spatiale	GO	COS Spectroscopy of the Stephan's Quintet Giant Shock
Yicheng Guo	University of California, Santa Cruz	SNAP	UV Snapshot of Low-redshift Massive Star-forming Galaxies: Searching for the Analogs of High-redshift Clumpy Galaxies
Frederick Hamann	University of Florida	GO	A Study of PG Quasar-driven Outflows with COS
Masao Hayashi	National Astronomical Observatory of Japan	GO	Resolving Internal Structures of the Progenitors of Early-type Galaxies in a Vigorously Forming Cluster at $z = 2.5$
Matthew Hayes	Observatoire Midi-Pyrénées	GO	Coupling the Emission of Ionizing Radiation and Lyman-alpha
Timothy Heckman	The Johns Hopkins University	GO	On the Nature of Highly Ionized Gas in the Halos of Normal Star-forming Galaxies
Anne Jaskot	University of Michigan	GO	Green Pea Galaxies: Extreme, Optically Thin Starbursts?
Inger Jorgensen	Gemini Observatory, Northern Operations	AR	Galaxy Evolution in the Densest Environments: *HST* imaging
Alexander Karim	Durham University	GO	Characterizing the Formation of the Primordial Red Sequence
Davor Krajnovic	Astrophysikalisches Institut Potsdam	GO	Where Cores Are No More: Assessing the Role of Dissipation in the Assembly of Early-type Galaxies
Mark Krumholz	University of California, Santa Cruz	AR	Tools for Stellar Population Synthesis in the Stochastic Regime
Claus Leitherer	Space Telescope Science Institute	GO	Pushing COS to the (Lyman-)Limit
Andrew Levan	The University of Warwick	GO	The Host and Location of the Candidate relativistic Tidal Disruption Event Swift 2058+0516
Andrew Levan	The University of Warwick	GO	Super-luminous Supernovae without Host Galaxies
Emily Levesque	University of Colorado at Boulder	SNAP	Calibrating Multi-wavelength Metallicity Diagnostics for Star-forming Galaxies
Britt Lundgren	University of Wisconsin – Madison	GO	The Evolving Gas Content of Galaxy Halos: A Complete Census of Mg II Absorption Line Host Galaxies at $0.7 < z < 2.5$
Ragnhild Lunnan	Harvard University	GO	Zooming in on the Progenitors of Ultra-luminous Supernovae with *HST*
Crystal Martin	University of California, Santa Barbara	GO	COS Gas Flows: Challenging the Optical Perspective
Michael McDonald	Massachusetts Institute of Technology	GO	Searching for 300,000 Degree Gas in the Core of the Phoenix Cluster with *HST*-COS
Ian McGreer	University of Arizona	GO	A Candidate Gravitationally Lensed Quasar at $z = 6.09$
Eileen Meyer	Space Telescope Science Institute	GO	Proper Motions at 500 Mpc: Measuring Superluminal Motions in Optical Jets with *HST*
Bahram Mobasher	University of California, Riverside	AR	Combined Study of High Spatial Resolution Color and Mass Maps with Dynamics of Galaxies
Francisco Mueller-Sanchez	University of California, Los Angeles	AR	The Physics of the Coronal Line Region in Seyfert Galaxies and its Role in Galaxy Evolution
Richard Mushotzky	University of Maryland	GO	*Hubble* Observations of *Kepler*-monitored Seyfert 1s

Cycle 21 Approved Programs

Name	Institution	Type	Title
Paul O'Brien	University of Leicester	GO	The Nuclear Outflow in PDS 456
Brian O'Shea	Michigan State University	AR	Unlocking the Secrets of Absorption Line Complexes in the Intergalactic Medium
Göran Östlin	Stockholm University	GO	ELARS—Extending the Lyman-alpha Reference Sample
Benjamin Oppenheimer	Universiteit Leiden	AR	Cosmic H I: a Tracer of the Physics Regulating Galaxy Formation over a Hubble Time
Richard Plotkin	University of Michigan	GO	Radio-quiet Quasars with Extremely Weak Emission Lines: A New Perspective on Quasar Unification
Mary Putman	Columbia University in the City of New York	GO	Warm Gas Flows in the Coma Cluster
Mary Putman	Columbia University in the City of New York	GO	Measuring the Properties of Dwarf Streams
Thomas Quinn	University of Washington	AR	The New Frontier of Cosmological Simulations: Robust Predictions of the Galaxy Population Properties at $z > 4$
David Radburn-Smith	University of Washington	GO	Feeding Galaxies: Cold Accretion Through Warps
Jeffrey Rich	Carnegie Institution of Washington	GO	Investigating the Impact of Merger-driven Shocks
Dominik Riechers	Cornell University	GO	A Simultaneous Measurement of the Cold Gas, Star-formation Rate, and Stellar-mass Histories of the Universe
Adam Riess	The Johns Hopkins University	GO	The Longest Period Cepheids, a Bridge to the *Hubble* Constant
Adam Riess	The Johns Hopkins University	SNAP	*HST* and *Gaia*, Light and Distance
Jane Rigby	NASA Goddard Space Flight Center	GO	The Morphology and Star Formation Distribution in a Big Cool Spiral LIRG
Andrew Robinson	Rochester Institute of Technology	GO	Is There a Kicked Supermassive Black Hole in E1821+643?
Steven Rodney	The Johns Hopkins University	GO	Frontier Field Supernova Search
Anna Rosen	University of California, Santa Cruz	AR	Simulating the Birth of Massive Star Clusters: Is Destruction Inevitable?
Kate Rubin	Max-Planck-Institut für Astronomie, Heidelberg	GO	Mapping Mg II Emission in the M82 Superwind: A Rosetta Stone for Understanding Feedback in the Distant Universe
Wiphu Rujopakarn	University of Arizona	GO	Dissecting the Intensely Star-forming Clumps in a $z \sim 2$ Einstein Ring
Tim Schrabback	Universität Bonn, Argelander Institute for Astronomy	SNAP	An ACS Snapshot Survey of the Most Massive Distant Galaxy Clusters in the South Pole Telescope Sunyaev-Zel'dovich Survey
Anil Seth	University of Utah	AR	The Structure of the Nearest Nuclear Star Clusters
Keren Sharon	University of Michigan	GO	Resolving the Cluster-lensed Sextuple Quasar SDSSJ2222+2745
Kartik Sheth	National Radio Astronomical Observatory	GO	Star Formation and Dissolution Across Dynamically Distinct Environments in NGC 1097
J. Michael Shull	University of Colorado at Boulder	GO	COS Spectra of High-redshift AGN: Probing Deep into the Rest-frame Ionizing Continuum and Broad Emission Lines
J. Michael Shull	University of Colorado at Boulder	GO	Deep COS Spectra of the Two Brightest Quasars that Probe the He II Post-Reionization Era
Brian Siana	University of California, Riverside	GO	The Ultraviolet Frontier: Completing the Census of Star Formation at Its Peak Epoch
Robert Simcoe	Massachusetts Institute of Technology	GO	The Structure of Mg II Absorbing Galaxies at $z = 2$–5: Linking CGM Physics and Stellar Morphology During Galaxy Assembly
Rachel Somerville	Rutgers, the State University of New Jersey	AR	Constraining the Physics of Dwarf Galaxy Formation from the Reionization Epoch to the Present
William Sparks	Space Telescope Science Institute	GO	Gas Physics in Cool-core Clusters: the Virgo Cluster
John Stocke	University of Colorado at Boulder	GO	Accretion Physics in Nearby FR1 Galaxies

Cycle 21 Approved Programs

Name	Institution	Type	Title
Jason Surace	California Institute of Technology	GO	Resolving the Reddest Extragalactic Sources Discovered by *Spitzer*: Strange Dust-Enshrouded Objects at $z \sim$ 2–3?
David Syphers	University of Colorado at Boulder	GO	The First Study of the Quasar Broad Line Region in the <550 Å Extreme UV
Nial Tanvir	University of Leicester	GO	Identifying and Studying gamma-ray Bursts at Very High Redshifts
Grant Tremblay	European Southern Observatory – Germany	GO	Mysterious Ionization in Cooling Flow Filaments: A Test with Deep COS FUV Spectroscopy
Tommaso Treu	University of California, Santa Barbara	AR	The Cosmic Evolution of Faint Satellites Galaxies as a Test of Galaxy Formation and the Nature of Dark Matter
Todd Tripp	University of Massachusetts – Amherst	GO	Directly Probing $>10^6$ K Gas in Lyman Limit Absorbers at $z > 2$
Remco van den Bosch	Max-Planck-Institut für Astronomie, Heidelberg	GO	The Most Massive Black Hole in a Compact Galaxy UGC 2698
Sylvain Veilleux	University of Maryland	GO	The Remarkable Ultraviolet Spectrum of Mrk 231
Carolin Villforth	University of Florida	GO	Do Mergers Matter? Testing AGN-triggering Mechanisms from Seyferts to Quasars
David Wake	University of Wisconsin – Madison	AR	Predicting the Performance of Satellite Dark Energy Surveys Using WFC3 Grism Spectroscopy
Bart Wakker	University of Wisconsin – Madison	GO	Constraining the Size of Intergalactic Clouds with QSO Pairs
Q. Daniel Wang	University of Massachusetts – Amherst	GO	Warm and Hot Gases in and around Cluster Galaxies at $z = 0.1$–0.2
Jessica Werk	University of California, Santa Cruz	AR	The Skeleton in the Closet: Testing the Effect of H II Region Self-Enrichment Using Archival STIS Data
Rik Williams	Carnegie Institution of Washington	AR	A New Window on Galactic Suburbia with CSI, CANDELS, and GOODS-S
Gillian Wilson	University of California, Riverside	GO	Is the Size Evolution of Massive Galaxies Accelerated in Cluster Environments?
David Wittman	University of California, Davis	GO	Probing Dark Matter with a New Class of Merging Clusters
Nadia Zakamska	The Johns Hopkins University	GO	Taking the Measure of Quasar Winds
Dennis Zaritsky	University of Arizona	GO	Galaxy Transformation in the Infall Regions of Clusters
Wei Zheng	The Johns Hopkins University	AR	Characterizing the Young Galaxies at Cosmic Dawn
Planetary Programs			
Daniel Apai	University of Arizona	GO	Patchy Clouds and Rotation Periods in Directly Imaged Exoplanets
Sarah Badman	University of Leicester	GO	Dual Views of Saturn's UV Aurora: Revealing Magnetospheric Dynamics
Susan Benecchi	Carnegie Institution of Washington	GO	Precise Orbit Determination for a *New Horizons* KBO
Amy Bonsor	Institute de Planétologie et d'Astrophyisque de Grenoble	GO	Constraining the Structure of the Kappa Cr B Planetary System, a Unique Subgiant, Orbited by Two Companions and a Debris Disk
Marc Buie	Southwest Research Institute	GO	Pluto Satellite Orbits in Support of *New Horizons*
Nuria Calvet	University of Michigan	GO	Gauging Dust Settling in 5–10 Myr-old Disks with COS
Imke de Pater	University of California, Berkeley	GO	Giant Impacts on Giant Planets
Cesar Fuentes	Northern Arizona University	AR	Deep Field TNO Colors within Archival Frontier Fields
Jean-Claude Gérard	Université de Liège	GO	Remote Sensing of the Energy of Jovian Auroral Electrons with STIS: A Clue to Unveil Plasma Acceleration Processes
William Grundy	Lowell Observatory	GO	Mutual Orbits and Physical Properties of Binary Transneptunian Objects
Dean Hines	Space Telescope Science Institute	GO	Imaging Polarimetry of the 2013 Comet ISON with ACS: A Study of the Heterogeneous Coma

Cycle 21 Approved Programs

Name	Institution	Type	Title
Catherine Huitson	University of Exeter	GO	The First Spectroscopic Phase Curve of a Transiting Planet: Understanding the Deeper Atmosphere
David Jewitt	University of California, Los Angeles	GO	*Hubble* Imaging of a Newly Discovered Main Belt Comet
Michael Jura	University of California, Los Angeles	GO	The Elemental Compositions of Extrasolar Minor Planets
John Krist	Jet Propulsion Laboratory	GO	The Eccentric Debris Ring around HD 202628: Signs of Planetary Perturbations
Marc Kuchner	NASA Goddard Space Flight Center	AR	SMACK: A New Tool for Modeling Images of Debris Disks
Philippe Lamy	Laboratoire d'Astrophysique de Marseille	GO	*Hubble* Imaging of the Nucleus of Comet ISON
Alain Lecavelier des Etangs	Centre National de la Recherche Scientifique, Institut d'Astrophysique de Paris	GO	Hydrogen, Deuterium and Nitrogen in the Beta Pictoris Disk
Jonathan Nichols	University of Leicester	GO	Observing Ganymede's Atmosphere and Auroras with COS and STIS
Jonathan Nichols	University of Leicester	GO	Discovering the Nature of the Star–Planet Interaction at WASP–12b
Marshall Perrin	Space Telescope Science Institute	GO	STIS Coronagraphy of Four Young Debris Disks Newly Uncovered from the NICMOS Archive
Laurent Pueyo	The Johns Hopkins University	GO	Confirmation and Characterization of Young Planetary Companion Hidden in the *HST* NICMOS Archive
Lorenz Roth	Southwest Research Institute	GO	Probing Io's Putative Global Magma Ocean through FUV Auroral Spot Morphology
Michael Salz	Universität Hamburg, Hamburger Sternwarte	SNAP	A Pilot Study to Characterize the Lyman-alpha Emission of Active Exoplanet Host Stars
Eric Schindhelm	Southwest Research Institute	AR	Reconstructing Lyman-alpha Radiation in T Tauri Stars
Mark Showalter	SETI Institute	GO	Reading the Record of Cometary Impacts into Jupiter's Rings
William Sparks	Space Telescope Science Institute	GO	Probing the Atmosphere of a Transiting Ocean World
Andrew Steffl	Southwest Research Institute	GO	Using *Hubble* to Resolve Fundamental Discrepancies in the Surface Composition of the Asteroid (21) Lutetia
Kevin Stevenson	University of Chicago	GO	Confirming a Sub-Earth-sized Exoplanet in the Solar Neighborhood
Harold Weaver	The Johns Hopkins University Applied Physics Laboratory	GO	*Hubble* Spectroscopy of Sungrazing Comet ISON
Ming Zhao	The Pennsylvania State University	GO	Near-IR Spectroscopy of the Highly Inflated, Hottest Known Jupiter KOI–13.01
Galactic Programs			
Nicholas Abel	University of Cincinnati – Clermont College	GO	The Life and Death of H_2 in a UV-rich Environment—Towards a Better Understanding of H_2 Excitation and Destruction
Joshua Adams	Carnegie Institution of Washington	AR	Main Sequence Star Counts as a Probe of IMF Variations with Galactic Environment
Iair Arcavi	Weizmann Institute of Science	GO	Determining the Progenitor of SN 2011dh as a Test of Supernova Shock Cooling Models
John Bally	University of Colorado at Boulder	GO	The First Ultraviolet Survey of Orion Nebula's Protoplanetary Disks and Outflows
Luciana Bianchi	The Johns Hopkins University	SNAP	Understanding Post-AGB Evolution: Snapshot UV Spectroscopy of Hot White Dwarfs
Howard Bond	Space Telescope Science Institute	GO	*HST* Observations of Astrophysically Important Visual Binaries
Howard Bond	Space Telescope Science Institute	GO	Tol 26 and the EGB 6 Class of Planetary-nebula Nuclei: What Happens to a Companion Star when a PN is Ejected?
Madelon Bours	The University of Warwick	GO	CSS 41177: An Eclipsing Double White-dwarf Binary

Cycle 21 Approved Programs

Name	Institution	Type	Title
Esther Buenzli	University of Arizona	GO	Evolution of Heterogeneous Cloud Structure through the T-Dwarf Sequence
Julio Chaname	Pontificia Universidad Católica de Chile	GO	Probing Cold Dark Matter Substructure with Wide Binaries in Dwarf Spheroidal Galaxies
You-Hua Chu	University of Illinois at Urbana–Champaign	GO	A Search for Surviving Companions of Type Ia Supernovae in the Large Magellanic Cloud
Seth Cohen	Arizona State University	AR	Using Resolved Stellar Populations to Tune the Pixel-by-pixel SED Fitting Technique
Martin Cordiner	NASA Goddard Space Flight Center	GO	Probing the Nature of Small-scale Structure towards rho Oph stars: A New Avenue in Diffuse Interstellar Band Research
Romano Corradi	Instituto de Astrofísica de Canarias	GO	The Necklace Nebula as a Probe of Close Binary Evolution
Arlin Crotts	Columbia University in the City of New York	GO	The Surprising Ejecta Geometry of Recurrent Nova T Pyx
Roelof de Jong	Astrophysikalisches Institut Potsdam	GO	The Vertical Disk Structure of Spiral Galaxies and the Origin of Their Thick Disks
Andrea De Luca	INAF, Instituto di Astrofísica Spaziale e Física	GO	Imaging the Crab Nebula when It Is Flaring in gamma-rays
Selma de Mink	Space Telescope Science Institute	GO	Massive Stars and Their Siblings: the Extreme End of the Companion Mass Function
Selma de Mink	Space Telescope Science Institute	GO	The Massive Monsters Living Deep in the Tarantula Nebula: How Massive Are They Really?
Nathalie Degenaar	University of Michigan	GO	Unravelling the Evolution and Accretion Morphology of an Extraordinary Black Hole X-ray Binary
Rosanne Di Stefano	Smithsonian Institution Astrophysical Observatory	AR	Masses or Mass Constraints for 116 Gravitational Microlenses from Archived *HST* Images
Nancy Evans	Smithsonian Institution Astrophysical Observatory	GO	The Dynamical Mass of Polaris, the Nearest Cepheid
Nancy Evans	Smithsonian Institution Astrophysical Observatory	GO	A Precision Measurement of the Mass of the Cepheid V350 Sgr
Hua Feng	Tsinghua University	GO	Multiwavelength Test for a Standard Accretion Disk around an Intermediate-mass Black Hole Candidate
Robert Fesen	Dartmouth College	GO	STIS Spectra of the Young SN Ia Remnant SN 1885 in M31
Gastón Folatelli	Institute for Physics and Mathematics of the Universe	GO	Direct Test for a Binary Progenitor of SN 2011dh in M51
Ryan Foley	Smithsonian Institution Astrophysical Observatory	GO	Understanding the Progenitor Systems, Explosion Mechanisms, and Cosmological Utility of Type Ia Supernovae
Andrew Fox	Space Telescope Science Institute	GO	The Closest Galactic Wind: UV Properties of the Milky Way's Nuclear Outflow
Ori Fox	University of California, Berkeley	GO	Late-time UV Spectroscopic Signatures from Circumstellar Interaction in Type IIn Supernovae
Claes Fransson	Stockholm University	GO	A 3D view of the SN 1987A Ejecta
Anna Frebel	Massachusetts Institute of Technology	AR	The Nucleosynthetic Origins and Chemical Evolution of Phosphorus in the Early Universe
Andrew Fruchter	Space Telescope Science Institute	GO	How Low Can They Go? Detecting Low-luminosity Supernova Progenitors
Boris Gänsicke	The University of Warwick	GO	RXJ0439.8–6809: the Hottest Pre-White Dwarf, or the First Double-degenerate Supersoft X-ray Source?
Peter Garnavich	University of Notre Dame	GO	A Look Inside a Star: The Evolved Main-Sequence Channel and Hydrogen-depleted Ultracompact Binaries

Cycle 21 Approved Programs

Name	Institution	Type	Title
Marla Geha	Yale University	GO	A Non-universal Initial Mass Function in the Ultra-faint Galaxy Coma Berenices
Stephan Geier	Universität Erlangen – Nürnberg	GO	The Hypervelocity Hot Subdwarf US 708—Remnant of a Double-detonation SN Ia?
Christopher Gelino	Jet Propulsion Laboratory	GO	Characterizing the Ultra-cold Brown Dwarf WD 0806–661B
Alexandros Gianninas	University of Oklahoma	GO	COS Spectroscopy of Pulsating, Metal-Rich, Extremely Low-mass White Dwarfs
Douglas Gies	Georgia State University Research Foundation	GO	Separating the Spectral Components of the Massive Triple-star System Delta Orionis
Ana Gomez De Castro	Universidad Complutense	GO	Mapping the Magnetospheric Structure at Outburst of the Pre-main-sequence Close Binary AK Sco
Sandra Greiss	University of Warwick	GO	The Temperatures, Masses and Pulsation Modes of Three ZZ Cetis in the *Kepler* Field
Fabien Grise	Instituto de Astrofísica de Canarias	GO	Unveiling the Nature of Ultraluminous X-ray Sources via UV Spectroscopy
Aaron Grocholski	Louisiana State University and A & M College	AR	Calibrating the Luminosity of Carbon Stars: An Archival Study of Galaxies in the Nearby Universe
Donald Hoard	Eureka Scientific, Inc.	GO	Time-resolved FUV Spectroscopy of a Unique White Dwarf in the *Kepler* Field
David Hogg	New York University	AR	Probabilistic Self-calibration of the WFC3 IR Channel
Ivan Hubeny	University of Arizona	AR	DISKSPEC: A Tool for Analyzing Observed Spectra of Accretion Disk Systems
Remy Indebetouw	University of Virginia	GO	Dissecting Star Formation in N159
Edward Jenkins	Princeton University	AR	Filling in the Gaps in a Study of Gas that Molds the Fermi Bubbles: An Archival Supplement to a Cycle 20 GO Program
Adam Jensen	Wesleyan University	AR	A New Look at Interstellar Silicon
Saurabh Jha	Rutgers, the State University of New Jersey	GO	UV Spectroscopy of a Peculiar White Dwarf Supernova
Nitya Kallivayalil	Yale University	GO	Proper Motion and Internal Kinematics of the SMC: Are the Magellanic Clouds Bound to One Another?
Pierre Kervella	Observatoire de Paris	GO	The Parallax and Mass of the Binary Classical Cepheid V1334 Cyg
Wolfgang Kerzendorf	University of Toronto	GO	To Be or Not to Be the Progenitor: The Question about Tycho-B
Robert Kirshner	Harvard University	GO	SAINTS: Images of SN 1987A
Chris Kochanek	The Ohio State University	GO	Unmasking the Supernova Impostors
Gloria Koenigsberger	Universidad Nacional Autónoma de México	GO	The Changing Wind Structure of the WR/LBV Star in HD 5980
Adam Kowalski	NASA Goddard Space Flight Center	GO	Taking the Temperature of Explosive Stellar Flares
Søren Larsen	Radboud Universiteit Nijmegen	GO	Do the Globular Clusters in the Fornax dSph Have Multiple Stellar Populations?
Jessica Lu	University of Hawaii	AR	Kinematics of the Massive Star-forming Region, Orion BN/KL
Dougal Mackey	Australian National University	GO	Extremely Faint, Diffuse Satellite Systems in the M31 Halo: Exceptional Star Clusters or Tiny Dwarf Galaxies?
Dougal Mackey	Australian National University	GO	Deep Photometry of Two Accreted Families of Globular Clusters in the Remote M31 Halo
Derck Massa	Space Science Institute	GO	Flux Calibration of the COS FUV Modes
Robert Mathieu	University of Wisconsin – Madison	GO	COS Spectroscopy of White Dwarf Companions to Blue Stragglers in NGC 188

Cycle 21 Approved Programs

Name	Institution	Type	Title
Jon Mauerhan	University of Arizona	GO	Constraining the Physical Properties of LBV Nebulae in the Galactic Center Environment
Justyn Maund	Queen's University of Belfast	GO	Stellar Forensics V: A Post-explosion View of the Progenitor of SN 2011dh
Bruce McCollum	Catholic University of America	GO	Uncovering the Nature of the Evolving Remnant Star of a Recent Stellar Merger
Kristen McQuinn	University of Minnesota – Twin Cities	GO	The Star-formation History of Leo P
Andrea Mehner	European Southern Observatory – Chile	GO	Essential UV Observations of Eta Carinae's Change of State
Tiffany Meshkat	Leiden Observatory	GO	Transmission Spectroscopy through the Debris Disk of Fomalhaut
Dan Milisavljevic	Harvard University	GO	Toward a Comprehensive Kinematic and Chemical Survey of the Young O-rich SNR 1E 0102–7219 in the SMC
Antonino Milone	Australian National University	GO	Multiple Stellar Populations in the Young Large Magellanic Cloud Cluster NGC 1856
Matteo Monelli	Instituto de Astrofísica de Canarias	GO	Multiple Populations in External Globular Clusters: the Fornax dSph, the LMC, and the SMC
Cristina Pallanca	Università di Bologna	GO	COSMIC-LAB: a BSS Orbiting a NS? The Companion to the Supermassive NS in NGC 6440
Ruth Peterson	Astrophysical Advances	AR	Determining Fe I Energy Levels with STIS 230H Near-UV Spectra of Metal-Poor Stars
Jacqueline Radigan	Space Telescope Science Institute	GO	Silver Linings: Using Cloud Maps to Understand the L/T Spectral Transition
John Raymond	Smithsonian Institution Astrophysical Observatory	GO	Ion Temperatures in a Collisionless Supernova Remnant Shock Wave
Seth Redfield	Wesleyan University	SNAP	A SNAP Survey of the Local Interstellar Medium: New NUV Observations of Stars with Archived FUV Observations
Bo Reipurth	University of Hawaii	GO	Structure, Excitation, and Evolution of Shocks: A Multiwavelength Study of Herbig-Haro 1/2
Bo Reipurth	University of Hawaii	GO	The HH 24 Jet Complex: Collimated and Colliding Jets from a Newborn Multiple Stellar System
Armin Rest	Space Telescope Science Institute	GO	Spectral Time Series of the Cas A Supernova
Russell Ryan	Space Telescope Science Institute	AR	Understanding the Population of Distant Ultracool Dwarfs from WISPS and 3d-*HST*
Kailash Sahu	Space Telescope Science Institute	GO	Detecting Isolated Black Holes through Astrometric Microlensing
Kailash Sahu	Space Telescope Science Institute	GO	Accurate Mass Determination of the Nearby Old White Dwarf Stein 2051B through Astrometric Microlensing
Gregory Schwarz	American Astronomical Society	GO	Fundamental Properties of Novae Outburst: Coordinated *HST* and *XMM* ToO Observations
Allen Shafter	San Diego State University	AR	A Multiwavelength Study of Recurrent Novae in the Bulge of M31
Nathan Smith	University of Arizona	GO	A Time-lapse Movie of the Kinematics across the Carina Nebula with ACS
Nathan Smith	University of Arizona	GO	WFC3-IR Imaging of Dense, Embedded Outflows from Intermediate-mass Protostars in Carina
Matthias Stute	IAAT, Eberhard Karls Universität, Tübingen	GO	R Aqr: A Prototype for Non-relativistic Astrophysical Jets and a Key for Understanding Jet Formation
Ben Sugerman	Goucher College	GO	Six in One Blow: Reconstructing the Circumstellar Environments of Supernovae in NGC 6946 with Light Echoes
Rachael Tomasino	University of Denver	GO	Co-latitudinal Radial-velocity Profile Confirmation Via Differential Proper Motion of the Bipolar Egg Nebula

Cycle 21 Approved Programs

Name	Institution	Type	Title
R. Brent Tully	University of Hawaii	SNAP	The Geometry and Kinematics of the Local Volume
Roeland van der Marel	Space Telescope Science Institute	GO	Proper Motions along the Orphan Stream: Finding the Parent, Orbit, and Milky Way Halo Shape
Schuyler Van Dyk	California Institute of Technology	GO	Detecting a Hot Companion to the Progenitor of the Type Ic Supernova 1994I in M51
Schuyler Van Dyk	California Institute of Technology	GO	The Stellar Origins of Supernovae
Enrico Vesperini	Indiana University Bloomington	AR	Effects of Dynamical Evolution on the Stellar Mass Function of Multiple Population Globular Clusters
Klaus Werner	Eberhard Karls Universität, Tübingen	GO	Trans-iron Group Elements in the Hot White Dwarf RE 0503–289
J. Craig Wheeler	University of Texas at Austin	AR	Multidimensional and Radiation Hydrodynamics Simulations of Superluminous Supernovae
Benjamin Williams	University of Washington	AR	Measuring of the Progenitor Masses of Historic Supernovae
Benjamin Williams	University of Washington	GO	The Influence of Environment on Star-forming Disks
Brian Wood	Naval Research Laboratory	GO	Tracking the Winds of Red Giants from the Star to the ISM
David Zurek	American Museum of Natural History	GO	Spectroscopic Confirmation of the First Symbiotic Star in a Globular Cluster
Large Programs			
Christopher Churchill	New Mexico State University	GO	A Breakaway from Incremental Science: Full Characterization of the $z < 1$ CGM and Testing Galaxy Evolution Theory
Bradley Peterson	The Ohio State University	GO	Mapping the AGN Broad-line Region by Reverberation
Tommaso Treu	University of California, Santa Barbara	GO	The Grism Lens-amplified Survey from Space (GLASS)
Treasury Programs			
Thomas Ayres	University of Colorado at Boulder	GO	Advanced Spectral Library II: Hot Stars
Jacob Bean	University of Chicago	GO	Follow The Water: The Ultimate WFC3 Exoplanet Atmosphere Survey
Daniela Calzetti	University of Massachusetts – Amherst	GO	LEGUS: Legacy ExtraGalactic UV Survey
Giampaolo Piotto	Università degli Studi di Padova	GO	The *HST* Legacy Survey of Galactic Globular Clusters: Shedding UV Light on Their Populations and Formation
Pure Parallel Program			
Matthew Malkan	University of California, Los Angeles	GO	WFC3 Infrared Spectroscopic Parallel Survey WISP: A Survey of Star Formation across Cosmic Time
AR Legacy Programs			
Garth Illingworth	University of California, Santa Cruz	AR	High-level Science Products from Deep ACS and WFC3/IR Imaging over the CDF-S/GOODS-S Region
Roeland van der Marel	Space Telescope Science Institute	AR	Proper Motions of Distant Halo Stars: New Clues to Milky Way Structure, Evolution and Mass

Staying Sharp: Keeping *Hubble* and *Webb* Seeing Clearly

M. Lallo, *lallo@stsci.edu*, **C. Cox,** *cox@stsci.edu*, **E. Elliott,** *eelliott@stsci.edu*, **G. Hartig,** *hartig@stsci.edu*, **M. Perrin,** *mperrin@stsci.edu*, **R. Soummer,** *soummer@stsci.edu*, **and R. van der Marel,** *marel@stsci.edu*

Hubble and *Webb* are two different types of space telescopes, operating in different environments. Though the tasks of maintaining their optical alignments share many of the same basic principles, the actual techniques and processes bear less resemblance, and it is interesting to compare and contrast the two telescopes in terms of wavefront sensing and control (WFS&C).

The telescopes

Hubble's optical design is a Ritchey-Chrétien Cassegrain telescope with a monolithic, 2.4-meter primary mirror and a 0.3-meter secondary mirror. The mirrors are glass, coated with aluminum and magnesium fluoride. They sit in a graphite-epoxy ring and truss structure approximately 5 meters long (Fig. 1). The *Hubble* optics are optimized for light at ~0.5 micron wavelength, and form well-corrected images across a region of sky ~20 arcminutes in diameter.

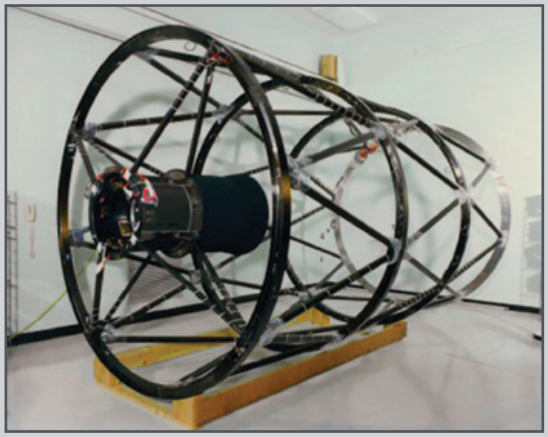

Figure 1: *Hubble*'s graphite-epoxy truss, which supports the primary and secondary mirrors. *Foreground*: the secondary-mirror housing, supported by the "spider." Not shown are the main ring and the primary mirror it supports, which are mounted at the far end of the truss. (Credit: Perkin-Elmer)

Hubble operates in low-earth orbit, which means that the radiant-heat loads rapidly fluctuate, and that the outer surface of the spacecraft undergoes large temperature swings. To minimize thermal effects on the optical quality, *Hubble* has layers of insulation to block heat from soaking into the interior, and the two telescope mirrors are actively heated to stabilize them at room temperature, where they have been held throughout the *Hubble* mission.

Hubble's single-piece primary mirror is fixed in place. Its mount offers limited low-order figure adjustment via 24 force actuators behind the mirror. *Hubble*'s primary mirror actuators were planned for use only if the mirror needed post-launch, low-order correction (mostly coma and astigmatism). These actuators were not used because the primary held its shape pre- and post-launch, and because the spherical aberration from *Hubble*'s primary mirror was outside of the correction capabilities of these mechanisms.

Hubble's secondary mirror can be positioned and oriented with six degrees of freedom. Post-launch the secondary mirror was moved multiple times in all six degrees of freedom to best align the telescope. In routine operations, however, *Hubble*'s image quality is maintained by just one adjustment: despace, i.e., moving the secondary mirror purely toward or away from the primary mirror (see Fig. 2).

The *Webb* telescope is a three-mirror anastigmat—an optical design minimizing astigmatism over a wide field. *Webb* features a 6.6-meter primary mirror composed of 18 separate, hexagonal segments of beryllium coated in gold. A backplane assembly—a carbon-composite trellis—supports the segments. Hinged, composite tubes will deploy from the backplane assembly and support the secondary mirror. The tertiary mirror is off-axis and directs light to a fourth, flat, steering mirror, which will automatically tip and tilt frequently during an observation to stabilize the image on the science camera (see Figs. 3–4). *Webb*'s field of view will be similar in size to *Hubble*'s, about 20 arcminutes across. While the optics are optimized for light at 2 microns—four times longer wavelength than *Hubble*—*Webb*'s short-wavelength sensitivity overlaps with a portion of *Hubble*'s, and at longer wavelengths it extends well into the thermal infrared, to beyond 20 microns.

When launched, *Webb* will take up station at Earth-Sun L2, about 1.5 million km away, or about four times the Earth–Moon distance. From this location, the Earth, Sun, and Moon remain behind the telescope's large sunshield, allowing the telescope to passively cool to about 35°K, or –400°F. Small fluctuations in the backplane temperature—much less than a degree—will degrade the optical alignment, and we expect to adjust the primary-mirror segments regularly. Each segment is expected to need such control in six degrees of freedom—a dramatically more complex scenario than for *Hubble*.

Wavefront sensing and control (WFS&C)

An ideal telescope would convert the flat wavefront of light from a star, situated anywhere in its field of view, into a perfectly spherical wavefront converging to a point on the surface of the detector. Any real telescope, however, introduces diffraction effects, contains irregularities in the mirror surfaces,

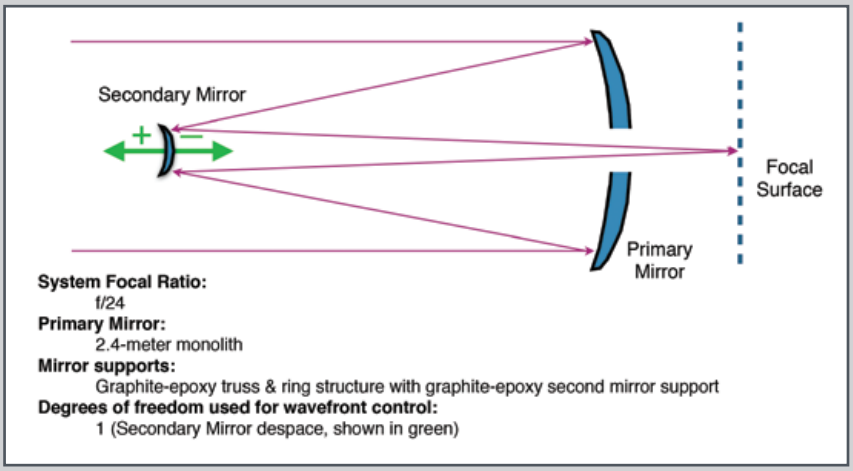

Figure 2: *Hubble*'s optical layout. As is standard practice, the secondary mirror is mounted to allow position and orientation changes in six degrees of freedom. This provides control over the mirror's angles, location in three dimensions, and orientation. In practice we need to control *Hubble*'s secondary mirror only in despace, as shown in green.

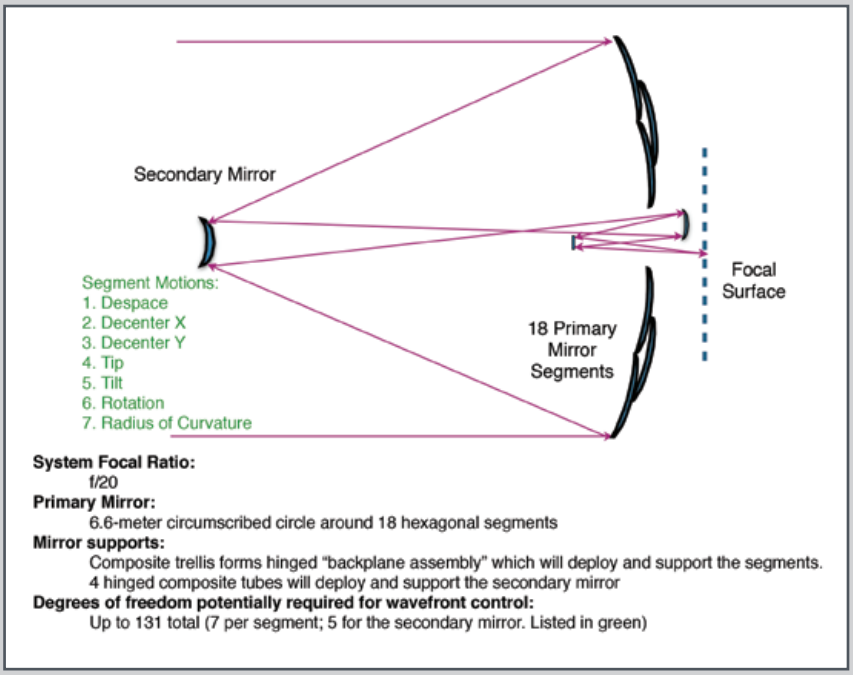

Figure 3: *Webb*'s optical layout. Light falls onto 18 individual 1.3-meter mirrors, each shaped to one of three different optical prescriptions. It then reflects off the secondary, the tertiary (which is fixed in place) and the fine steering mirror before coming to a focus for the science instruments. At the start of the *Webb* mission, the mirror segments will be aligned to work together as one, and secondary mirror adjustments will be made in order to optimize image quality across *Webb*'s field of view. This process will utilize many or most of the 131 degrees of freedom (7 DOF for each of the 18 segments, and 5 DOF for the secondary mirror, since rotation and radius of curvature adjustments should not be needed). To maintain image quality thereafter, we expect to normally need fewer: 108 to 113, still far more than *Hubble*'s single adjustment.

and exhibits aberrations intrinsic to its design, all of which have the effect of spreading the tight natural distribution of light from a point source like a star. Additionally, errors in the alignment of the optics—in their positions or orientations—further alter the distribution of light. This instrumental signature is the telescope's point-spread function (PSF).

Continued page 22

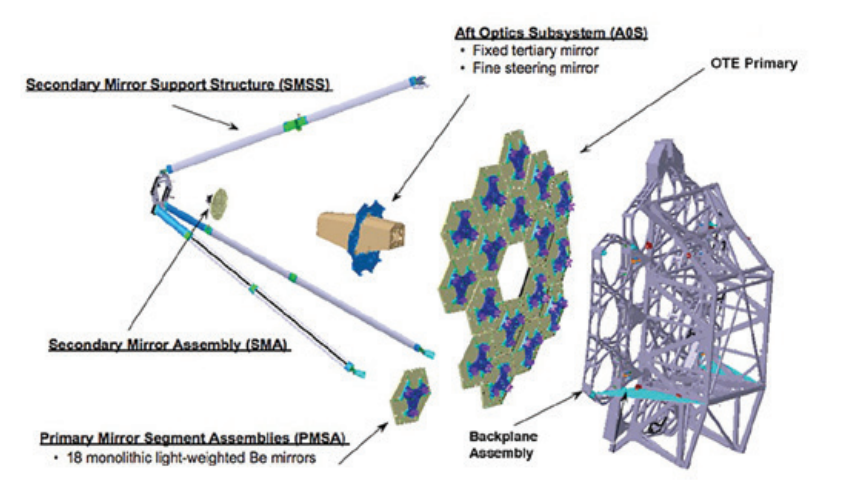

Figure 4: *Webb*'s optics and support structures. The primary mirror segments are mounted to the backplane assembly, as are the secondary mirror supports. After deployment of the folding backplane and secondary mirror supports, gross alignment errors will be removed. Thereafter, small changes in the temperatures of these support structures during normal science operations will cause them to distort, necessitating much finer control of the optics in order to maintain image quality. (Credit: BATC)

For any given optical system there is a well-known mathematical relationship between an image formed by that system and the *wavefront* corresponding to that image. Via techniques known as phase retrieval, this mathematical relation is algorithmically inverted to solve for wavefront errors from an image, or suite of images, collected by science instruments. In practice, noise, sampling, jitter, finite spectral bandpass, flat-fielding error, and detector dynamic range all limit the ability of phase retrieval to determine the wavefront from the images. There are numerous approaches to mitigating these error effects, such as defocussing (discussed later) and/or collecting multiple images to span the field-of-view and range of wavelengths. These mitigation approaches are termed "diversity," and they can significantly increase the accuracy and speed of phase-retrieval-based wavefront sensing.

Webb will use focus diversity by shifting the focus in the Near Infrared Camera (NIRCam) through use of insertable lenses mounted in that camera's filter and pupil wheels. It will use field diversity to separate errors in the primary mirror segments from misalignments of the secondary mirror. In routine operations, *Hubble* requires neither focus diversity nor field diversity to obtain wavefront information sufficient for maintaining image quality at the science instruments.

For both missions though, the wavefront sensing is or will be performed by periodically using phase retrieval to analyze star images (effectively point sources) taken with the same cameras that are used for the science to determine the wavefront error. Some part of this will be intrinsic to the telescope and unavoidable, while some amount will be due to the correctable misalignments and overall shape of the mirrors. Detailed models of the complete optical systems are used to separate these two contributions. In both missions, this wavefront sensing analysis is done on the ground and is not autonomous. Based on the results, we may decide to *control* the mirror positions to reduce this error, thus restoring the desired image quality.

Science-image-based phase retrieval has a history that precedes *Hubble*, and was proposed by Perkin-Elmer for use with the *Hubble* mission. Post-launch this approach quickly became the method of choice for characterizing *Hubble* by groups both inside and outside of the Institute, accurately validating *Hubble*'s Corrective Optics Space Telescope Axial Replacement (COSTAR) instrument, by verifying through image analysis the predictions of pre- and post-COSTAR wavefront errors. These successes led ultimately to exploration of the overall approach and its selection and validation for *Webb* by groups at NASA/GSFC, NASA/JPL, the Institute, Ball Aerospace & Technologies Corporation, and in academia.

Hubble **WFS&C**

Over *Hubble*'s long mission, we have found that the primary and secondary mirrors do not change shape enough to be noticed in the PSF. Tips, tilts, and off-center motions of these mirrors are also so small that they go unnoticed. We do, however, see significant changes in focus caused by variations in the distance between the primary and secondary mirrors. These disparities are caused by small temperature changes in the truss as *Hubble* orbits the Earth and points in different directions (see Fig. 5). The small but measurable focus errors due to temperature changes have been reasonably well understood and modeled, and no mirror control is performed to compensate for this effect, which occurs over hours to days.

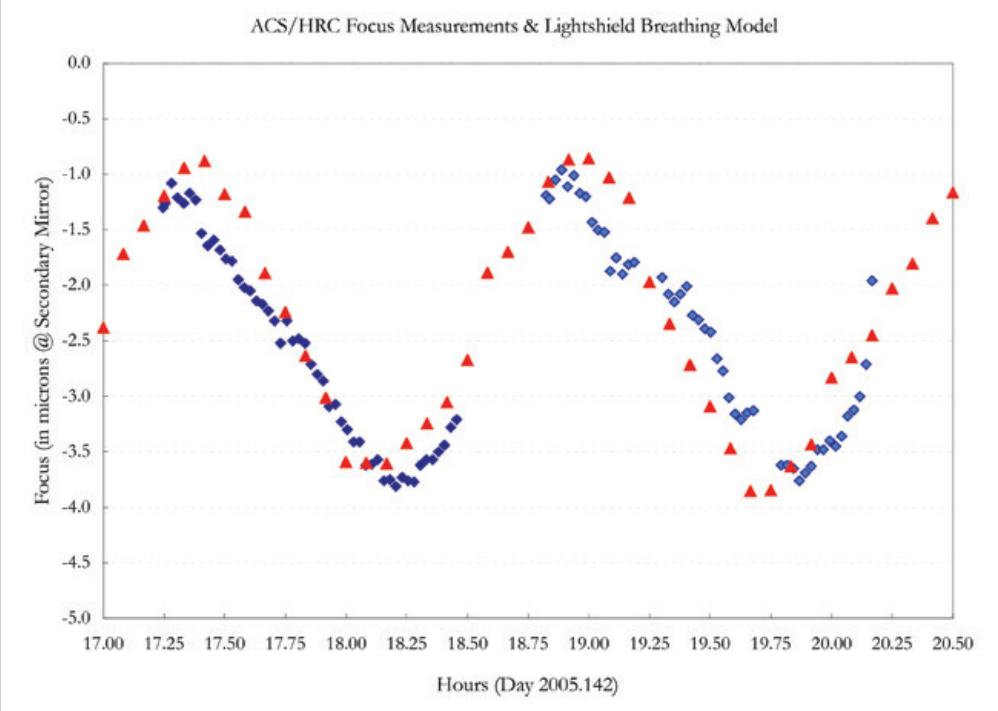

Figure 5: Measured and modeled variation of *Hubble*'s focus error over a *Hubble* orbit, expressed as despace at the secondary mirror. One micron of despace at the secondary mirror produces a small but measurable effect on the PSF, corresponding to a focus error of 6 nanometers rms.

A more significant effect on *Hubble*'s focus is the long-term, gradual shrinkage of the entire truss due to outgassing of water and other molecules from the graphite-epoxy material. This outgassing has caused *Hubble*'s focus to trend throughout its mission, as shown in Figure 6. If left uncorrected, by now this effect would have built up a wavefront error of many times the design specification. To compensate, we have commanded dozens of focus adjustments, each time backing the secondary mirror away from the primary mirror. These adjustments are typically 3–4 microns every few years, based on monthly measurements of the PSF.

For *Hubble*, the phase retrieval method used to determine wavefront error from the observed PSF expresses the result in terms of a polynomial of aberration terms. The software is typically set to solve for only certain "low-order" aberrations like focus, astigmatism, and sometimes coma, but among these, only the focus error varies enough to require periodic corrections. The *Hubble* phase retrieval operates on science images that are very close to being "in focus." The sharp star images formed by the telescope are also undersampled at the detector, meaning that the PSF falls on fewer pixels than needed to optimally represent it (Fig. 7). This can present a challenge to a fitting algorithm like phase retrieval, but due in large part to the limited parameters that are being fit, we can accurately determine the amount of defocus even in a sharp *Hubble* PSF.

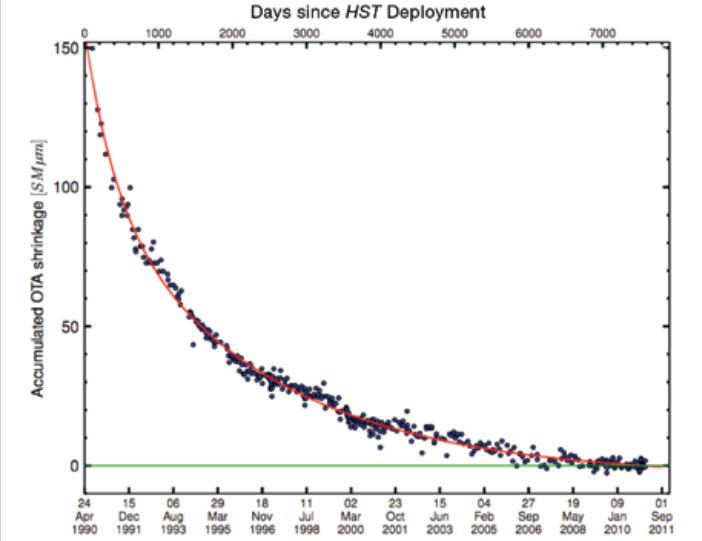

Figure 6: Shrinkage of *Hubble*'s truss due to outgassing. A total shrinkage of about 150 microns—only three thousandths of one percent of the truss's length—dominates *Hubble*'s wavefront error. The *Hubble* program of WFS&C has corrected this long-term trend in focus by backing the secondary mirror away from the primary every couple of years to restore focus at the science instruments.

Webb WFS&C

Unlike *Hubble*'s truss, the large, cold, carbon-composite structure holding *Webb*'s secondary mirror and 18 primary mirror segments is not expected to shrink significantly over time. The structure will, however, unavoidably deform when repointing of the telescope changes the angle of the sunshield with respect to the sun. Over the mission of five or more years, the sunshade material will degrade, causing temperatures to rise, which will produce a long-term evolution of the PSF. We may also find the PSF

Continued page 24

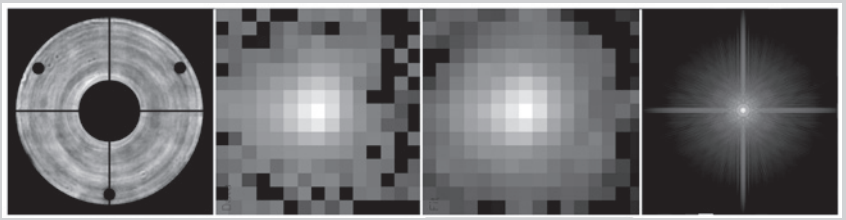

Figure 7: *Hubble* phase-retrieval images. *Far left:* a representative map of phase variations in the pupil. Note the concentric ring-like structure is wavefront error that is known to the phase-retrieval algorithm, and is due to unavoidable irregularities when the mirror was polished. *Center left:* central region of the observed PSF (star image), showing the pixels that sample the image. *Center right:* phase retrieval's best-fit model PSF. *Far right:* a wide view of a model PSF, shown using a logarithmic presentation to accentuate the structure of low-level light outside the core.

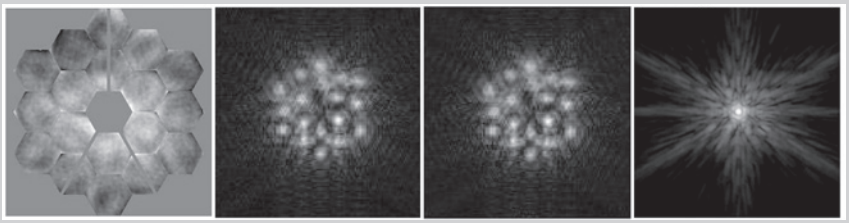

Figure 8: *Webb* phase-retrieval images. *Far left:* a simulated map of phase variations in the pupil, showing the 18 mirror segments. *Center left:* central region of a simulated, out-of-focus PSF. *Center right:* the best-fit, model PSF. *Far right:* a wide view of a model PSF, at 2-microns wavelength, shown using a logarithmic presentation to accentuate the structure of low-level light outside the core. (Credit: BATC)

affected by unanticipated mechanical changes in the structure. The *Webb* WFS&C program is designed to address these issues and deliver an optimal PSF to the science instruments.

Compared with *Hubble*, the more complex telescope design of *Webb* requires the phase-retrieval algorithm to extract much more information about the wavefront from the observed PSF in order to guide more complex control of the mirrors. Instead of simply determining a single parameter (i.e., focus aberration), which scales directly with secondary mirror despace, the sophisticated algorithms developed to support *Webb* will produce a map of the best fitting observed wavefront, compare that with the required or a desired *target* map, then determine the set of commands needed to control the positions and orientations ("poses") of each of the 18 segments to achieve that target wavefront. The relationship between the mirror poses and the wavefront is much more complicated for *Webb* than with *Hubble*, and sometimes the solutions will be degenerate, with various sets of adjustments producing indistinguishable PSFs. In such cases, practical considerations—economy of motion, conservation of the actuators, and ensuring that mirror segments avoid contact with each other—will influence the final choice of mirror commands.

Star images taken through NIRCam's special lenses will increase the amount of information measurable in the PSF by introducing a precisely known defocus. This spreads the PSF out over more pixels, facilitating a more accurate and detailed phase retrieval (see Fig. 8).

Without corrections, *Webb*'s total wavefront error could wander outside of its specification over periods of days to weeks, depending on the amount of thermal perturbations. Therefore, the current plan is to correct the aberrations as needed on an approximately biweekly timescale, based on wavefront sensing every two days. Figure 9 shows one particular model of possible fluctuations of the wavefront error during a year of representative science observations. As was the case with *Hubble*, much about *Webb*'s stability will not be known until it is operating on orbit. We will continue to refine models before launch, and utilize a control scheme that is flexible enough to adapt as we better understand behavior in flight and develop optimal control cadences.

Webb's initial optical alignment

We have described how *Webb*'s WFS&C program will maintain the optical quality of the PSF during routine science operations, and compared the program to *Hubble*'s. The first test of these WFS&C procedures will be the initial alignment of the optics after the backplane assembly and secondary-mirror supports are deployed, when gross alignment errors at the millimeter level will be removed. These are very large adjustments compared with the tens of nanometers of fine control typically expected for the routine WFS&C program to follow. Nevertheless, the same wavefront sensing and mirror management tools will be used in both cases. The one-time WFS&C program after deployment will also involve special operations to support the unique conditions and scenarios that are part of the observatory commissioning.

The approach to performing *Webb*'s WFS&C resulted from a joint effort of NASA/GSFC, NASA/JPL, Ball Aerospace and Technology, Northrop Grumman Aerospace Systems, and the Institute. Ball will also be responsible for the initial alignment of the telescope.

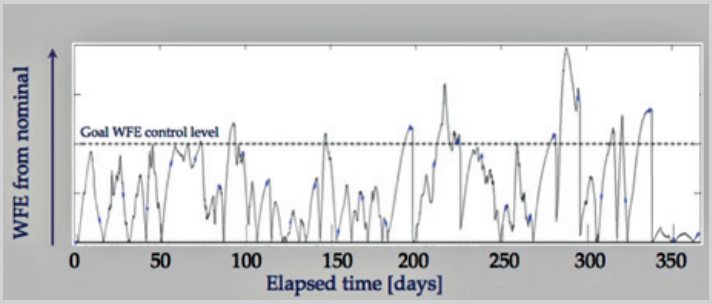

Figure 9: Simulation of how *Webb*'s wavefront might vary over time, showing irregular drifts away from its nominal best alignment. This does not include the contributions to fixed wavefront error inherent in the telescope optics and science instruments. Just as with *Hubble*, active control corrects *Webb*'s optical state when aberrations grow too large. The primary cause of these drifts is thermal expansion and contraction as the telescope's attitude varies with respect to the Sun. Changes in backplane temperature at the tenth Kelvin level can induce measurable wavefront errors. The wavefront evolution shown here was estimated from telescope pointings in a notional, year-long observing schedule. We used simplified thermal models derived from detailed thermal simulations performed, for shorter time periods, at the Goddard Space Flight Center.

Table 1: Comparison of *Hubble* and *Webb* WFS&C

	Hubble	***Webb***
Number of telescope mirrors	2	21
Total degrees of freedom to be used for control	1	113–131 (all possible motions of 18 primary mirror segments and secondary mirror, and potential curvature adjustments)
Control for temperature effects?	No	Yes
Wavefront sensing frequency	Normally once per month.	Normally every 2 days.
Wavefront control frequency	Typically every 1–3 years in recent times. Every few months very early in the mission.	Expected between few weeks to a few months.
Wavefront sensing input	Star images from science cameras; observed with existing amounts of focus aberration.	Star images from science cameras, with intentional defocusing to improve analysis.
Wavefront sensing & control output	Optical aberration terms like focus, astigmatism, and coma; secondary mirror despace command.	Optical aberration terms; map of wavefront; differences compared with a target wavefront; mirror control file containing commands to adjust the mirrors.
Optimize image for the entire field of view?	No, not necessary for the field angles of the science instruments.	Probably required during commissioning; possibly unnecessary thereafter, but planned.
Initial alignment when deployed	Minor adjustments to 5 DOF rigid-body motions of the secondary mirror.	Large adjustments to all primary mirror segments and secondary mirror will be required.

PSF modeling tools

The Institute provides tools to the community to model *Hubble* and *Webb* PSFs:
http://www.stsci.edu/hst/observatory/focus/TinyTim
http://www.stsci.edu/jwst/software/webbpsf

Webb Update

Rachel Osten, *osten@stsci.edu*

Summer 2013 proved to be a busy time for the *James Webb Space Telescope*, and significant progress was made on several fronts. Key hardware and instruments were delivered, and testing commenced. Momentum is building in the *Webb* project. We are planning special activities for outreach to the community at the January 2014 American Astronomical Society (AAS) meeting in Washington, DC.

And then there were three: NIRCam delivered to GSFC

The Near Infrared Camera (NIRCam) joined two other *Webb* instruments—Mid-Infrared Instrument (MIRI) and Fine Guidance Sensor/Near-Infrared Imager and Slitless Spectrograph (FGS/NIRISS)—at the Goddard Space Flight Center (GSFC). NIRCam arrived on July 27, 2013, from Lockheed Martin Advanced Technology Center in Palo Alto, California. Principal investigator Marcia Rieke led the team at the University of Arizona and Lockheed which built NIRCam.

NIRCam is the primary near-infrared imager on board *Webb*. It operates in the range of 0.6–5 microns. In addition to science observations, this instrument also works as a wavefront sensor, confirming the precise alignment of the mosaic of 18 individual primary mirrors.

NIRCam will make essential contributions to accomplishing *Webb*'s science goals. It is a versatile instrument for direct imaging, offering a wide-field survey mode, a small-source mode, and a channel for coronagraphic imaging. The short-wavelength (SW) and long-wavelength (LW) channels cover 2.21 × 2.21 arcmin^2, with 2-pixel sampling of the diffraction-limited point-spread function at 2 and 4 microns. Because of its importance to the *Webb* observatory in wavefront sensing, NIRCam carries a redundant imaging module and focal plane assembly.

A wide variety of filters offer high-, medium-, and narrow-band direct imaging. A grism offers slitless spectroscopy in the 2.4–5 micron range, with spectral resolving power of 2000. Figure 1 compares NIRCam's sensitivity to that of other ground- and space-based imagers on large telescopes.

After NIRCam arrived from the west coast at GSFC in Greenbelt, Maryland on July 27, 2013, an aliveness test was performed to verify the instrument's responses to inputs (Fig. 2). The next stop was vibration testing at the Applied Physics Laboratory in Laurel, Maryland. Formal delivery of NIRCam to GSFC is expected to occur in Fall 2013.

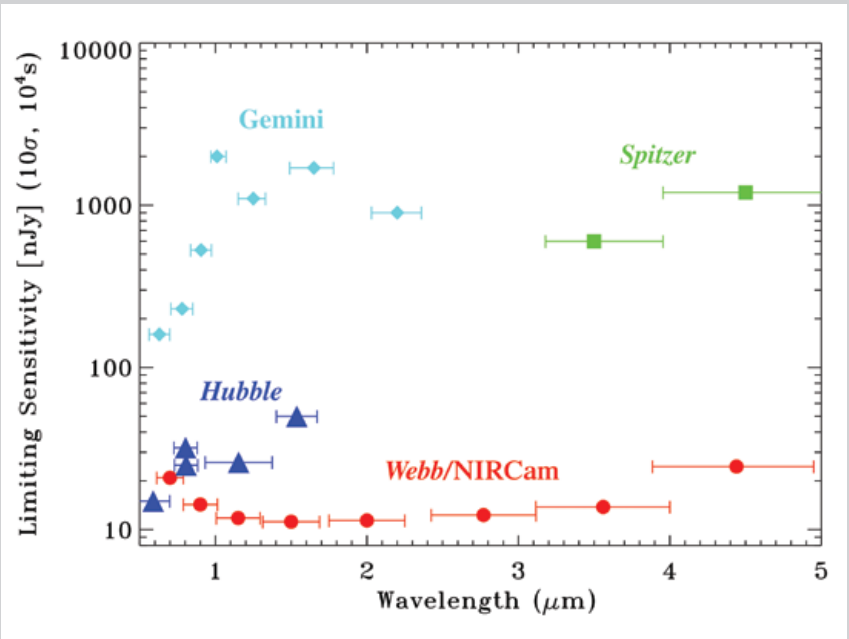

Figure 1: Sensitivity comparison for different imaging modes of *Webb*'s NIRCam. Blue triangles show sensitivities for *Hubble* and green squares show sensitivities for *Spitzer*. Cyan diamonds show ground-based instruments on Gemini. Red circles are required sensitivities from NIRCam in a 10,000-second integration for a signal-to-noise ratio of 10.

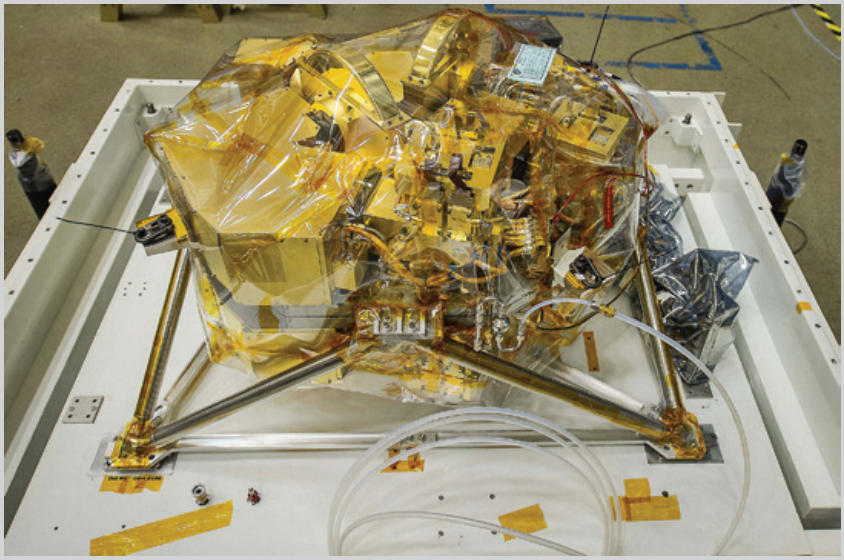

Figure 2: A close-up of the NIRCam optics module, which arrived at NASA's Goddard Space Flight Center in Greenbelt, Maryland, on July 27, 2013. This image was taken in the clean room at GSFC. Image credit: NASA/ Chris Gunn.

Other mission milestones

The *Webb* program recently achieved two additional milestones. The Near-Infrared Spectrograph (NIRSpec)—the last of *Webb*'s science instruments to arrive at GSFC—was shipped from Germany in September 2013 and arrived at GSFC on September 20, 2013. NIRSpec will join the other instruments at GSFC for integration into the science instrument module and subsequent testing in 2014.

On August 22nd, the primary backplane support of *Webb*'s hexagonal primary mirrors arrived at NASA's Marshall Space Flight Center in Huntsville, Alabama, for testing. The backplane supports the mirrors, instruments, and other telescope elements. For more information on this hardware development, see the accompanying article by Blake Bullock.

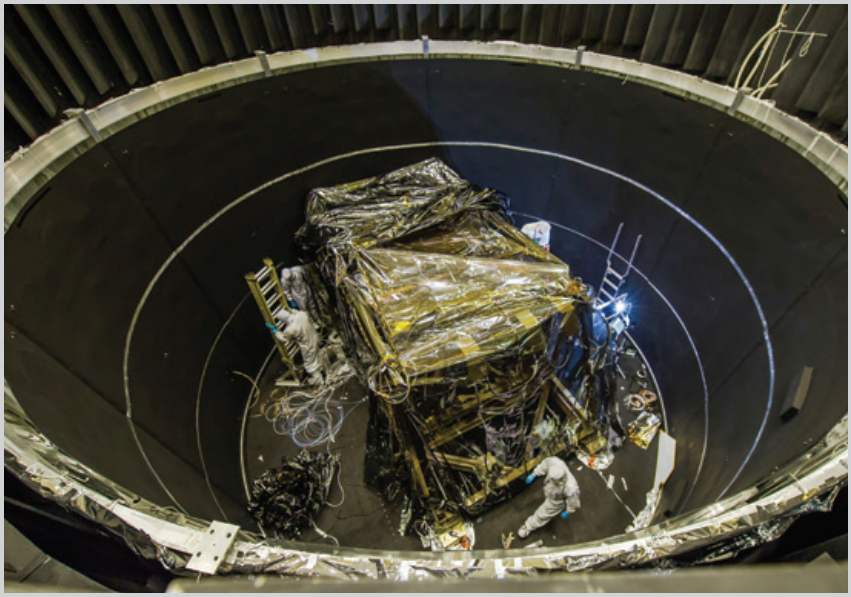

Figure 3: A view of the inside of the thermal vacuum chamber at GSFC, showing engineers working with the ISIM and its system-integration fixture, in preparation for the first thermal vacuum testing, which started on August 29, 2013. The ISIM structure, visible in this photo, is covered in protective blankets. The thermal vacuum chamber is large—approximately 27 by 40 feet. Image credit: NASA/Chris Gunn.

Continued page 28

Update from page 27

Testing, testing, testing

The Integrated Science Instrument Module (ISIM) consists of the four science instruments and nine instrument-support systems. The integration of the FGS/NIRISS and MIRI instruments with the ISIM structure is complete, and the first of three thermal-vacuum tests started on August 29, 2013, at GSFC. The primary purpose of the first thermal-vacuum test was risk reduction—performing dry runs of critical test procedures to identify possible improvements in the testing procedures before the second and third thermal-vacuum tests, which will follow in 2014 and 2015. This series of tests of the integrated science payload is designed to simulate *Webb*'s operating environment in deep space. Figure 3 gives a view of the inside of the thermal vacuum chamber at GSFC. This space-environment simulator tests the ISIM at 35 K. FGS/NIRISS and MIRI were in place for the first test; all four instruments will be installed for the two subsequent tests.

AAS

The winter 2014 AAS meeting in Washington DC will offer several opportunities for the community to learn more about *Webb*. There will be a dedicated session on *Webb* science on Wednesday morning, January 8, 2014, at 10 a.m., with speakers addressing key topics for *Webb*. The list of speakers and subject areas is:

– Marla Geha, Yale University, galaxy evolution
– John Johnson, Harvard University, exoplanets
– Alicia Soderberg, Harvard University, supernovae
– Matthew Tiscareno, Cornell University, solar system
– Mark Wyatt, Cambridge University, star/planet formation

Wednesday afternoon, January 8, 2014, at 12:45 p.m., a joint *Webb* and *Hubble* town-hall meeting will be held. The speakers include Ken Sembach, head of the Institute's *Hubble* Mission Office; Eric Smith, the acting director of the *Webb* program at NASA Headquarters; and Nobel Laureate Adam Riess, affiliated with the Johns Hopkins University and the Institute.

The Institute booth at the AAS meeting will host a number of interactive sessions with the science community. The NIRSpec team at the Institute has been constructing tools and algorithms to assist with the complex multi-object spectroscopy (MOS) mode of the NIRSpec instrument. There will be demonstrations of the planning tool for the NIRSpec microshutter array at the Institute booth to solicit community input to the *Webb* MOS observation planning process.

The meeting will also feature Google+ "hangouts." These are on-line chats during which scientists describe how they plan to use *Webb* in concert with other observatories.

Wide-Field Slitless Spectroscopy with *Webb*'s NIRISS

Van Dixon, *dixon@stsci.edu*, **& Chris Willott,** *Chris.Willott@nrc-cnrc.gc.ca*

The *James Webb Space Telescope*'s Near Infrared Imager and Slitless Spectrograph (NIRISS) will offer several innovative observing modes, one of which is wide-field slitless spectroscopy (WFSS). This mode provides a mean resolving power ($\lambda/\Delta\lambda$) of 150 over the wavelength range 0.8–2.25 microns. The wavelength coverage has been optimized for the detection of Lyα emission lines and breaks in the spectra of galaxies at redshifts 6 to 17, to probe the first stars and ionizing sources in the early universe.

In WFSS, a grism placed in the optical path renders each object in the field as a spectrum. The powerful multiplex capability of WFSS has recently been illustrated with the WFC3 instrument on *Hubble*. In crowded fields grism spectra often overlap, complicating their analysis. To alleviate this problem, NIRISS employs two identical grisms oriented with orthogonal dispersion directions: GR150R disperses spectra into rows on the detector, while GR150C disperses into columns.

To explore its ability to observe high-redshift galaxies—and our ability to identify them—we modeled a NIRISS observation of the massive lensing galaxy cluster MACS J0647+7015. Using published

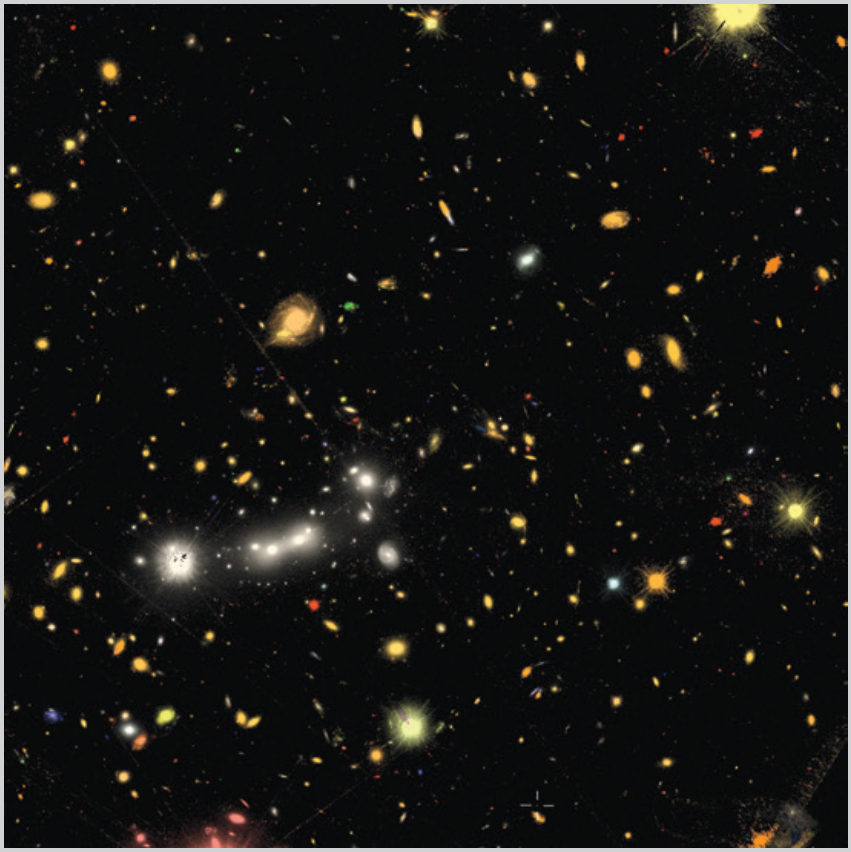

Figure 1: Simulated direct image of the CLASH field (Postman et al. 2012). This color composite combines F090W, F150W, and F200W images. The crosshair near the bottom of the field marks the high-redshift galaxy discussed in the text. The dispersion directions of the two NIRISS grisms are aligned with the crosshairs.

images, photometry, and redshifts from the CLASH survey (Postman et al. 2012), we constructed a series of simulated direct and dispersed images in the six filters available for WFSS with NIRISS. Figure 1 is a color composite of the direct images through the F090W, F150W, and F200W filters. Figure 2 presents dispersed images through the F200W filter. Direct images assume a total integration time of one hour per filter; dispersed images, ten hours. The NIRISS field of view is 2.2 arcminutes on a side.

We added 180 simulated high-redshift ($6 < z < 15$) galaxies distributed uniformly in space, redshift, and magnitude to each image. We used SOURCE EXTRACTOR (Bertin & Arnouts 1996) to identify all objects

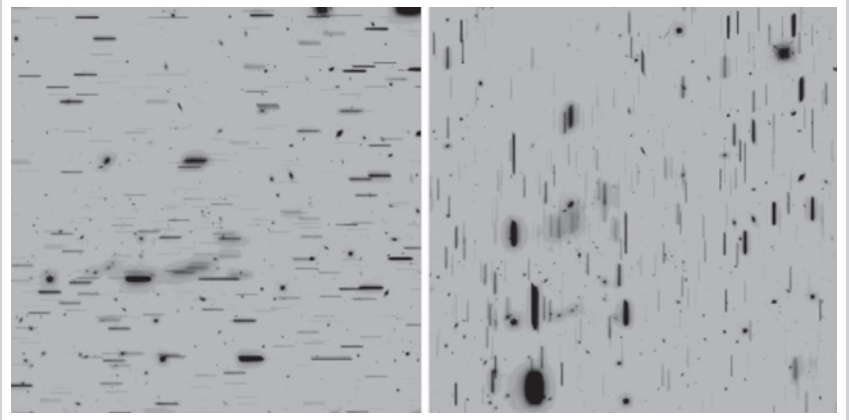

Figure 2: Simulated GR150R (*left*) and GR150C (*right*) images of the CLASH field through the F200W filter. GR150R disperses into rows on the detector, while GR150C disperses into columns.

Continued page 30

NIRISS
from page 41

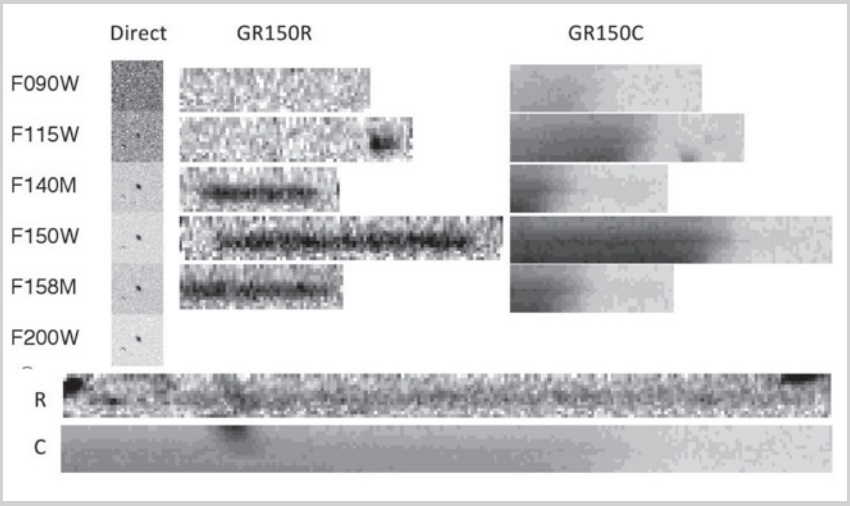

Figure 3: Postage stamps of the direct and dispersed images of a $z = 9.3$ galaxy through each of the six NIRISS filters available for WFSS. The GR150C spectra are contaminated by flux from a nearby galaxy.

in the F200W direct image and perform photometry on each. We used the AXE software package (Kümmel et al. 2009) to extract and calibrate each spectrum and to estimate the contamination due to overlapping spectra. Figure 3 presents postage-stamp images of a $z = 9.3$ galaxy (marked with a crosshair in Figure 1) through each filter. The galaxy is relatively bright (mag = 26.4) through the F200W filter, but undetectable in F090W. While a nearby galaxy obliterates the GR150C spectra, the GR150R spectra are unscathed, demonstrating the utility of our two-grism design.

For each galaxy and each grism, we combine the data obtained through all six filters into a flux- and wavelength-calibrated spectrum, then fit the spectrum with a simple high-redshift model consisting of a power-law continuum and a Lyα emission line. The model flux drops to zero at wavelengths shorter than Lyα. We fit the spectra with a variety of other templates (ellipticals, spirals, starbursts, quasars) to identify lower-redshift objects, as well. The GR150R spectrum of the $z = 9.3$ galaxy is shown in Figure 4. The black points represent the data, the red curve represents the error array (computed by AXE), and the blue curve is our best-fit model.

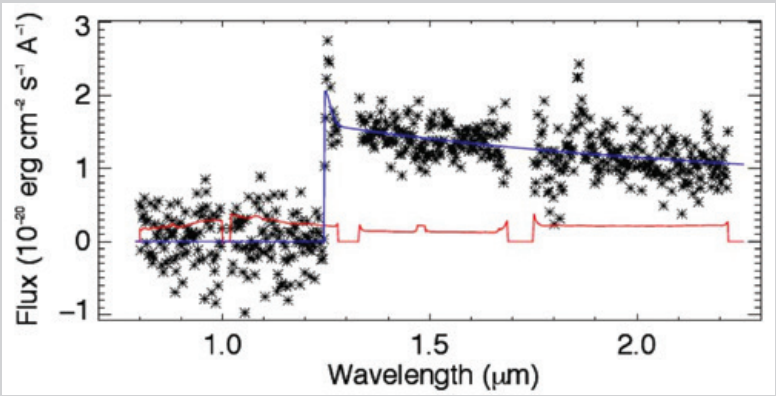

Figure 4: GR150R spectrum of a $z = 9.3$ galaxy. Black points represent the data, the red curve is the error array, and the blue curve is our best-fit model, which combines a power-law continuum with a Lyα emission line.

Work is now under way to analyze a large sample of simulated galaxies and determine how best to mitigate the effects of spectral overlap for deep observations in crowded fields. Redshifts of simulated galaxies much fainter than that in Figure 4 can be determined via spectral breaks and/or emission lines. Targeting high-redshift galaxies magnified by foreground lensing clusters, such as those in the *Hubble* Frontier Fields, will enable a more detailed study of the intrinsically low-luminosity galaxies within the epoch of reionization. Our simulations demonstrate that WFSS with NIRISS will provide a powerful tool for the exploration of the high-redshift universe.

NIRISS is provided to the *Webb* project by the Canadian Space Agency (**http://www.asc-csa.gc.ca/eng/satellites/jwst/contribution.asp**). René Doyon (Université de Montréal) is the principal investigator, and COM DEV Canada is the prime contractor. More information about NIRISS, including tools to simulate and analyze WFSS images, is available on the NIRISS website at STScI (**http://www.stsci.edu/jwst/instruments/niriss**).

References

Bertin, E. & Arnouts, S. 1996, A&AS, 317, 393
Kümmel, M., Walsh, J. R., Pirzkal, N., Kuntschner, H., & Pasquali, A.J. 2009, PASP, 121, 59
Postman, M. et al. 2012, ApJS, 199, 25

Observing Galaxy Assembly with the *James Webb Space Telescope*

Rogier A. Windhorst, *Rogier.Windhorst@asu.edu*

The advantages of *Webb*

Three factors will make *Webb* exquisitely suitable for detecting the faintest and farthest galaxies, and for charting the history of their assembly: its large aperture compared with *Hubble*, its superb infrared (IR) detectors, and the dark IR sky background at its operating location, the second Lagrange point, L2.

The history of galaxy assembly began when the first stars were born—at First Light, about 200 million years after the Big Bang. At that time, the universe was ~20× smaller than it is today. Starlight that originated then, and is observed now, has been shifted in wavelength toward the IR portion of the spectrum, where *Webb*'s performance is optimized. An additional advantage of the IR is its ability to penetrate dust, which can obscure the processes of galaxy assembly at shorter wavelengths. *Webb* is designed to study the epoch of First Light and the entire subsequent process of galaxy assembly.

The process of galaxy assembly

Galaxies are the basic building blocks of the universe, where the supply of atoms and molecules in dark-matter (DM) halos cycles continuously through the birth and death of stars. Analytical theories and numerical models have suggested—and *Hubble* observations have shown—that galaxies build up over cosmic time in a hierarchical manner. The first star clusters and dwarf galaxies, born from the essentially unpolluted hydrogen and helium left over from the Big Bang, formed around the earliest, most massive, so-called "Population III" stars. Their first associations were low-mass, star-forming objects, which grew into larger structures—galaxies—by hierarchical clustering and merging under self-gravity of the DM halos.

In massive DM halos, the process of assembling galaxies accelerated, with more frequent mergers of progressively larger galaxies, and gas converted into stars at a faster rate. This acceleration resulted in bulge-dominated galaxies forming most of their stars early on, with a peak at redshifts $z \simeq 3$, when the universe was only ~2 billion years old. The result was the early-type or elliptical galaxies that we see in the local universe today. In these galaxies, fewer stars formed recently, as *GALEX* and *Hubble*'s Wide Field Camera 3 (WFC3) have shown in great detail (e.g., Rutkowski et al. 2012).

Lower-mass halo environments resulted in less violent galaxy assembly, with lower-mass galaxies forming with smaller bulges and more dramatic spiral-disk structures. This process, fed by a steady inflow of gas and the mergers of minor galaxies, peaked at redshifts $z \simeq 1$–2, when the universe was 2–3× smaller than today and only 3–6 billion years old. After this peak of the cosmic star-formation rate, galaxies evolved more passively, slowly running out of the gas needed to make significant generations of new stars. The outcome is today's Hubble sequence of elliptical and spiral galaxies, which has been in place for roughly the last half of the Hubble time. In earlier times, the process of galaxy assembly was more chaotic, and the deep-field images (Figs. 1–2) simply do not show the familiar galaxy structures that we observe nearby.

Systematic factors affecting galaxy assembly

Three systematic factors in star formation provide context for the fundamentally new contributions that *Webb* will make in the field of galaxy formation. Star formation is rather inefficient, with most starbursts using up only a small fraction of the available gas. Drawn out over cosmic time, the process of galaxy assembly is therefore vulnerable to factors that can deplete the gas supply available for star formation. *Webb*'s unique observing powers—dust penetration, high spatial resolution, and exquisite photometric sensitivity—will enable us to study the roles and interplay of these factors.

1. ***Gas clearing by supermassive black holes.*** In a bulge-dominated galaxy, a supermassive black hole (SMBH), sinking to the galaxy's gravitational center, consumes a small but consistent ~0.2% fraction of the baryonic mass (Ferrarese & Ford 2005; Haring & Rix 2004). The massive BHs left over from the initial Population III stars, which accreted gas and merged hierarchically over cosmic time, likely seeded SMBHs, and the exchange of gravitational radiation facilitated final-stage BH mergers. SMBHs probably grew in lockstep with the process of galaxy assembly itself, at least in the more massive, bulge-dominated early-type galaxies.

   SMBHs are important for galaxy formation, because they have bad eating habits. They eat irregularly and gobble up steady flows of gas from their surrounding accretion disks. But they

Continued page 32

Figure 1: The *Hubble* WFC3 Early Release Science field in 10 filters reaching a depth of $AB \simeq 26.5–27.0$ mag over 40 arcmin^2 (only 15 arcmin^2 shown here) at 0.07–0.15 arcsec resolution full width at half maximum from 0.2–1.7 micron (filters: *UV*, *U*, *B*, *V*, *i*, *z*, *Y*, *J*, *H*; Windhorst et al. 2011). *Webb* will provide imaging at 0.05–0.2 arcsec resolution to a depth $AB \simeq 31.5$ mag (1 nJy) from 1–5 micron, and at 0.2–1.2 arcsec resolution from 5–29 micron, tracing young and old stellar populations—and dust—during the entire process of galaxy assembly over the last 13.5 billion years.

can also suddenly swallow huge chunks of food, including stars, and possibly even entire star clusters. When they eat, the inner accretion disk—which spins rapidly, generating strong magnetic fields—heats up to the point that a relativistic jet of particles forms, and a large amount of gas flows out from the region just outside the Schwarzschild radius. If the viewing angle is right, this extremely bright active nucleus is visible as a quasar or a Seyfert galaxy. Its associated outflow can deposit large amounts of mechanical energy into the intergalactic medium (IGM). For the more massive, bulge-dominated galaxies, this feedback mechanism can shut down the consumption of in-falling gas for a long time, significantly moderating the process of galaxy assembly.

Astronomers will use *Webb*'s unique spatial resolution and sensitivity to investigate SMBHs and correlate their growth with other characteristics of galaxy formation.

2. ***Dust generation and gas clearing by supernovae and stellar winds.*** Stars themselves provide feedback mechanisms in galaxy formation. The combined supernovae output from massive stars in a star-forming galaxy will deposit significant gas, mechanical energy, and dust particles into the IGM. The steadier mass loss from more numerous, lower-mass supergiants in the last stages of their lives also pollutes the IGM with gas and dust. The combination of these processes can be so intense that most of the subsequent starbursts and feeding of SMBHs occurs in regions shrouded by dust. Indeed, another bad eating habit of SMBHs is that they gobble their prodigious meals under a tablecloth of dust, making the process hard to observe with facilities other than *Webb*.

3. ***Starvation by cosmic expansion.*** Galaxies have—or soon will—run out of gas to form significant numbers of new stars. During the last half of the Hubble time, the more massive galaxies have already begun to run out, which has stabilized the Hubble sequence, and has caused elliptical galaxies to be almost, but not completely, "red and dead." Eventually, dark energy (DE), which dominates the expansion of the universe, may permanently drive *all* galaxies away from one another. In the last 4.5 billion years, the expansion rate has accelerated, and it may eventually stop all galaxy assembly, leaving each galaxy to consume its remaining, surrounding gas—and its smaller neighbors—while it still can.

Figure 2: The *Hubble* Ultra-Deep Field (HUDF) data from 750 ACS+WFC3 orbits (2997 exposures totaling 522 hours or nearly 22 full days) in the filters *B*, *V*, *i*, *I*, *z*, *Y*, *J*, *JH*, and *H* (Koekemoer et al. 2013). This image is based on the same data as Illingworth et al. (2012) and Ellis et al. (2013), but displayed at a weighted double log-stretch with a hard color-grayscale, to illustrate fainter features and the possible image crowding expected in *Webb*'s (ultra-)deep fields. This *Hubble* image has 0.06 arcsec drizzled pixels, while *Webb* will have ~0.03 arcsec pixels—or smaller when drizzled. Green circles indicate 76 Lyman-break-dropout galaxies at $z = 7–8$ (Bouwens et al. 2012; Schenker et al. 2013). Yellow circles indicate the six possible dropouts at redshifts $z \simeq 9$ (Ellis et al. 2012), and the red circle indicates the only $z \simeq 10–12$ galaxy candidate that is common to various authors (Yan et al. 2010; Bouwens et al. 2011; Ellis et al. 2012). The HUDF data have pushed *Hubble* to its limits, and *Webb* is needed to provide substantially larger and deeper samples of the first galaxies at redshifts $z \geq 10$, when the universe was less than 500 million years old.

The process of galaxy assembly is thus complex and often rather messy. Dust hides it, and its nature has changed significantly over the last 13.5 billion years. Progress awaits *Webb*, which will probe more deeply into the dust than *Hubble* can, and will offer higher spatial resolution and sensitivity than *Spitzer* has.

Viewing galaxy assembly over cosmic time with *Webb*

Webb will see the faintest galaxies after the epoch of First Light, when the universe was ~20× smaller than it is today. Figure 1 shows a ten-band image from the *Hubble*'s WFC3 and Advanced Camera for Surveys (ACS), in an area of about 15 square arcmin, covering 0.2–1.7 micron in wavelength. The exposure time with each filter was about two hours, and the image reaches to $AB \simeq 26.5–27$ mag (Windhorst et al. 2011).

Continued page 34

Galaxy
from page 41

Figure 2 shows a similar image, but in nine filters on the *Hubble* Ultra Deep Field (HUDF), where each filter was exposed for about 24–100 hours, for a total of 522 hours, reaching almost 100× fainter than Figure 1, or $AB \simeq 30.5$ mag, covering 0.4–1.7 micron in wavelength (Beckwith et al. 2006; Bouwens, Illingworth et al. 2012; Ellis et al. 2013; Schenker et al. 2013; Koekemoer et al. 2013).

At longer wavelengths (1–29 micron), *Webb*'s Near-Infrared Camera (NIRCam; 0.6–5 micron) plus its Mid-InfraRed Instrument (MIRI; 5–29 micron) will redo Figure 1 to similar depths in just minutes per filter. They will redo images like Figure 2 in several hours per filter. The latter will be a day-long *Webb* exposure, probing deeper than the 522-hour *Hubble* depth of Figure 2—equivalent to detecting a firefly from the distance of the Moon. Stated differently, *Webb* will be able to see faint objects in the near-IR to mid-IR that were simply impossible to see with *Hubble* or *Spitzer*.

Webb will see the onset of galaxy assembly, which commenced with the first dwarf galaxies, just after the epoch of First Light. To find significant numbers of the first super star clusters and dwarf galaxies at redshifts $z \simeq 10$–20—when galaxy assembly begins—*Webb* will rely on: (a) its 6.5-meter-diameter mirror for exquisite spatial resolution; (b) its very low background at L2, well away from Sun, Earth and Moon; (c) its huge collecting area for tremendous image depth; and (d) its sensitivity over the near-IR to mid-IR wavelength range.

With the appropriate scheduling, *Webb* can also expose for many days per filter, enabling it to reach considerably deeper than Figure 2, to the point that the wings of foreground galaxies will start overlapping in their outskirts, which means that the objects of First Light will need careful identification. While this task will be akin to looking for needles in a haystack, at least the needles will be numerous, and the foreground haystack can be well determined, modeled, and carefully subtracted. The First Light objects also have significantly different colors than the foreground, so they can be identified in significant numbers. Observers can make corrections for blocking by the known objects in the foreground, thereby retrieving a complete assessment of the First Light population in the background.

Webb is ideally suited for gravitational lensing, which is facilitated by image crowding and the ability to model the gravitational foreground. *Webb*'s lensing studies will, for example, open a window to the first dwarf galaxies. Rich clusters or groups of galaxies in the foreground will amplify the galaxies in the background. Even the halos of random foreground galaxies may be sufficiently dense to lens dwarf galaxies at redshifts $z \geq 10$–20 (Wyithe et al. 2011). Without lensing, many of those galaxies would be too faint to observe.

The continuous near- to mid-IR wavelength coverage of *Webb* will allow it to find dusty, star-forming galaxies at all redshifts, including any highly dust-embedded objects of First Light. So reddened by dust that they remain invisible to *Hubble*, these objects are too dim to be seen by *Spitzer*. This category includes star-forming galaxies with embedded SMBHs that are also too dusty to be seen by *Hubble*, or too faint for detection by *Spitzer*.

For imaging studies, *Webb*'s NIRCam and MIRI will reveal hidden star formation throughout the universe and over most of cosmic time—including the most obscured phases of galaxy assembly and SMBH growth.

For spectroscopic studies, *Webb*'s Near-Infrared Spectrograph (NIRSpec; 1–5 micron) and MIRI (5–29 micron) will measure the redshifts, rotation curves, dynamical masses, and chemical composition of even the faintest galaxies as they assemble over cosmic time. In the near IR, NIRSpec has a fine set of gratings with low to intermediate resolution ($R \simeq 100$–2700), and so does MIRI in the mid-IR. In typical one-day integration times, NIRSpec will obtain spectra for objects with $AB \simeq 28$–29 mag, and emission-line fluxes of few$\times 10^{-19}$ in cgs units. This is more than 10× fainter than can be achieved from the ground.

Webb's Near-Infrared Slitless Spectrograph (NIRISS) will be able to survey substantial sky areas, looking for weak emission lines or continuum breaks in the spectra of faint galaxies. (See article on NIRISS by V. Dixon and C. Willott elsewhere in this *Newsletter*.) NIRISS can yield significant numbers of Lyman-break and Lyman-alpha emission-line galaxies at redshifts $z \simeq 7$–30, as well as Balmer-break galaxies at redshifts $z \simeq 1$–11. This covers the entire epoch of First Light and galaxy assembly, including the epoch at redshifts $z \geq 9$–10, which is essentially out of reach for *Hubble* and *Spitzer*. The same advantage for imaging and object detection is also true of NIRCam and MIRI—and of NIRSpec for higher-resolution spectroscopy. NIRCam, NIRISS, and MIRI imaging will estimate galaxy redshifts, and NIRSpec and MIRI spectroscopy will measure precise redshifts, even for the faintest objects. These measurements, together with the imaging data from NIRCam, FGS, and MIRI, will determine galaxy luminosities, ages, masses, dust-content, and star-formation rates—all the ingredients needed to measure the properties of galaxies over the entire chronology of galaxy assembly.

Viewing the growth of supermassive black holes

Webb's high spatial resolution, combined with its ability to penetrate dust in the near-to-mid-IR, will be essential to identifying SMBHs that are actively feeding—as well as ones that are more dormant. Here, the synergism of NIRCam and MIRI will be used to find weak active galactic nuclei (AGN) candidates,

no matter if the SMBHs are feeding actively or not, or are well shrouded by dust. Further, the use of the complementary spectroscopic capabilities of NIRSpec and NIRISS to identify AGN candidates through their emission lines, will establish how much AGN or SMBH feeding activity is going on in any epoch, and in any type of galaxy. The results will reveal the relationships between the SMBH feeding rate and galaxy luminosity, age, mass, dust content, and star formation. In addition, the coronagraphs in NIRCam, MIRI and NIRISS will be able to find the host galaxies of quasars at $z \geq 6$, which will call for carefully suppressing and subtracting the signal of the central quasar point source (e.g., Mechtley et al. 2012). This full suite of data will enable *Webb* to delineate the entire process of galaxy assembly from every angle, including the role of SMBHs.

Synergy of *Webb* with other facilities

Last but not least, we call attention to the powerful synergy that has existed for nearly two decades between *Hubble* and the 8–10-m class ground-based telescopes, such as Gemini, Keck, and the Very Large Telescope. We fully expect a similar interaction to exist in the next decade and beyond between *Webb* and the future 20–40-m ground-based telescopes, such as the Extremely Large Telescope, Giant Magellan Telescope, and the Thirty Meter Telescope. While *Hubble* and *Webb* are clearly unprecedented in wide-field, faint-object detection and image characterization, the ground-based facilities can provide higher-resolution images of known objects—but over smaller fields of view—as well as spectra at higher resolution. Ground-based and space-based facilities complement each other nearly perfectly. Also, current sub-mm facilities, such as ALMA, and X-ray facilities such as *Chandra* and *XMM*—and including their future X-ray sequels—provide a unique capability of finding weak AGN when light in no other wavelength range can poke though the dense veil of dust.

References

Beckwith, S. V. W., et al. 2006, AJ, 132, 1729
Bouwens, R. J., Illingworth, G. D., Labbe, I., et al. 2011, Nature, 469, 504
Bouwens, R., Illingworth, G. D., Oesch, P., et al. 2012, ApJ, 709, L133
Ellis, R. S., et al. 2013, ApJ, 763, L7
Ferrarese, L. & Ford, H. 2005, Space Sc. Rev. 116, 523
Haring, N, & Rix, H. 2004, ApJ, 604**,** L89
Koekemoer, A. M., et al. 2013, ApJS, in press (arXiv1212.1448K)
Mechtley, M., Windhorst, R. A., Ryan, R. E., et al. 2012, ApJ, 756, L38
Rutkowski, M. J., et al. 2012, ApJS, 199, 4
Schenker, M. A., et al. 2013, ApJ, 768, 196
Windhorst, R. A., Cohen, S. H., Hathi, N. P., et al. 2011, ApJS, 193, 27
Wyithe, J. S. B., et al. 2011, Nature, 469, 181
Yan, H.-J., Windhorst, R. A., Hathi, N. P., et al. 2010, RAA, 10, 867

Webb: The Stiffest Backbone in Space

Blake Bullock, *blake.bullock@ngc.com*

Across the country, teams of highly skilled engineers and technicians are building the backbone of the mighty *James Webb Space Telescope*. This four-story-tall scaffolding, called the backplane, is one of the largest cryogenic structures ever built. While its sheer size and visual complexity are impressive, the backbone's engineering breakthrough is its amazing ability to remain almost perfectly still and rigid under extreme environmental conditions.

Imagine the magnitude of the tasks to design and build a structure to both withstand the violent rocket launch from the humid shores of Kourou, French Guiana, and then not flex more than 38 nanometers—approximately 1/1,000 of the diameter of a human hair—after it arrives at its station at L2, one million miles from Earth, where it will operate at temperatures as low as –400° F.

The role of *Webb*'s backplane is to support the primary mirror—18 hexagonal segments of polished beryllium—and the science instrument module containing the flight cameras and spectrographs. Fully loaded, it will weigh over 7,000 lbs., more than three times the weight of the structure itself.

It takes a team to invent and build unique hardware like the *Webb* backplane, and NASA has called on the diverse talents of many aerospace contractors. Northrop Grumman Aerospace Systems[1] of

Continued page 36

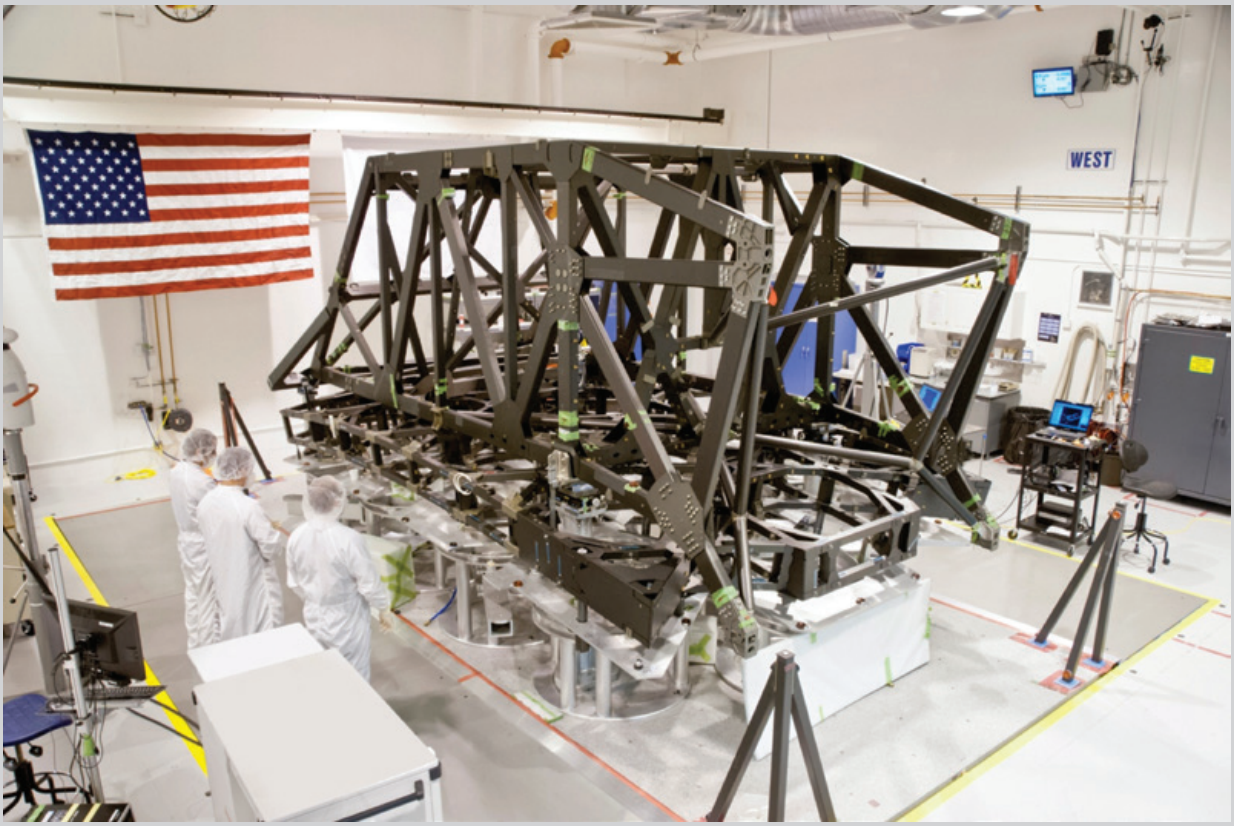

Figure 1: Complete backbone of the *James Webb Space Telescope* (Photo credit: ATK).

Redondo Beach, California, is responsible for the design and development of the entire observatory, including the telescope, the deployable sunshield, and the spacecraft bus. Ball Aerospace[2] of Boulder, Colorado, ATK[3] of Magna, Utah, and ITT Exelis[4] of Rochester, New York, are among the 193 suppliers across the country contributing expertise and facilities to build components and systems for *Webb*.

In June, ATK completed the last piece of the support frame, a critical component at the core of the structure, which brings together *Webb*'s center section, hinged wings, secondary mirror support structure, and the integrated science instrument module. In all, ATK designed, engineered, and constructed more than 10,000 parts for this piece, many from ultra-lightweight graphite. To ensure the stiffness and stability *Webb* requires, every connection point within this structure was manufactured with high precision, down to customized metallic fittings made of special materials, such as Invar and titanium.[5]

In August 2013, ATK shipped the *Webb* backbone structure to NASA's Marshall Space Flight Center in Huntsville, Alabama, for cryogenic thermal testing, which will occur in the x-ray and cryogenic facility.[6] From there, the structure will be shipped to Northrop Grumman for structural static testing, during which a team of engineers and technicians will carefully push, pull, and press on the hardware. Then, the structure will be ready to accept the telescope and instruments for the ultimate cryogenic-vacuum test, in Chamber A at Johnson Space Center, in Houston, Texas.[7]

Notes

[1]**http://www.northropgrumman.com**
[2]**http://www.ballaerospace.com**
[3]**http://www.atk.com**
[4]**http://www.exelisinc.com**
[5]Behind the *Webb*, episode 18, On the wings of Webb **http://webbtelescope.org/webb_telescope/behind_the_webb/episodes/18**
[6]**https://optics.nasa.gov/facilities/xraycal.html** Press release: **http://www.nasa.gov/centers/marshall/news/news/releases/2013/13-099.html#.UjxmfBDAGyb**
[7]**http://www.nasa.gov/centers/johnson/engineering/integrated_environments/altitude_environmental/chamber_A/index.html**

Barbara A. Mikulski Archive for Space Telescopes

Anton Koekemoer, *koekemoer@stsci.edu*, **for the MAST team**

The Barbara A. Mikulski Archive for Space Telescopes (MAST) is one of NASA's premier astronomy data centers, along with the High Energy Astrophysics Science Archive Research Center (HEASARC) and the NASA/IPAC Infrared Science Archive (IRSA). MAST is the primary archive repository for data from several large, active space missions (*Hubble*, *Kepler*, *XMM*-OM and *Swift*-UVOT), as well as legacy data from past missions (*GALEX*, *FUSE*, *IUE*, *EUVE*, and others), planned data from future missions, such as *James Webb Space Telescope*, and all-sky surveys such as the Very Large Array—Faint Images of the Radio Sky at Twenty-centimeters (VLA-FIRST), Guide Star Catalog (GSC) and Digitized Sky Survey (DSS).

MAST supports the scientific research carried out by the astronomical community by facilitating access to its collections, offering expert user support and software for calibration and analysis, and providing value-added scientific data products. These include high-level science products (HLSPs) such as mosaics, catalogs, and spectra delivered to MAST by science teams, as well as enhanced products accessible via the *Hubble* Legacy Archive (HLA). As of September 2013, the total volume of MAST's data holdings was approximately 270 terabytes (TB), with an average of 18 TB of data downloaded per month. Current MAST news and updates are continuously posted on our main archive site (**http://archive.stsci.edu**) and on social media, including Facebook (**https://www.facebook.com/MASTArchive**) and Twitter (**https://twitter.com/MAST_News**).

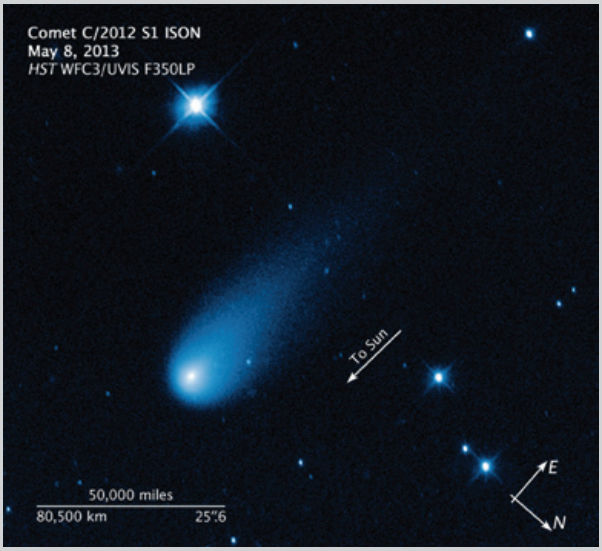

Figure 1: An image of comet ISON taken with *Hubble*, released on May 9, 2013 (provided by the *Hubble* Heritage Team, P.I.: Z. Levay). Eight different programs have observed, or are scheduled to observe, the comet before and after perihelion.

Comet ISON High-Level Science Products Available in MAST

Comet ISON is being intensely studied as it approaches perihelion, or its closest approach to the sun. In anticipation of the potential for unique advances in our understanding of comet physics that will be enabled by this event, a number of *Hubble* proposals have been scheduled to observe the comet both before and after perihelion. The reduced data from these programs are being made available to the community via MAST as high-level science products. The website for the project (**http://archive.stsci.edu/prepds/ison**) provides the program numbers of all the approved *Hubble* proposals and provides further details about the observations, as well as access to the high-level science products as they become available. The first datasets from these projects are now available for interactive display and download, including all the observations that were used to create the *Hubble* Heritage images released on May 9, 2013.

New High-Level Science Products from the Multi-Cycle Treasury Programs

All three Multi-Cycle Treasury (MCT) programs have completed their observations during this cycle and are continuing to release a variety of new HLSPs, bringing the total to over 4 TB of mosaics and other products delivered to the archive by these teams. These can be accessed from the main HLSP page (**http://archive.stsci.edu/hlsp**). As of September 2013, these data have been used in a total of 111 refereed papers published by these teams and by the community (with more currently in press); recent science highlights are summarized here:

The Cosmic Assembly Near-Infrared Deep Extragalactic Legacy Survey (CANDELS; P.I.: S. Faber and H. Ferguson; **http://archive.stsci.edu/prepds/candels**) has successfully completed the entire observing program of 902 orbits (including the supernova component), covering five fields using the Wide Field Camera 3 (WFC3) with the F125W and F160W filters, and the Advanced Camera for Surveys (ACS) with the F606W and F814W filters, together with additional filters in some fields (ACS F435W, F775W, and F850LP, and WFC3 F275W and F105W). Full details are provided in Grogin et al. (2011) and Koekemoer et al. (2011). To date, full-depth combined v1.0 mosaics in WFC3 and ACS have been released for three of the fields (UDS, COSMOS and GOODS-S), while v0.5 mosaics have been released for all data on the EGS field and for 13 out of the total of 14 GOODS-N epochs. The remaining releases are on schedule for delivery over the coming months. The CANDELS team has also now released two full v1.0 photometric multi-wavelength catalogs for the UDS field (35,932 sources; Galametz et al. 2013) and for GOODS-S (34,390 sources; Guo et al. 2013), as well as a catalog of 20,000 sources

Continued page 38

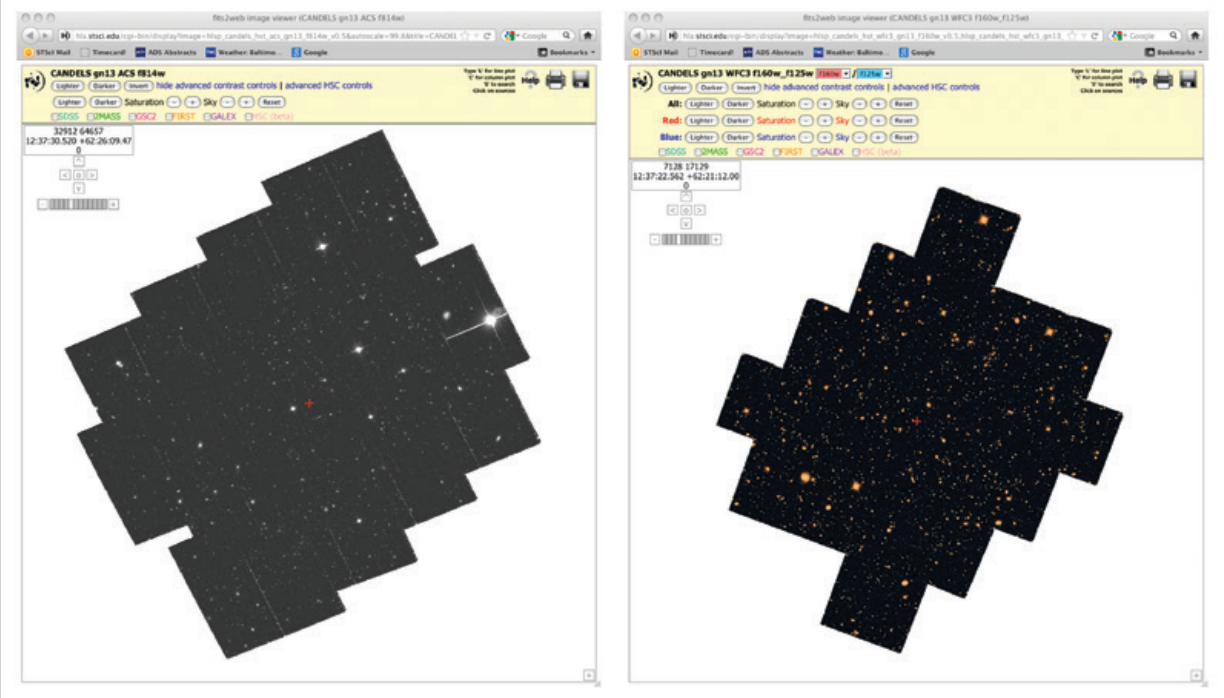

Figure 2: The most recent mosaic delivery by the CANDELS team (P.I.: S. Faber and H. Ferguson; see Grogin et al. 2011 and Koekemoer et al. 2011), showing the epoch 13 mosaics of the GOODS-N field (*left*: ACS F814W; *right*: WFC3 F125W and F160W), using the interactive display browser available via the MAST website.

from GOODS-S that was used to train a total of 11 different photometric redshift codes (Dahlen et al. 2013). As of September 2013, the community had downloaded over 37 TB of the CANDELS survey's high-level science products and mosaics to 1303 distinct IP addresses. Recent science highlights include high-redshift supernovae, galaxy structure and black holes, and galaxy evolution in the early universe.

The Cluster Lensing and Supernova Survey with *Hubble* (CLASH; P.I.: M. Postman; **http://archive.stsci.edu/prepds/clash**; see Postman et al. 2012) has also completed their entire observing program of 25 clusters, for a total of 524 orbits (including the supernova component). The most recent data releases from the team include first-release mosaics, at 65 milliarcsec/pixel, for two new clusters (CLJ1226+3332 and MACSJ1423+24), as well as full photometric catalogs and higher resolution mosaics, at 30 milliarcsec/pixel, for three additional clusters (Abell 1423, MACSJ0429-02, and RXJ2248-4431). Each cluster has been observed with up to 16 *Hubble* filters, including four ultraviolet filters in the ultraviolet-visible channel of the Wide Field Camera 3 (WFC3/UVIS), seven optical filters in Advanced Camera for Surveys (ACS), and five filters in the infrared channel of WFC3 (WFC3/IR).

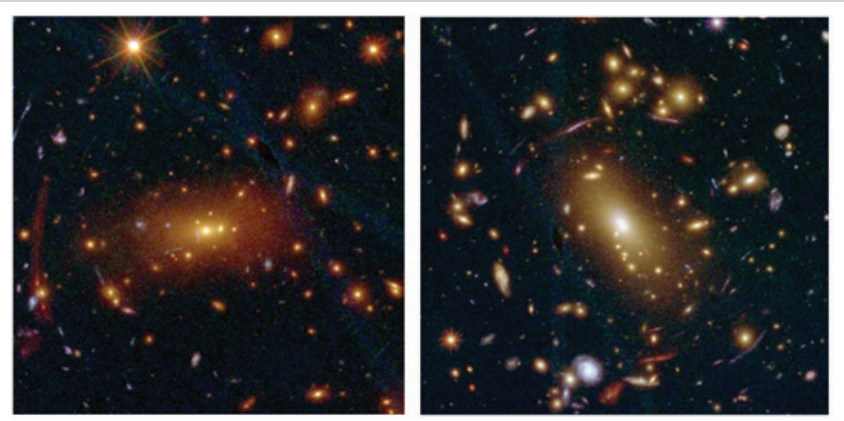

Figure 3: CLASH mosaics (P.I.: M. Postman; see Postman et al. 2012) of the two most recently released clusters, CLJ1226+3332 (*left*), and MACSJ1423+24 (*right*), constructed from the full 16-filter *Hubble* datasets.

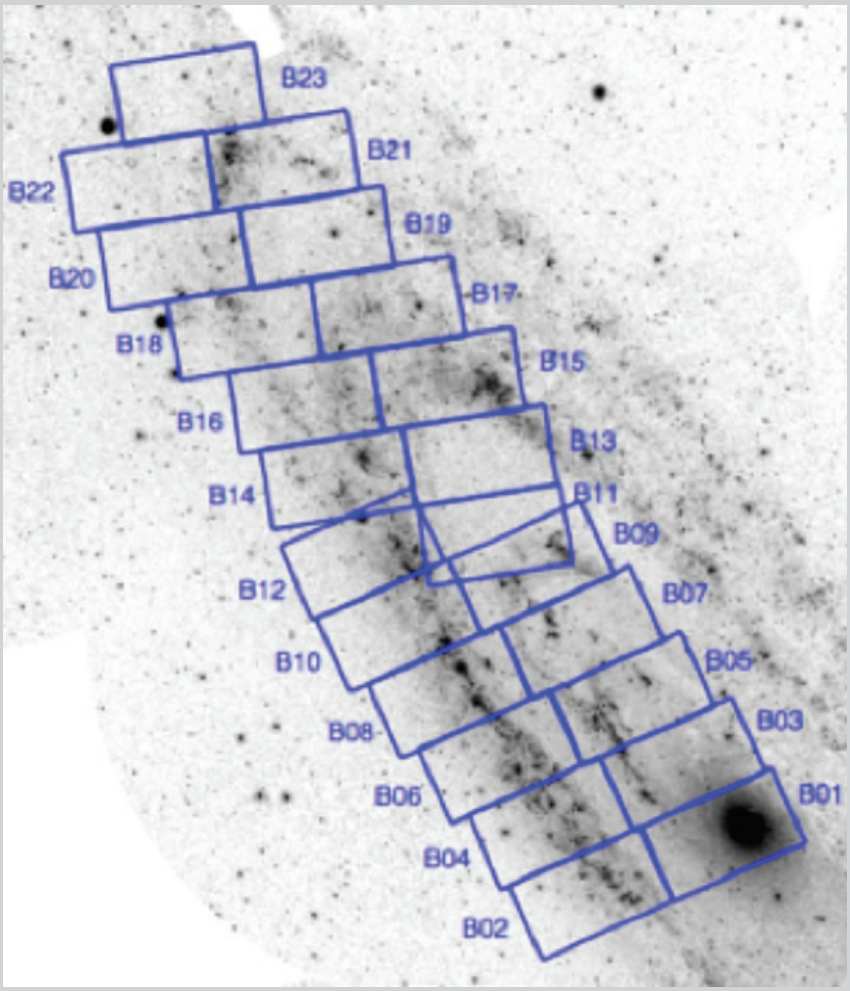

Figure 4: The full layout of the completed PHAT survey over the Andromeda galaxy (M31), showing the relative locations of all 23 "bricks" that were used to tile the north-eastern sector of the galaxy (image graphic provided by the PHAT Team, P.I.: J. Dalcanton; see Dalcanton et al. 2012).

As of September 2013, the community had downloaded over 2.5 TB of the CLASH survey's high-level science products and mosaics to 1061 distinct IP addresses. Recent science results from the survey include distant galaxy candidates at redshifts 9–10, lensed galaxies at redshift 6, and the physical properties of clusters.

The Panchromatic *Hubble* Andromeda Treasury Program (PHAT; P.I.: J. Dalcanton; **http://archive.stsci.edu/prepds/phat**; Dalcanton et al. 2012) has also completed their 834-orbit observing program of 23 "bricks" that tile the Andromeda galaxy in a total of six filters (ultraviolet coverage with WFC3/UVIS F275W and F336W, optical coverage with ACS F475W and F814W, and infra-red coverage with WFC3/IR F110W and F160W). As of September 2013, the community had downloaded over 5 TB of the PHAT survey's mosaics and other products to 522 distinct IP addresses. Recent science highlights include supernova remnant progenitor masses, the dynamics and structure of M31, and the properties of its stellar populations.

Other Recent Releases of High-Level Science Products

The *Hubble* eXtreme Deep Field project (XDF; Illingworth et al. 2013) available from MAST at **http://archive.stsci.edu/prepds/xdf**, delivered mosaics consisting of combined data from all optical and infrared observations obtained by *Hubble* over the original *Hubble* Ultra-Deep Field (HUDF) area, with just a few exceptions (small amounts of data taken with unusual or rarely used filters, and spectroscopic data, are not included). Data used in this project were taken from the original HUDF, UDF09, and UDF12 programs (Beckwith et al. 2006; Bouwens et al. 2011; Ellis et al. 2013; Koekemoer et al. 2013), as well as GOODS (Giavalisco et al. 2004), CANDELS (P.I.: S. Faber and H. Ferguson), supernova follow-up programs (P.I.: A. Riess), and other projects. The observations used include five filters from ACS (F435W, F606W, F775W, F814W and F850LP) and four filters from WFC3 (F105W, F125W, F140W,

Continued page 40

Figure 5: Image showing the XDF dataset (provided by the XDF Team, Illingworth et al. 2013), consisting of combined data from all optical and infrared observations obtained by *Hubble* over the original *Hubble* Ultra-Deep Field (HUDF) area (with just a few exceptions, such as small amounts of data taken with unusual or rarely used filters and spectroscopic data, which are not included). This image shows the full set of five ACS and four WFC3/IR filters, combined from all observations obtained on this area.

Figure 6: WFC3 image of the field around a candidate high-redshift protocluster from the BoRG survey (P.I.: M. Trenti; see Trenti et al. 2012), which could be the most distant such grouping ever observed in the early universe. The protocluster is evident as a collection of red "dropout" galaxies, which are detected only in the reddest filters (F125W and F160W).

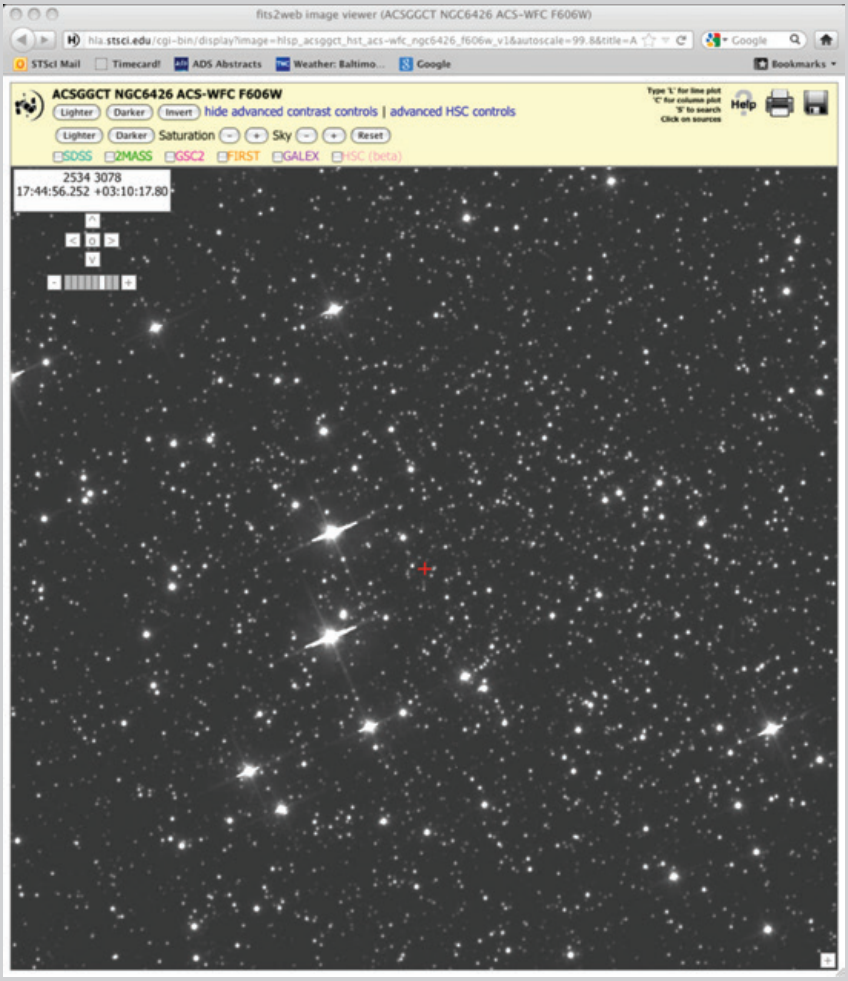

Figure 7: ACS image of the central part of the cluster NGC 6426, displayed using the MAST interactive display browser. This is one of six new clusters added to MAST from the ACS Globular Cluster Survey (P.I.: A. Sarajedini; see Sarajedini et al. 2007).

F160W). Further details are available from the above website listed on page 39, which also presents the full-depth combined mosaic datasets.

The Brightest of Reionizing Galaxies (*BoRG*) *Program* (P.I.: M. Trenti, **http://archive.stsci.edu/prepds/borg**) has recently delivered combined images to MAST for 29 new fields. BoRG is an ongoing Pure-Parallel Program that obtains WFC3 imaging in four filters (F606W, F098M, F125W, F160W) on random sightlines at high Galactic latitudes (above 30 degrees), as well as folding in WFC3 parallel data obtained from other programs, for example those obtained in parallel to the Cosmic Origins Spectrograph (COS) Guaranteed Time Observer (GTO) observations. Scientific results from this program so far include galaxy luminosity functions at redshifts beyond 7, containing a possible protocluster at these redshifts. All the released images are available at the MAST webpage for this project, which also provides access to interactive displays of the datasets.

The ACS Globular Cluster Survey (P.I.: A. Sarajedini; see Sarajedini et al. 2007), a Treasury Program obtaining uniform imaging of 65 of the nearest globular clusters using ACS, has delivered high-level science products to MAST for 6 new clusters from program 11586: IC 4499, NGC 6426, NGC 7006, Palomar 15, Pyxis, and Ruprecht 106. This project aims to observe globular clusters in the F606W and F814W filters, providing a homogeneous dataset extending up to 7 magnitudes fainter than the stellar main-sequence turnoff, and suitable for a broad range of scientific investigations. So far this survey has produced new scientific results on stellar evolution, intermediate-mass black holes, binary stellar systems in globular cluster cores, relative ages of globular clusters, and a wide range of other scientific results. Please visit the project page at MAST (**http://archive.stsci.edu/prepds/acsggct**) to access the mosaics and source catalogs, including interactive displays.

Continued page 42

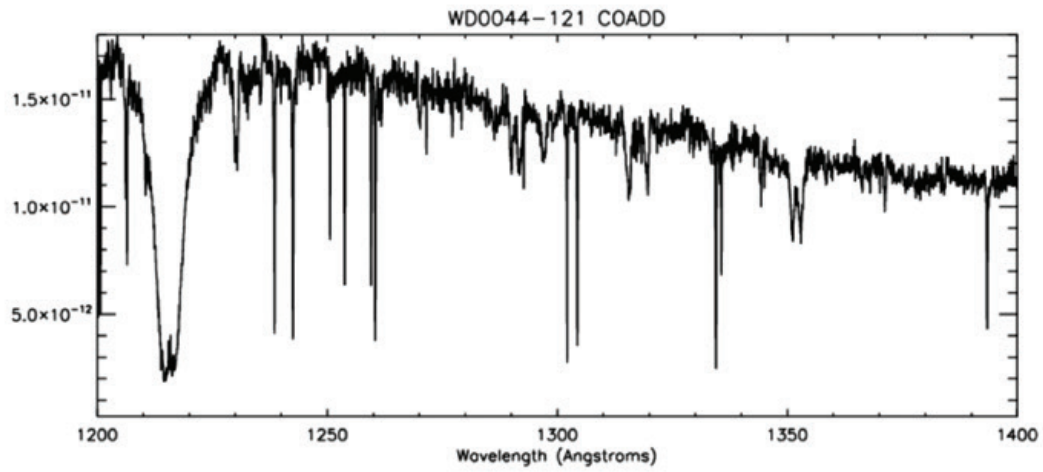

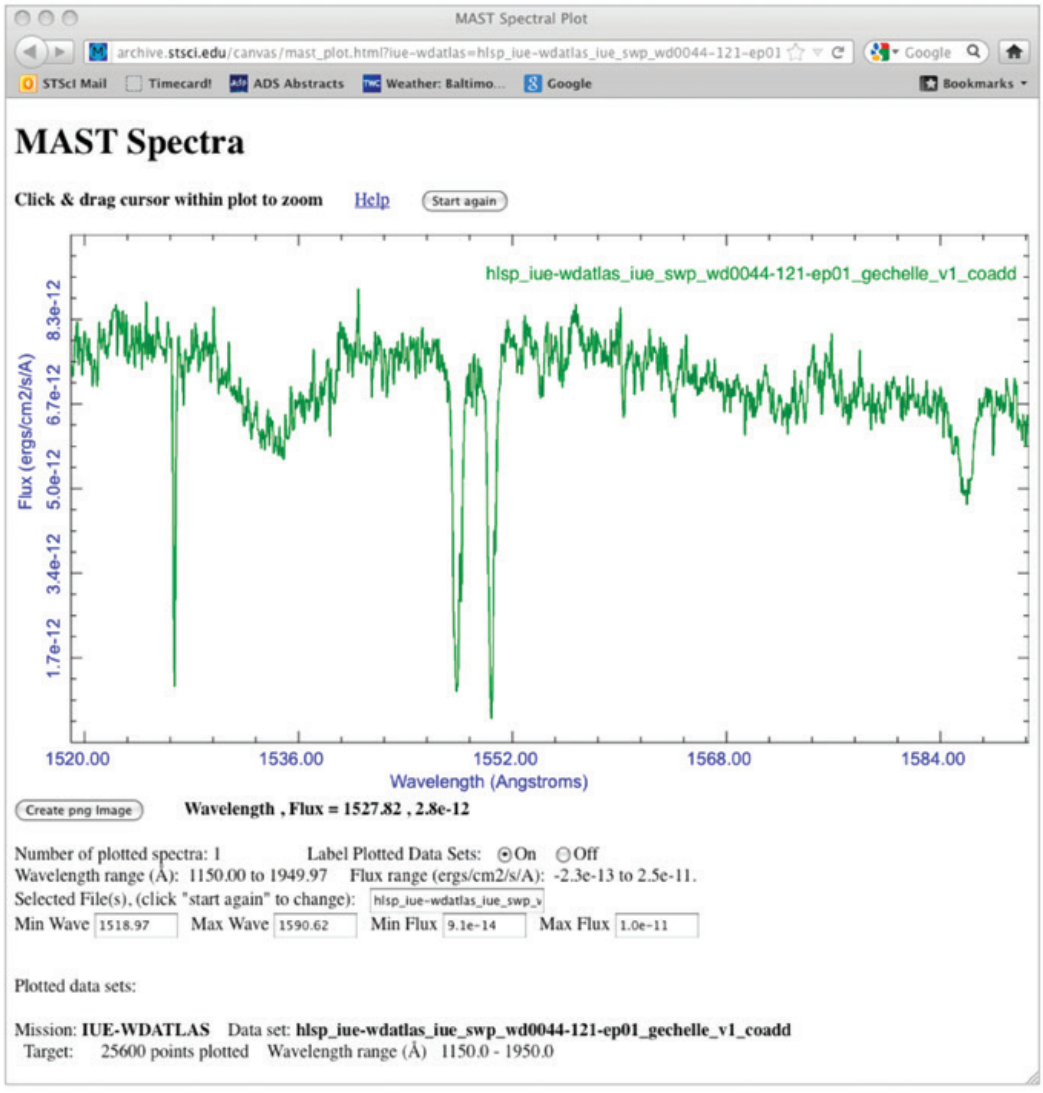

Figure 8: (*Top*) example co-added spectrum of the star WD0044-121, from the Holberg et al. (1998) *IUE* White Dwarf Spectral Atlas. Co-adding each *IUE* spectrum for a target increases the signal-to-noise substantially. (*Bottom*) the spectral plotting tool, which enables the viewer to zoom in on any section of the spectrum. The full-depth, combined FITS files are all available for download as well.

Figure 9: WFC3 image of the new Horsehead Nebula high-level science products available from MAST (provided by the *Hubble* Heritage Team, P.I.: Z. Levay), showing the detailed structure of the nebula revealed by the new WFC3/IR F110W and F160W observations.

The *IUE* White Dwarf Atlas of high-resolution, echelle spectra (created by Holberg et al. 1998) now has a new home at MAST. This project extracted echelle spectral orders in the wavelength range 1150–1950 Angstroms, and further co-added multiple epochs of observations obtained on each star to increase the overall signal-to-noise of the final spectrum (as shown in the example figure). These files have been ingested into the MAST holdings, reformatted to the data format recommended by MAST, and integrated with our HLSP Target Search page. Additional metadata (coordinates, exposure times, etc.) have been included in these FITS files from the original files to further enhance their scientific value. The total atlas consists of 55 white dwarfs, spanning a range of types and effective temperatures. Please visit the project page (**http://archive.stsci.edu/prepds/iue-wdatlas**) for a table of stars within the atlas, which also provides an interactive plotting tool with which to examine the spectra, as well as access to all the new FITS files.

The Horsehead Nebula: to commemorate *Hubble*'s 23rd anniversary, the *Hubble* Heritage Team has observed the famous Horsehead Nebula with the new WFC3 infrared camera. This new view of the Horsehead is strikingly different from the familiar view in visible light, revealing structures hidden by the

Continued page 44

MAST
from page 43

dense dust and gas. This image complements the 2001 *Hubble* Heritage image that had been obtained with the WFPC2 camera. The new WFC3 observations were obtained in October/November 2012 and include 9 tiles in a 3 × 3 mosaic pattern, where a small shift between tiles allows for the removal of detector artifacts (see Proposal 12812, P.I.: Z. Levay for details.) The broad-band F110W and F160W filters highlight unique physical processes occurring in and around the nebula, and they combine to produce a dramatic new color image. The full-depth combined mosaics have all been delivered to the MAST archive as high-level science products, and are available for download from the project webpage (**http://archive.stsci.edu/prepds/heritage/horsehead**), which also offers interactive display capabilities for browsing the image datasets.

Hubble Legacy Archive

The HLA has made available Data Release 7.1, which includes several new data deliveries, as well as a number of user-interface enhancements. Specifically, new mosaics are provided that have been delivered by the CANDELS, CLASH, and PHAT MCT programs, as well as the UD12, XDF and Heritage programs, allowing direct access and browsing capabilities for these datasets. The user interface enhancements include additional options to overlay the *Hubble* Source Catalog (HSC), as well as enabling the image astrometry to be shifted using corrections derived during the construction of the HSC.

The Beta 0.2 version of the HSC is also now available. The primary goal of the HSC is to combine the tens of thousands of individual visit-based, general-purpose source lists from the HLA into a single master catalog, using algorithms described in Budavari and Lubow (2012). The HSC currently contains data from ACS/WFC and WFPC2 SOURCE EXTRACTOR source lists. The primary enhancements for Beta 0.2 are improvements in the matching algorithms, development of an HSC Summary Search form, and access to a version of the HLA interactive display that allows the user to overlay the catalog on HLA images.

For further details, please see the HLA page (**http://hla.stsci.edu**) where updates continue to be posted as they become available.

Kepler Updates

The *Kepler* team has recently released Q15 and Q16 data to the public. In addition, the Q0–Q14 datasets have been reprocessed with an improved light-curve algorithm, and with corrected timestamps. Previously the barycentric times reported in the Flexible Image Transport System (FITS) files were measured in the Coordinated Universal Time (UTC time standard, rather than the intended Barycentric Dynamical Time (TDB) time standard. With this release, the timestamps are now in the correct system for all files except for the target pixel files, which will be updated in the future. For further details and updates, please consult the MAST *Kepler* website (**http://archive.stsci.edu/kepler**).

In addition, MAST has added the second part of the *Kepler*/Isaac Newton Telescope Survey (KIS), extending the KIS coverage to ~97% of the *Kepler* field. In addition to nearly doubling the number of sources, the H-alpha (narrow-band) fluxes have also been included in the *Kepler* Target Search forms. There can be multiple measurements of the same source within the KIS catalog, as discussed in further detail in the original KIS paper (Greiss et al. 2012).

As always, please feel free to contact the MAST help desk (**archive@stsci.edu**) with questions, or contact us through Facebook (MASTArchive) or Twitter (@MAST_News) to provide suggestions on how we can improve our sites and services.

References

Beckwith, S. V. W., et al. 2006, AJ, 132, 1729
Bouwens, R., et al. 2011, ApJ, 737, 90
Budavari, T. & Lubow, S. 2012, ApJ, 761, 188
Dahlen, T., et al. 2013, ApJ, 775, 93
Dalcanton, J., et al. 2012, ApJS, 200, 18
Ellis, R. S., et al. 2013, ApJ, 763, L7
Galametz, A., et al. 2013, ApJS, 206, 10
Giavalisco, M., et al. 2004, ApJ, 600, L93
Greiss, S., et al. 2012, AJ, 144, 24
Grogin, N. A., et al. 2011, ApJS, 197, 35
Guo, Y., et al. 2013, ApJS, 207, 24
Holberg, J. B., Barstow, M. E., & Sion, E. M., 1998, ApJS, 119, 207
Illingworth, G., et al. 2013, ApJS, 209, 6
Koekemoer, A. M., et al. 2011, ApJS, 197, 36
Koekemoer, A. M., et al. 2013, ApJS, 209, 3
Postman, M., et al. 2012, ApJS, 199, 25
Sarajedini, A., et al. 2007, AJ, 133, 1658
Trenti, M., et al. 2012, ApJ, 746, 55

The CANDELS Multi-Cycle Treasury Program

H. Ferguson, *ferguson@stsci.edu*, **& the CANDELS team**

The Cosmic Assembly Near-IR Deep Extragalactic Legacy Survey (CANDELS) is one of three Multi-Cycle Treasury (MCT) programs approved in 2010. The 900-orbits' worth of observations finished in August 2013. The observations were designed to document the first third of galactic evolution from $z = 8$ to 1.5 (lookback times of 13 to 9 billion years ago) via deep imaging of more than 250,000 galaxies with the Wide Field Camera 3 infrared channel (WFC3/IR) and the Advanced Camera for Surveys (ACS). Together with the CLASH cluster observations, another aim has been to find and characterize Type Ia supernovae (SNe Ia) beyond $z > 1.5$, and to establish their accuracy as standard candles for cosmology. The survey targets five premier multi-wavelength sky regions; each has multiwavelength data from *Spitzer* and other facilities, and has extensive spectroscopy of the brighter galaxies. The use of five widely separated fields mitigates cosmic variance and yields statistically robust and complete samples of galaxies down to 10^9 solar masses out to redshift $z \sim 8$. The data are immediately public, and high-level science products have been appearing regularly in the Mikulski Archive for Space Telescopes (MAST). Further information on the observations and data reduction can be found in the *Institute Newsletter* (Vol. 28, Issue 1; **https://blogs.stsci.edu/newsletter/2011/02/08/candels/**) and on the CANDELS website, **http://candels.ucolick.org**, as well as in two overview papers (Grogin et al. 2011 and Koekemoer et al. 2011).

Even while the data have been pouring in, both the CANDELS team and the wider community have been busy trying to make progress on some of the science goals with only a portion of the data. By

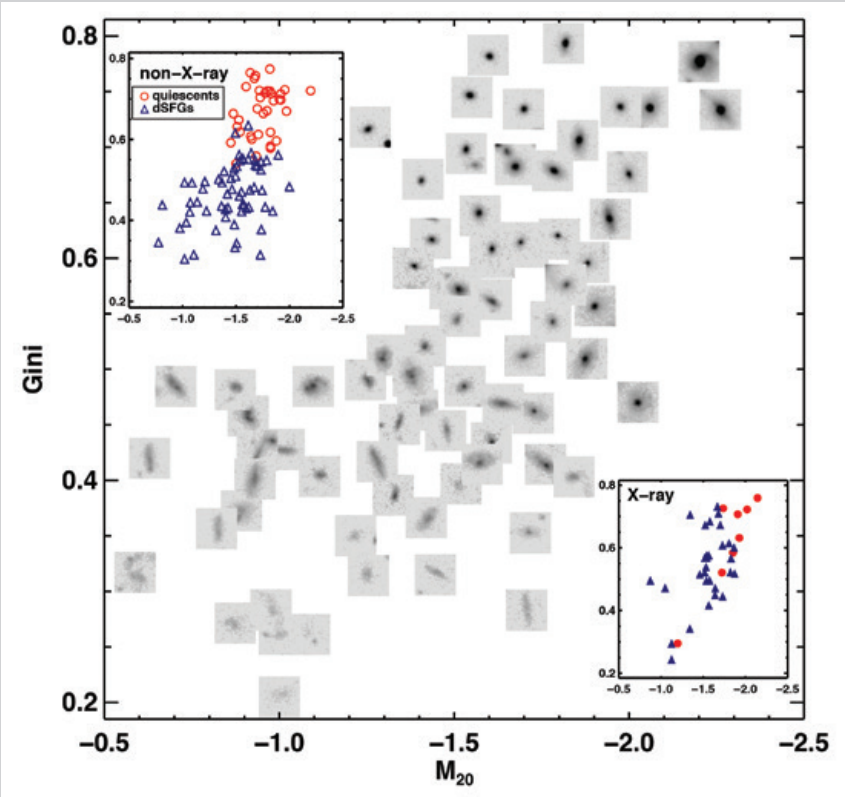

Figure 1: The morphology of extremely red galaxies at $z \sim 2$ from Wang et al. (2012). Objects are selected on the basis of the ratio of their *Spitzer* 3.6 micron fluxes relative to their *Hubble* 0.9 micron fluxes, and then separated into star forming (*blue triangles*) and quiescent (*red circles*) based on their 24-to-3.6 micron flux ratio. The passive galaxies have different visual morphologies, and differ as well in their central concentration (M_{20}) and their relative distribution of pixel flux values (Gini), as can be seen clearly in the upper-left inset. This segregation is less true for X-ray-selected AGN shown in the lower-right inset. The images are from the WFC3 with the F160W filter.

Continued page 46

CANDELS
from page 45

the end of June 2013, the team published 28 papers and submitted 11 others. While harder to identify, there are roughly 20 papers using CANDELS data from outside the team, either published or available as preprints.

We focus here on a few of the science highlights, typically from about a third of the full survey data.

Galaxies and AGN Hosts at Cosmic High Noon

The CANDELS survey provides high-resolution data in the rest-frame optical for galaxies at $z \sim 2$, when cosmic star formation and active galactic nuclei were at their peak. A solid—but perhaps not particularly surprising—result comes from studies of the relation between star-formation activity and galaxy morphology: passive galaxies at $z \sim 2$ already look like spheroids, by and large. This result is seen clearly using different sample selection and different kinds of morphological analysis in CANDELS papers by Wuyts et al. (2011), Wang et al. (2012), Bell et al. (2012), Lee et al. (2013) and others. Perhaps the most visually striking illustration of this is in Figure 1, from Wang et al., which looks specifically at extremely red objects selected on the basis of the ratio of their *Spitzer* 3.6 micron fluxes relative to their *Hubble* 0.9 micron fluxes, and then separates these red galaxies into star forming and quiescent based on their 24-to-3.6 micron flux ratio. The inset at the upper left shows that the quiescent galaxies generally lie in the spheroid portion of the Gini-M_{20} diagram (Lotz et al. 2004). Indeed, the morphology of galaxies appears to be the best predictor of whether or not they are passive. It is a better predictor than stellar mass, for example (Bell et al. 2012). In addition to being spheroidal in shape, passive galaxies at $z \sim 2$ are generally quite small: their half-light radii are much smaller than spheroids of the same mass today, and they are smaller than star-forming galaxies of the same stellar mass at the same epoch. Ongoing work from CANDELS is providing better constraints on the size evolution of such galaxies (e.g., Cassata et al. 2011, 2013) and attempting to identify the compact star-forming progenitors of these "red nuggets" (Barro et al. 2013; Williams et al. submitted). Barro et al. identify blue nuggets that have roughly the required stellar surface densities to become red nuggets if star formation is shut off. Comparing number densities of blue and red nuggets in the redshift range $1 < z < 3$, it appears possible to match the evolution in the number density of red nuggets if the transition timescale from blue to red is about 1 Gyr and the population of blue nuggets is replenished. This suggests a fast track for creation of early, compact spheroids, followed by slower mechanisms to produce the larger spheroids (and grow the compact ones) at later epochs, as illustrated schematically in Figure 2.

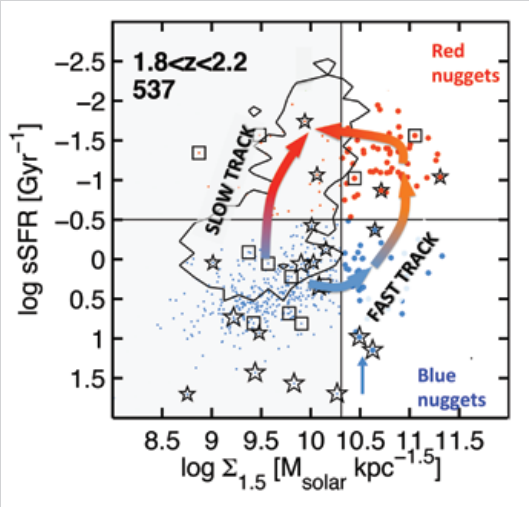

Figure 2: Schematic illustration from Barro et al. (2013) of the evolution from compact star-forming galaxies—aka "blue nuggets"—to compact quiescent galaxies (red nuggets), neither of which are common in the nearby universe. Galaxies in the lower left corner of the diagram are star-forming, but have stellar surface-mass densities that are too low to be the direct progenitors of the red nuggets. Some mechanism (presumably either mergers or internal dynamical instabilities) drives gas to the center and creates enough stars in the central regions to move the galaxy into the blue-nugget region on the lower right. The star formation then shuts off on a timescale of about ~1 Gyr, forming the compact red nuggets in the upper right portion of the diagram. Later those grow in size (but not much in stellar mass) via minor, mostly gas-poor mergers. At the same time, larger star-forming galaxies in the lower left portion can also populate the normal quiescent galaxy sequence as they cease forming stars. The data points in the diagram are estimates of stellar surface-mass densities and specific star-formation rates from CANDELS data. The points labeled with stars and squares are X-ray-detected AGN.

A popular paradigm for explaining the transition from star-forming to quiescent galaxies has been to invoke mergers and feedback from AGN. The merging process drives gas to the center of the galaxy, fueling star formation and the AGN. This can help to explain the tight correlation between the stellar mass in galaxy bulges and the mass of central black holes observed locally. Because the merger triggers the AGN activity, we might expect the host galaxies of AGN to look disturbed, or at least not to have re-grown their disks. CANDELS observations of AGN hosts at $z \sim 2$ do not confirm this expectation. Using visual morphology classifications from the CANDELS team compared the hosts of X-ray-selected AGN at $z \sim 2$ to a mass-matched sample at the same redshifts (Kocevski et al. 2011). There was no indication that the AGN hosts were more disturbed than non-AGN galaxies of the same stellar mass, and about 50% of the AGN hosts had a disk component. The sample does not include the most luminous AGN, so perhaps the merger scenario works for them, but that remains to be seen.

Galaxies near Cosmic Dawn

Another theme of CANDELS has been to study galaxies close to the epoch of re-ionization, at $z > 6$. Compared to the *Hubble* Ultra-Deep Fields (HUDFs), CANDELS offers additional volume to constrain the shape of the bright end of the luminosity function (LF), as well as deep multiwavelength data to help constrain stellar populations and AGN fractions. Indeed, the CANDELS data have already been used by a variety of groups to explore galaxy evolution at these high redshifts (e.g., Yan et al.

2012; Finkelstein et al. 2012; Oesch et al. 2013; Bouwens et al. 2013; Schenker et al. 2013; McLure et al. 2013). Galaxies are identified via their Lyman break, which for these redshifts occurs at ~1216 Å in the rest frame. Shorter-wavelength photons are scattered out of the line of sight by intervening hydrogen in the intergalactic medium. Different investigators use slightly different criteria for selecting high-z candidates, but generally derive similar number densities per unit redshift when they account for their selection biases. There is some disagreement at the bright end of the luminosity function, at $z \sim 7$–8, with Yan et al. (2012) finding a few more bright candidates than expected from the extrapolation of the evolution trend seen in the best-fit luminosity functions at lower redshift from the Bouwens group. Such disagreements should be easy to resolve as further data from CANDELS and the WFC3 parallel programs are incorporated. In spite of such discrepancies, the consensus is that the faint-end slope is very steep, and that it is therefore likely that dwarf galaxies are responsible for re-ionization, provided the ultraviolet (UV) photons can escape.

There has also been a lot of interest in investigating the evolution of the UV spectral-slopes of high-redshift galaxies, spurred by the tantalizing report of very steep slopes from the early HUDF analysis (Bouwens et al. 2010). More recent analysis suggests that the bluest galaxies are not significantly bluer than local metal-poor galaxies like NGC 1705, and hence do not require metal-free stars (Fig. 3). Nevertheless, there is systematic evolutionary trend at fixed UV luminosity such that higher-redshift objects have bluer rest-frame colors. The evidence also tends to favor a mild slope-luminosity relation in the sense that lower-luminosity galaxies are bluer than higher-luminosity ones, but this needs to be confirmed with more data. Both trends are in this sense expected if galaxies are increasing in metallicity and dust content with both mass and redshift. If the red colors are indeed due to dust, then the fact that luminous star-forming galaxies at $z \sim 8$ have some dust suggests that supernovae and not just Asymptotic Giant Branch (AGB) stars are responsible, because not enough time would have elapsed for the AGB stars to appear.

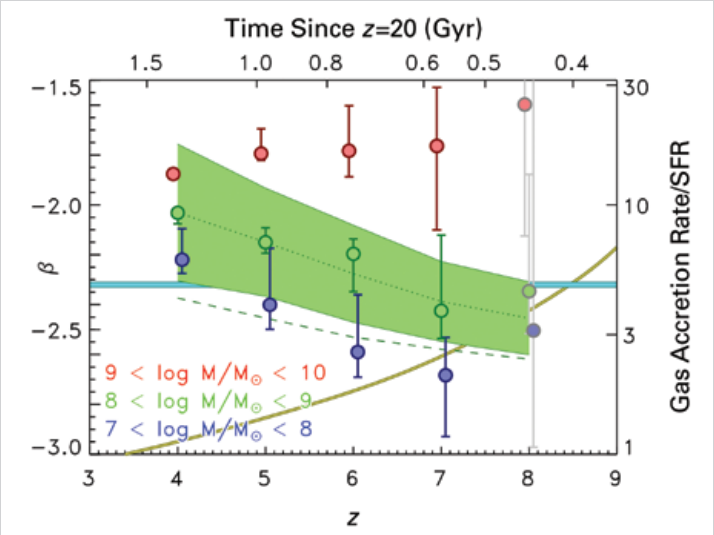

Figure 3: The evolution of the rest-frame UV spectra slopes of star-forming galaxies at very high redshift, from Finkelstein et al. 2012. The spectral slope β measures the steepness of the spectral-energy distribution $f_\lambda \propto \lambda^\beta$ at a rest wavelength $\lambda \sim 1500$ Å (more negative numbers are bluer). The points show medians for galaxies in various bins of redshift and stellar mass. The cyan bar shows the spectral slope of NGC 1705, one of the bluest galaxies in the local universe. The green-shaded region highlights the slopes expected from the models of Finlator et al. 2011 for the middle mass range. The yellow curve shows the relation, and the right-hand axis shows the relation between the star-formation rate and the gas accretion rate from Papovich 2011. Galaxies at these redshifts are accreting gas at rates higher than their star-formation rates, which may hinder the escape of ionizing photons.

Supernovae

Both the CANDELS and the CLASH MCT programs have scheduled their observations to facilitate finding high-redshift supernovae. SNe Ia are the best known standard candles for measuring cosmological distances. Together, the programs have identified more than 100 high-redshift supernovae of all types, with a handful at $z > 1.5$. At these high redshifts, dark energy should have a negligible influence on the distance-luminosity relation. On the other hand, the progenitor of a typical SN Ia at $z > 1.5$ will be considerably more massive and probably less metal-rich than a typical SN Ia progenitor today. Therefore, any departures from the matter-dominated distance-luminosity relation are more likely to be due to supernova evolution than dark energy. Observations of supernovae at these high redshifts will provide a strong lever arm for constraining the evolution of the luminosity and luminosity-light-curve-shape relation for SNe Ia. Followup observations of high-z candidates have been aimed at getting host-galaxy redshifts, supernova light curves, and supernova spectra where feasible.

The observations will also constrain the progenitor models for SNe Ia by constraining the relation between the star-formation rate and the SN Ia rate, both within a given cosmological volume, and for supernova hosts compared to control samples at the same redshift. So far, the rate of discovery of SNe Ia at $z > 1.5$ has fallen roughly at the low end of the range predicted. Detailed analysis is under way to determine the implications for SNe delay times.

As expected, the supernova searches have produced new record-holders for the highest-redshift supernova. This started with the first observation from CANDELS, which was a test frame to validate the dithering strategy, taken on the HUDF. There was about a 1-in-50 chance of having a supernova appear in that frame, but that is exactly what happened. This supernova, dubbed "primo" by the team, has a spectroscopic redshift of 1.55 and became the highest-redshift spectroscopically confirmed SN Ia (Rodney et al. 2012). This has since been superseded by two supernovae, one of which (dubbed "Wilson") at $z = 1.91$, is shown in Figure 4. SN Wilson was initially confusing, because the colors did not

Continued page 48

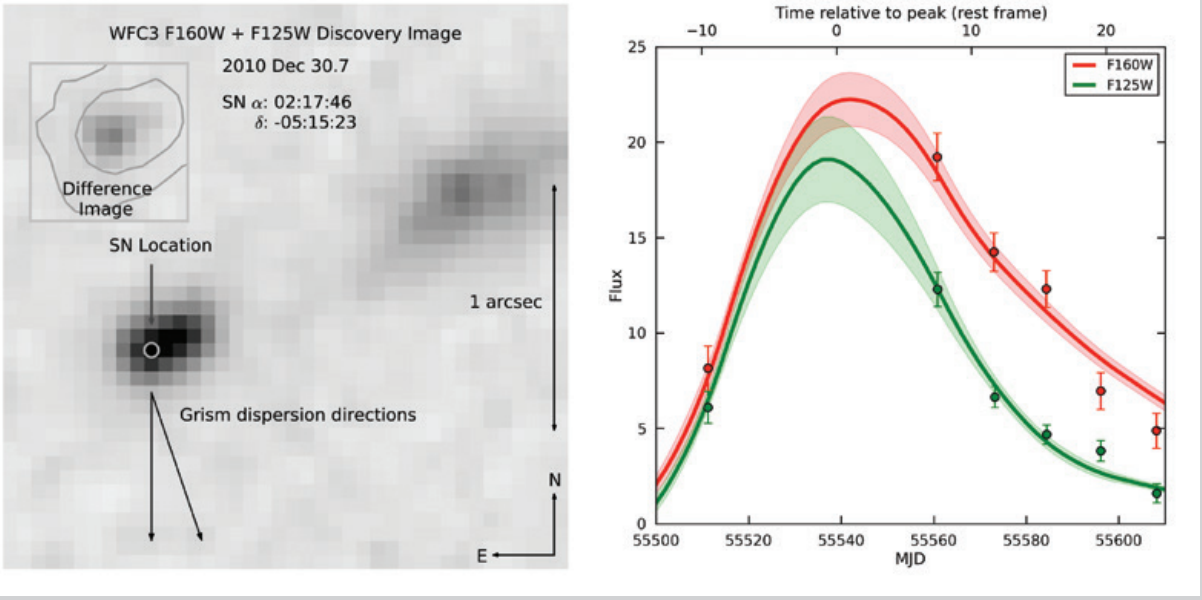

Figure 4: Supernova UDS10Wil (Wilson) from Jones et al. 2013. On the *left* is the discovery image. The main panel shows the host galaxy and its surroundings. The inset shows the difference image. On the *right* is the light curve in the F160W and F125W bands, overlayed with an SN Ia template. The shaded regions show the light-curve shapes that are consistent with typical local SN Ia.

match what was expected for a very young SN Ia of its apparent brightness. It gradually became clear that this was because the supernova was actually there in the first epoch—it having been caught very early on the rise. Of course, it was hard to confirm this without waiting until the supernova faded away more than 100 days later. We also obtained a spectrum with the WFC3 grism, but the signal-to-noise ratio of the spectrum is lower than expected because the supernova was older than we thought it was at the time the grism observations were scheduled. Thus, while the spectrum is consistent with an SN Ia at $z = 1.9$, it cannot strongly rule out other supernova types. Nevertheless, this is a very good candidate, because there is a good host redshift and two-band light curve that matches the shape expected for an SN Ia.

Other News

In addition to the science highlights above, it is worth noting a few developments that are of interest to community users of the CANDELS data. The first multi-wavelength catalogs are now available via the Mikulski Archive for Space Telescopes (**http://archive.stsci.edu/prepds/candels/**) or the Astrophysical Journal (ApJ). The cataloging team used galaxy-template fitting to deal with the crowding issues in *Spitzer* and deep ground-based data, and hence the catalogs are significantly deeper and more reliable than position-matched catalogs. The catalogs are extensively documented in papers by Galametz et al. 2013 and Guo et al. 2013. These catalogs provide the data for computing photometric redshifts and physical quantities such as stellar masses and star-formation rates. Within the CANDELS team, roughly a dozen independent estimates of photometric redshift and stellar mass were computed. Dahlen et al. 2013 describe the results of extensive comparison between the different photometric-redshift estimates, resulting in a procedure for combining different estimates that appears likely to produce smaller scatter and better estimates of the uncertainties. Similar comparisons for stellar masses are in progress. Structural parameters measured via GALFIT are available from van der Wel et al. 2013. Visual classifications have been carried out by CANDELS team members and by thousands of volunteers through Galaxy Zoo. Catalogs of those classifications are in the works.

CANDELS included a set of UV observations obtained only in the Great Observatories Origins Deep Survey–North field. These observations have not achieved nearly the desired sensitivity. Our initial strategy was to bin the WFC3 UV–visible data on 2 × 2 chip to reduce the readout noise. However, after the program had started it became clear that the impact of charge-transfer inefficiency (CTI) would be worse than the impact of read noise. Fortunately, the WFC3 team developed a technique for post flashing the detector (**https://blogs.stsci.edu/newsletter/2013/04/05/notes-from-the-wfc3-team/**). Filling the potential wells on the charge-coupled device (CCD) with just ~12 electrons significantly mitigates the CTI losses for low-background observations. Because the post flash adds background noise, the advantages of binning are negligible. We thus changed strategies to incorporate post flash and stop

binning. However the data reduction has proved challenging. Our goal at the moment is to focus on the post-flashed data for producing science-quality products. The resulting noise levels in the images will be a factor of ~2 worse than anticipated at the outset of the project.

Finally, as an outreach effort, the CANDELS team has been maintaining a research blog at **www.candels-collaboration.blogspot.com**. By the end of June 2013, there were 109 blog posts averaging just under 100 page-views per day. From the team's perspective, it has been a useful exercise to try to provide a summary of the work that is accessible and interesting both to our colleagues in astronomy and to non-astronomers. We hope it has been interesting and entertaining to its audience.

References

Barro, G., Faber, S. M., Pérez-González, Pablo G., et al. 2013, *CANDELS: The Progenitors of Compact Quiescent Galaxies at z ~ 2,* ApJ, 765, 104

Bell, E. F., van der Wel, A., Papovich, C., et al. 2012, *What Turns Galaxies Off? The Different Morphologies of Star-forming and Quiescent Galaxies since z ~ 2 from CANDELS*, ApJ, 753,167

Bouwens, R. J., Illingworth, G. D., Oesch, P. A., et al. 2013, *UV-Continuum Slopes of >4000 z ~ 4–8 Galaxies from the HUDF/XDF, HUDF09, ERS, CANDELS-South, and CANDELS-North Fields,* ApJ, submitted

Bruce, V. A., Dunlop, J. S., Cirasuolo, M., et al. 2012, *The morphologies of massive galaxies at 1 < z < 3 in the CANDELS-UDS field: compact bulges, and the rise and fall of massive discs,* MNRAS, 427, 1666

Cassata, P., Giavalisco, M., Guo, Y., et al. 2011, *The Relative Abundance of Compact and Normal Massive Early-type Galaxies and Its Evolution from Redshift z ~ 2 to the Present,* ApJ, 743, 96

Cassata, P., Giavalisco, M., Williams, C. C., et al. 2013, *Constraining the Assembly of Normal and Compact Passively Evolving Galaxies from Redshift z = 3 to the Present with CANDELS,* ApJ in press

Dahlen, T., Mobasher, B., Faber, S. M., et al. 2013, *A Critical Assessment of Photometric Redshift Methods: A CANDELS Investigation*, ApJ, submitted

Finkelstein, S. L., Papovich, C., Salmon, B., et al. 2012, *CANDELS: The Evolution of Galaxy Rest-frame Ultraviolet Colors from z = 8 to 4*, ApJ, 756,164

Grogin, N. A., Kocevski, D. D., Faber, S. M, et al. 2011, *CANDELS: The Cosmic Assembly Near-infrared Deep Extragalactic Legacy Survey*, ApJS, 197, 35

Jones, D. O., Rodney, S. A., Riess, A. G., et al. 2013, *The Discovery of the Most Distant Known Type Ia Supernova at Redshift 1.914*, ApJ, 768, 166

Koekemoer, A. M., Faber, S. M., Ferguson, H. C., et al. 2011, *CANDELS: The Cosmic Assembly Near-infrared Deep Extragalactic Legacy Survey,The Hubble Space Telescope Observations, Imaging Data Products, and Mosaics*, ApJS, 197, 36

Lee, B., Giavalisco, M., Williams, C. C., et al. 2013, *CANDELS: The Correlation between Galaxy Morphology and Star Formation Activity at z ~ 2,* ApJ, 774, 47

McLure, R., et al. 2013, *A new multifield determination of the galaxy luminosity function at z = 7–9 incorporating the 2012 Hubble Ultra-Deep Field imaging*, MNRAS, 432, 2696.

Oesch, P. A., Bouwens, R. J., Illingworth, G. D., et al. 2013, *Probing the Dawn of Galaxies at z ~ 9–12: New Constraints from HUDF12/XDF and CANDELS Data,* ApJ, 773, 750

Rodney, S. A., Riess, A. G., Dahlen, T., et al. 2012, *A Type Ia Supernova at Redshift 1.55 in Hubble Space Telescope Infrared Observations from CANDELS*, ApJ, 746, 5

Schenker, M. A., et al. 2013, *The UV Luminosity Function of Star-forming Galaxies via Dropout Selection at Redshifts z ~ 7 and 8 from the 2012 Ultra Deep Field Campaign*, ApJ, 768, 196

Wang, T., Huang, J.-S., Faber, S. M., et al. 2012, *CANDELS: Correlations of Spectral Energy Distributions and Morphologies with Star formation Status for Massive Galaxies at z ~ 2*, ApJ, 752, 134

van der Wel, A., Bell, E. F., Haussler, B., et al. 2012, *Structural Parameters of Galaxies in CANDELS,* ApJS, 203, 24

Williams, C. C., Giavalisco, M., Cassata, P., et al. 2013, *The progenitors of the compact early-type galaxies at high-redshift,* ApJ, submitted

Wuyts, S., Forster-Schreiber, N. M., van der Wel, A., et al. 2011, *Galaxy Structure and Mode of Star Formation in the SFR-Mass Plane from z ~ 2.5 to z ~ 0.1,* ApJ, 742, 96

Yan, H., Finkelstein, S. L., Huang, K.-H., et al. 2012, *Luminous and High Stellar Mass Candidate Galaxies at z ~ 8 Discovered in the Cosmic Assembly Near-infrared Deep Extragalactic Legacy Survey*, ApJ, 761, 177

Cluster Lensing And Supernovae Survey with *Hubble* (CLASH)

Marc Postman, *postman@stsci.edu*

The composition of our universe is most intriguing. It is "dark," with 23% of the mass-energy density made up of weakly interacting (and as-yet-undetected) non-baryonic particles (a.k.a. dark matter, DM), and 73% due to the as-yet-unknown physics that accelerates the expansion of the universe (a.k.a. dark energy). To shed new light on these mysteries, we coupled *Hubble*'s panchromatic imaging capabilities—the Wide Field Camera 3 (WFC3) and Advanced Camera for Surveys (ACS)—with the gravitational-lensing power of 25 massive galaxy clusters to test models of the formation of cosmic structure and to probe the high-redshift universe with unprecedented precision. Our 524-orbit Multi-Cycle Treasury (MCT) program, dubbed CLASH (Postman et al. 2012), successfully completed all its observations in July 2013.

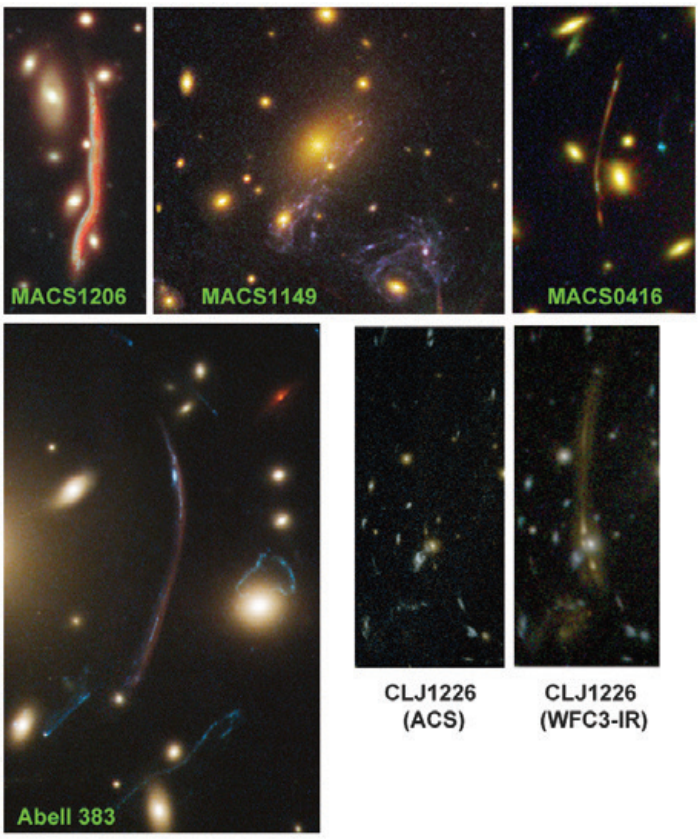

Figure 1: A montage of some of the strongly lensed galaxies lying behind 5 of the 25 clusters observed in the CLASH Multi-Cycle Treasury program. All of these background galaxies are at redshifts greater than 1. As seen particularly in the panels in the *lower right*, the IR channel of WFC3 is an extremely powerful tool for detecting distant lensed galaxies.

The four primary science objectives of the CLASH program are to (1) map the distribution and characterize the nature of dark matter in galaxy clusters; (2) detect type Ia supernovae (SNe Ia) out to redshift $z \sim 2$, to constrain the dark energy equation of state, measure the rate at which they occur, and constrain how their light curves may evolve with time (important for understanding whether SNe Ia are equally good standard candles over a wide range in redshift); (3) detect and characterize the most distant galaxies, focusing especially on the epoch when the universe was less than 800 million years old; and (4) characterize the internal structure and evolution of galaxies in and behind the CLASH clusters.

The mass profiles and central concentrations in CLASH clusters

Gravitational lensing enables precise maps of the distribution of mass in lenses, which are galaxy clusters in the case of CLASH. Lensing also enables high-resolution studies of background galaxies, which are sometimes referred to as arcs due to their curved appearance when they are magnified. The two main limitations on the accuracy of the derived mass distributions are the number of sources identifiable as having multiple images and the number of such sources with reliable redshifts. With deep *Hubble* imaging in 16 broadband filters, ranging from the ultraviolet (UV; 0.225 microns) to the near infrared (NIR; 1.6 micron), CLASH was designed to increase both numbers.

Prior to CLASH, *Hubble* observations demonstrated that many strongly lensed galaxies are fainter than 25.5 AB magnitude, which puts them beyond the reach of spectrographs on ground-based telescopes. CLASH's 16-band photometry provides both deep imaging—the 5σ point-source limit is ~27 AB mag—and accurate photometric redshifts, with errors ~$0.03\ (1 + z)$ for many arcs (see Jouvel et al. 2013).

Figure 1 shows a montage of images centered on some of the more prominent arcs seen in CLASH clusters. Figure 2 shows a CLASH cluster with 47 multiply lensed arcs from 12 unique sources, which span the range $1.1 \leq z \leq 5.8$. Prior to CLASH, only 3 multiply lensed sources were known in this cluster, all from a single background galaxy at $z = 1.03$.

To map the dark-matter distribution in a cluster, we combine weak-lensing data, primarily from multi-band images taken with the Subaru Prime Focus Camera (Suprime Cam), with strong-lensing data from *Hubble*. Weak lensing is measured mostly at large radii from the cluster, where the distortions of

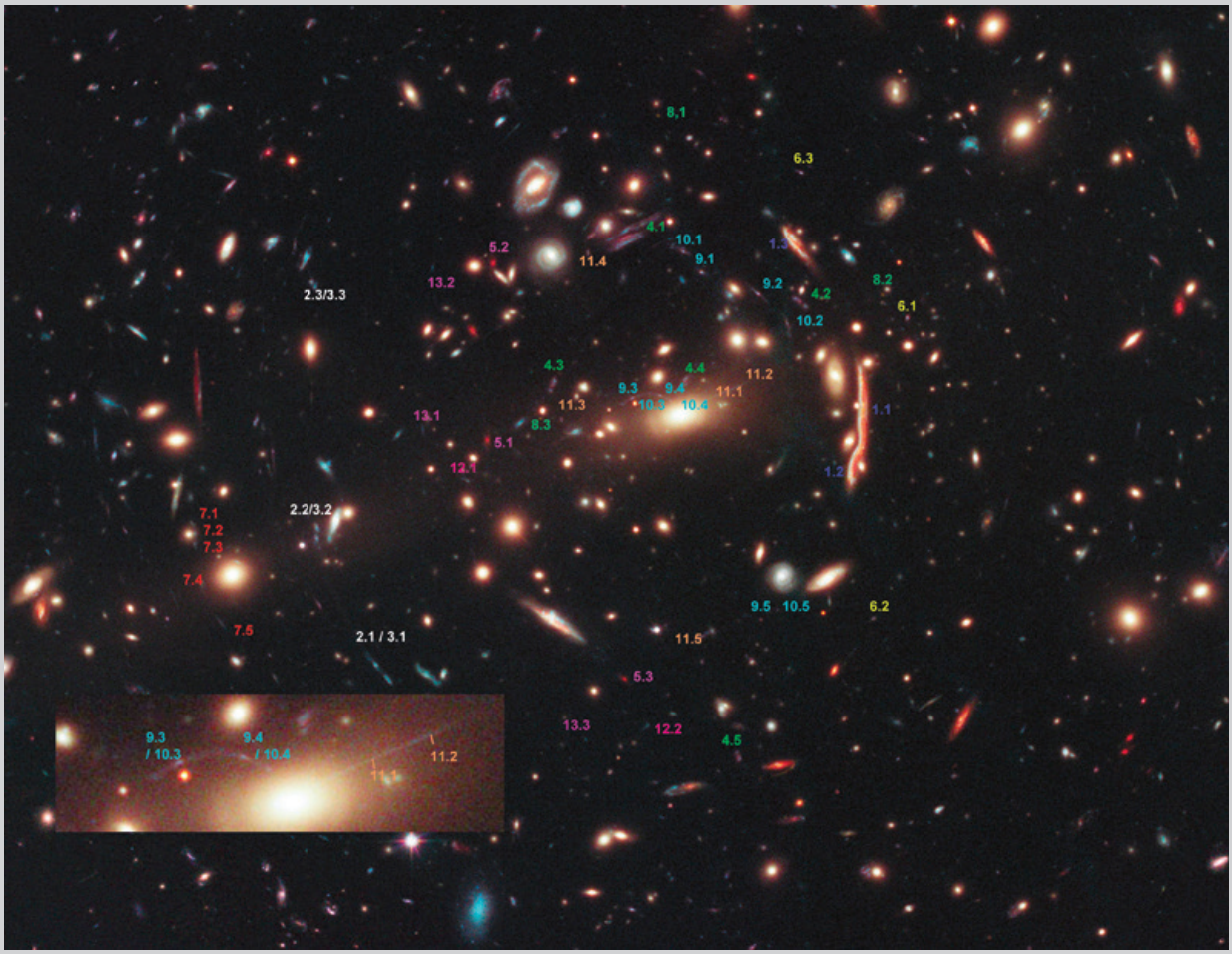

Figure 2: CLASH image of the galaxy cluster MACS J1206.2-0848 ($z = 0.440$). The 47 multiply imaged background sources (all but three of which are newly discovered in CLASH) are identified with color-coded ID numbers. See Zitrin et al. 2012a for full details.

the shapes of background galaxies are detected statistically. In this regime—Suprime Cam covers a region around a cluster at least 5 Mpc across—the galaxies are not multiply lensed but only slightly distorted. The combined information from Subprime Cam and *Hubble* allows us to generate a complete, two-dimensional picture of each galaxy cluster.

One of the predictions of the cold-dark-matter (CDM) model of structure formation is that there is a relationship between the compactness (or concentration) of the cluster's central distribution of matter and the virial mass of a cluster-scale dark matter halo. A halo is the overdense region containing the dark matter that, in this case, generates the cluster's gravitational potential well. Prior to CLASH, several studies found that clusters were significantly over-concentrated, in some cases by factors of 2 or more when compared to the predictions of numerical simulations. These findings caused tension between the observations and the theory. Nevertheless, it was not clear if this tension indicated problems with CDM theory or a selection bias in the data, because the best-studied clusters were often known to be the strongest lenses, and such systems may have systematically higher central-mass concentrations. In CLASH, 20 out of the 25 clusters were selected by their X-ray properties rather than their lensing characteristics. Specifically, the X-ray selected clusters display relatively smooth spherical distributions of hot gas. By choosing potentially relaxed systems at late stages of structural evolution, our sample for testing the CDM paradigm was far less biased.

Figures 3 and 4 show the preliminary relation between mass and concentration for 12 of 20 CLASH clusters selected by X-ray. The relation agrees with the expectations from CDM-based numerical simulations in a spatially flat universe with a sub-critical density of matter. Indeed, after analysis with the full suite of CLASH optical and X-ray data, one of the previously more discrepant clusters, Abell 2261, now agrees with predictions (Coe et al. 2012). The earlier tensions between observed and modeled cluster-mass profiles now seem far less significant (Merten et al. 2014).

CLASH data also allow us, for the first time, to directly test whether the dark-matter fluid is pressureless. In General Relativity, a gravitational potential well is shaped by its mass-energy content. However, in that

Continued page 50

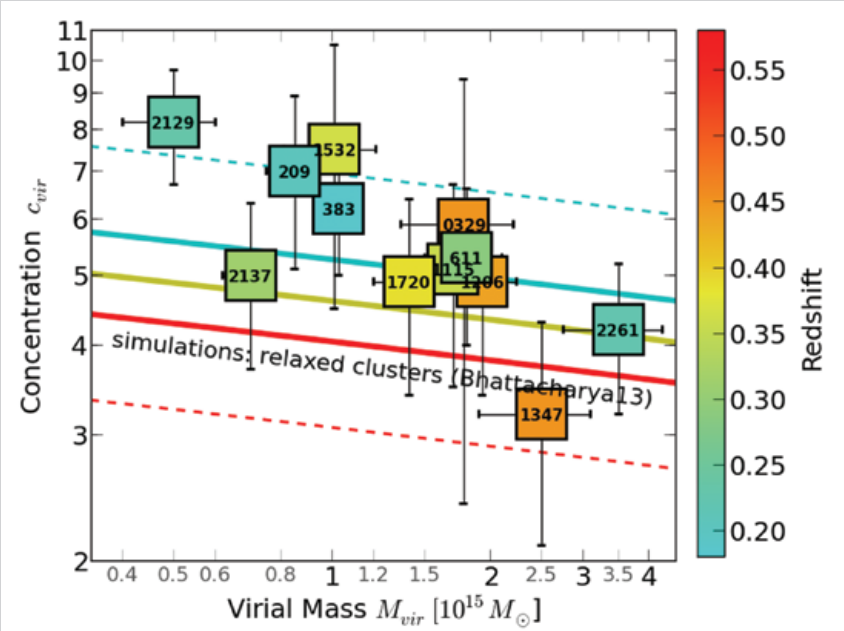

Figure 3: The relation between cluster mass and concentration for 12 of the 20 CLASH clusters selected by X-ray (Merten et al. 2014). Data points and predictions from *N*-body simulations (Bhattacharya et al. 2013) are color-coded by redshift. The numbers inside data points identify the cluster (e.g., 2129 = MACSJ2129.4-0741).

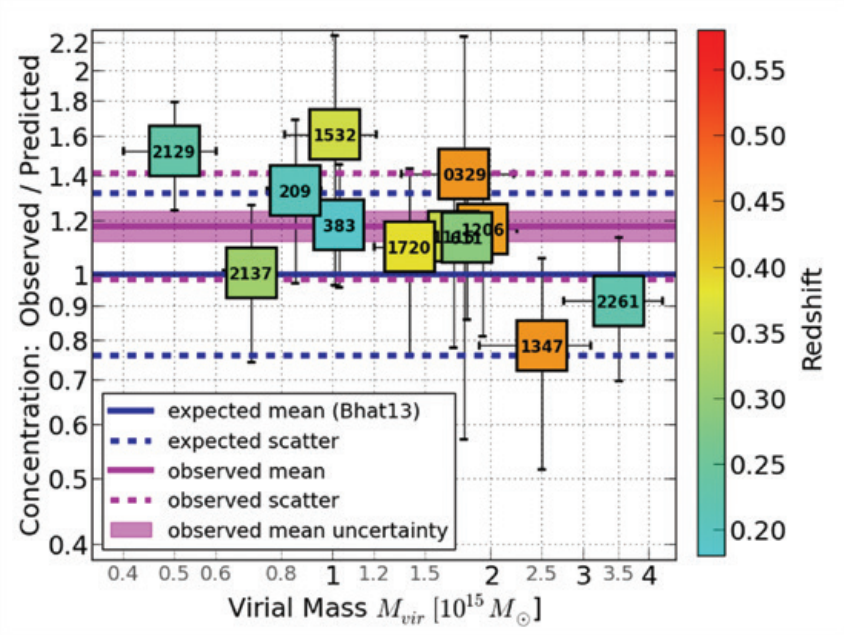

Figure 4: The relation between cluster mass and concentration ratio, which is the observed concentration value divided by the predicted value. The mean value of this ratio is 1.19 ± 0.07. The deviation from unity is <3σ and is smaller than the scatter predicted by the simulations (Bhattacharya et al. 2013).

well different types of particles respond to the gravitational potential, $\Phi(r)$, in different ways (e.g., Faber & Visser 2006). Dark matter is the dominant component that determines the gravitational potential well of a cluster and if the equation of state of the dark matter has a pressure term, then relativistic particles (photons) and non-relativistic particles (galaxies) flowing in a cluster will yield different mass profiles. In particular, the equation of state (EoS) is $w = [p_r(r) + 2p_t(r)] / [c^2 3\rho(r)]$, where $p_r(r)$ and $p_t(r)$ are the radial and tangential pressure profiles. We have obtained a constraint on the amplitude of the pressure terms in the CLASH cluster MACS J1206.2-0848, which has over 600 spectroscopically confirmed

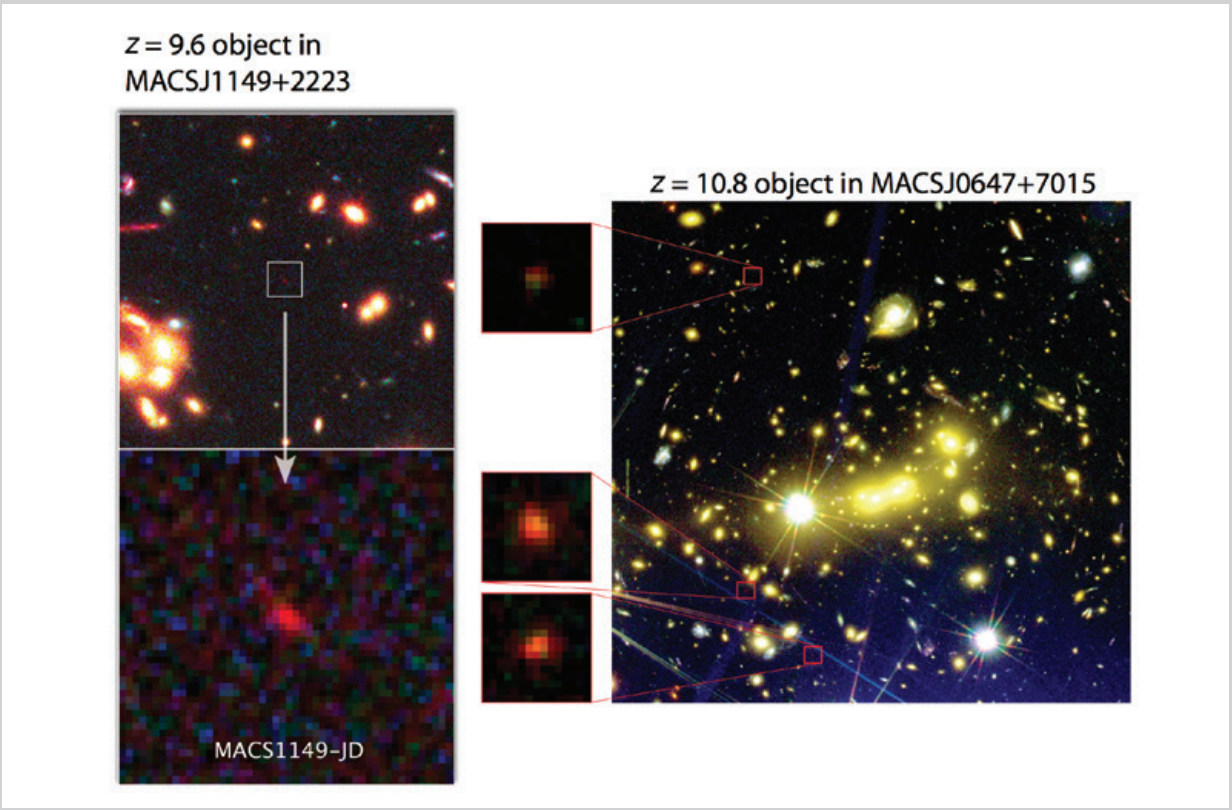

Figure 5: Two very distant galaxies ($z > 9$) discovered in the CLASH data. The galaxy at $z \sim 11$, behind MACSJ0647+7015, is believed to be a multiply lensed object, appearing at three different positions on the sky. The positions of the arcs from a multiply lensed galaxy can be used as an additional constraint on its redshift.

cluster members. That constraint is $w = -0.003 \pm 0.137$ (statistical error) $\pm$ 0.170 (systematic error), which is consistent with zero. Because the baryonic content of clusters is only ~15% of the total mass, the above EoS constraint is primarily on the DM fluid (Sartoris et al. 2013).

Probing the high-redshift universe with cluster lensing

Gravitational lensing is a highly efficient tool for discovering high-redshift galaxies. Lensing magnifies both an object's flux and size, while preserving the object's surface brightness. The typical magnification produced by a CLASH cluster is 2–4 over an area of ~1 square arcminute, and the magnification can rise well above 10 in some smaller regions. The CLASH sample includes five clusters that were known to be powerful lenses, with Einstein radii >30 arcsec and shallow mass profiles. We included these clusters with the hope we would detect several very highly magnified galaxies at $z > 7$, when the universe was less than 800 million years old.

Our observational strategy paid off. CLASH discovered three strongly lensed images of a galaxy at $z \sim 10.8$ in one of our clusters, which corresponds to an era only ~420 Myr after the Big Bang (Coe et al. 2013). This galaxy is a robust candidate for the most distant galaxy yet known. This breakthrough came shortly after CLASH discovered another lensed galaxy at $z \sim 9.6$ (Zheng et al. 2012). Figure 5 shows the CLASH images of these two galaxies.

The galaxies at redshifts 9.6 and 10.8 lie behind two of our five "high-magnification" clusters. Both appear to be dwarf starburst galaxies with stellar masses between 10^8 to 10^9 solar masses, which are producing new stars at rate of one to four solar masses per year. Both galaxies are also very compact, having half-light radii <0.2 kpc (unlensed). Both have apparent fluxes that are 8–15 times brighter than an identical field galaxy at the same redshift. Thus, these two galaxies will be prime targets for the spectrographs on the *James Webb Space Telescope*.

The rate at which CLASH discovers galaxies at $z > 9$–10 is consistent with lensing extrapolations from observed luminosity functions at lower redshifts ($z \leq 8$). This agreement suggests that low-luminosity galaxies may be a major source of the reionization of the universe. The *Hubble* Frontier Fields program should provide even stronger constraints on the evolution of the star-formation rate per unit volume—a key parameter used to assess the amount of ionizing radiation in the universe at a given place and time.

Furthermore, with accurate lens models in hand, we can reconstruct the unlensed source

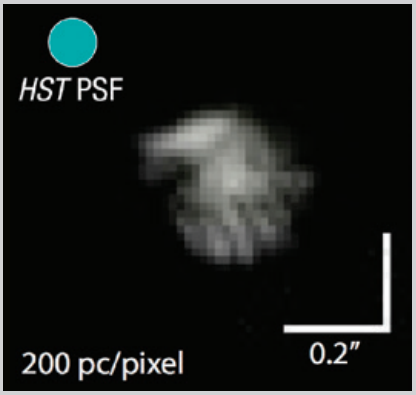

Figure 6: A galaxy at $z = 6.15$ (look-back time of 12.6 Gyr) as seen after it is "de-lensed" using our CLASH model for the cluster mass distribution. The spatial resolution seen here is about four times better than could be achieved with *Hubble* alone. Several knots are seen in the galaxy's internal structure, suggesting regions of active star formation.

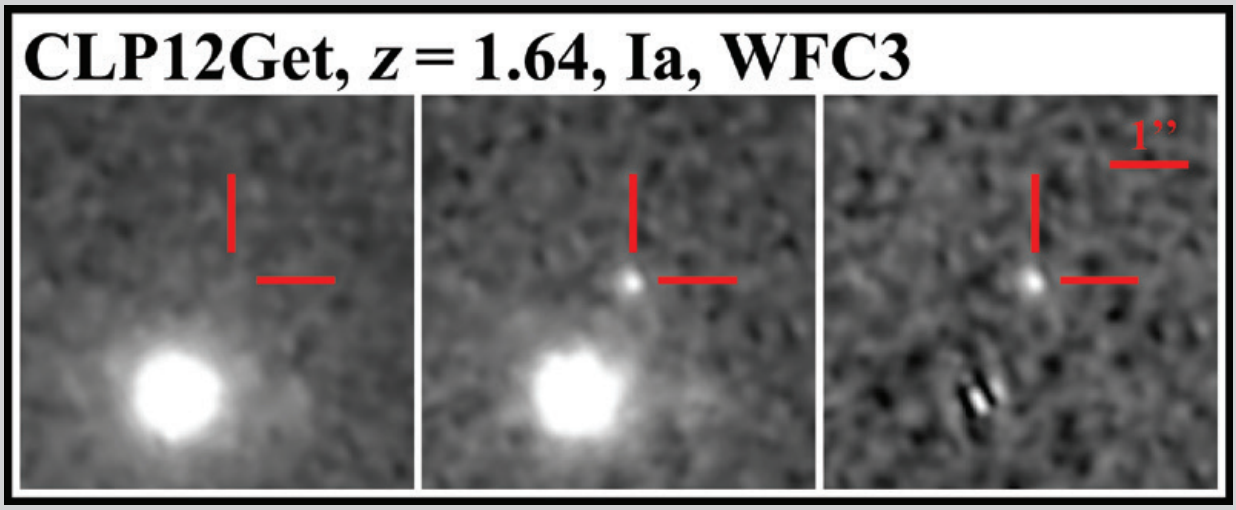

Figure 7: From *left* to *right*: the host galaxy ($z = 1.64$) before the SN explosion, the galaxy and the SN, and a subtraction of the previous two panels in which only the SN is present. All panels are in the WFC3 F160W band, which is similar to the *H*-band.

shape at a spatial resolution that significantly exceeds that of *Hubble*'s normal imaging. This advantage allows us to study the internal structure of distant galaxies at spatial resolutions of <200 parsecs at the source. Figure 6 shows an example of such an object for a galaxy at $z \sim 6$ (Zitrin et al. 2012b).

Constraints on the high-redshift Type Ia supernova rate

SNe Ia play diverse roles in the universe. They are catalysts of star formation, sources of iron-group elements, and perhaps the agents responsible for accelerating high-energy cosmic rays, just to name a few. Over the past two decades, SNe Ia have also been used as standard candles to measure extragalactic distances. And yet, we still do not know exactly what type of stellar system leads to these explosions. One way to constrain the various models of SNe Ia progenitors is to measure their explosion rate at different redshifts, i.e., at different ages of the universe. CLASH observations, combined with those from the Cosmic Assembly Near-infrared Deep Extragalactic Legacy Survey (CANDELS), allow us to conduct a survey aimed at discovering the most distant SNe Ia. To do this, we exploited *Hubble*'s parallel imaging mode: while one camera was trained on the "prime" field containing the core of a galaxy cluster, the other camera was trained on a nearby, "parallel" field of galaxies, far enough away to not be affected by strong lensing. Each parallel field was visited four times, with a cadence of 14–21 days. We discovered 39 supernovae in CLASH: 27 in the parallel fields and 12 in and around the galaxy clusters in the prime fields. Of these, we classify approximately half as SNe Ia. Figure 7 shows one of our high-redshift SNe, which is classified as a Type Ia at a redshift of $z = 1.64$. The light from this SN has taken approximately 9.5 billion years to reach us.

Preliminarily, we find that the SNe Ia rates are consistent with those measured by previous studies (see Fig. 8). While we did not find any SNe at $z > 2$, the sensitivity of WFC3 in the near-infrared has allowed us, for the first time, to place an upper limit on the SN Ia rate beyond $z \sim 2$. That limit and the CLASH SN Ia rates will be published in a forthcoming paper by Graur et al. (2014), with an accompanying paper on the CANDELS rates by Rodney et al. (2014).

Galaxy evolution in dense environments

With *Hubble*-quality imagery in 16 bandpasses spanning the UV to the IR, CLASH observations provide an unprecedented peek into the structure, content, and star-formation history of cluster galaxies. Our initial cluster science from CLASH is focusing on the galaxy most impossible to ignore in a cluster: the Brightest Cluster Galaxy (BCG). BCGs are often situated at the bottom of the potential well of the cluster, so it can be thought of as a 10^{12} solar mass galaxy with a 10^{15} solar mass dark matter halo. As such, BCGs likely experience a uniquely privileged history of mergers and interaction, which strongly affects the BCG's structure and stellar content. One of the primary unsolved problems of galaxy formation is how the regulation of gas cooling and star formation occurs in the centers of massive halos like those hosting BCGs.

All of the CLASH BCGs have been detected in rest-frame UV. Some of the UV emission comes from elderly stars, the so-called UV-upturn population. About half of the CLASH BCGs also exhibit UV excesses associated with clumps and filaments. Figure 9 shows the dramatic star-forming structures seen in two of the CLASH BCGs. CLASH has provided the first high-resolution images of such systems at $z > 0.2$ over the full, UV-to-NIR spectral range. The luminosity and number of UV and H-alpha filaments and

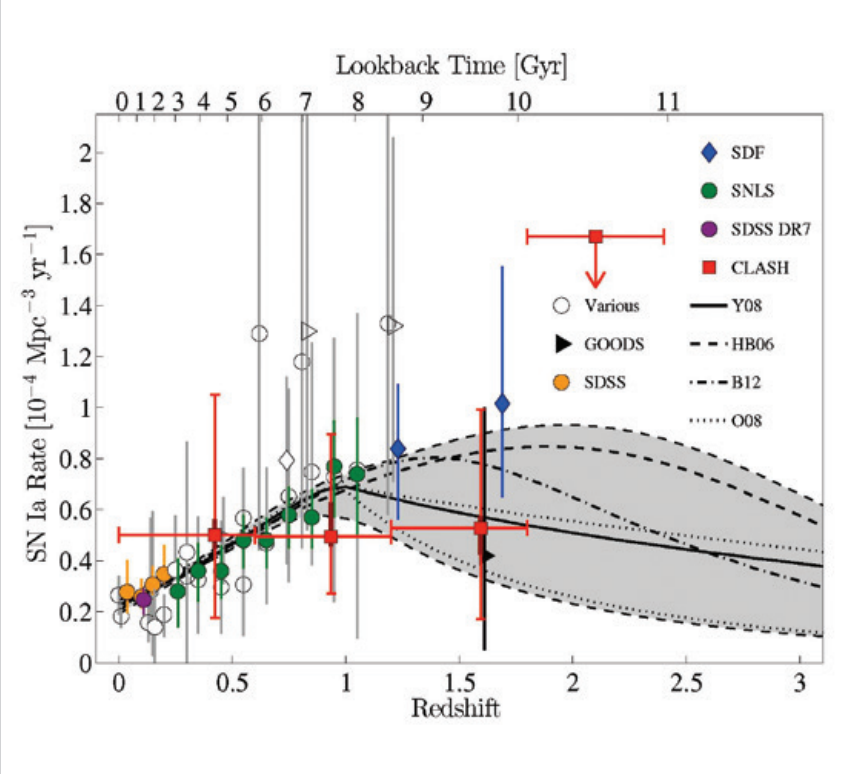

Figure 8: Preliminary measurements of the Type Ia supernova rates from CLASH (filled, red squares) compared to rates from the literature and best-fitting SN Ia rate histories derived by convolving a power-law delay-time distribution (DTD) with different star-formation histories (SFHs). Circles denote data from surveys with measurements out to $z \sim 1$. Filled circles denote the most accurate and precise measurements at $z < 1$. The GOODS rates are shown as downturned triangles and the Subaru Deep Field rates are shown as diamonds. The $z > 1.5$ rates from these two surveys are colored in black and blue, respectively. The thick curves are convolutions of several SFHs with the best-fitting power-law DTDs. The shaded area is the confidence region resulting from the combined 68% statistical uncertainties on the values of the power-law index fit with the above SFHs. The thin dashed lines indicate the 68% statistical uncertainty region obtained without the new CLASH measurements. The horizontal error bars delineate the CLASH redshift bins. Thicker, darker vertical error bars for the CLASH data points include systematic errors from uncertainties in the dust model and classification. The thinner, lighter vertical error bars for CLASH data points are the far more dominant Poisson uncertainties. The vertical error bars for the other data are sums of the statistical and systematic uncertainties. Details (with complete citations for all data shown here) will be published in Graur et al. 2014.

knots in these two galaxies indicate star formation at rates close to 50 solar masses per year. More detailed results will be forthcoming in the next year when follow-up observations are obtained with *Hubble*'s Space Telescope Imaging Spectrograph and Cosmic Origins Spectrograph.

The road ahead

While the CLASH program is now complete, the work to extract scientific knowledge from the data will be ongoing for many years. In the next year, we will be performing a variety of analyses on the full 25-cluster sample. We will investigate the use of CLASH results to calibrate cluster mass for the next generation of cosmological surveys, such as the Dark Energy Survey and surveys based on the Sunyaev-Zel'dovich effect, using the Atacama Cosmology Telescope and the South Pole Telescope, as well as next-generation cluster surveys using X-rays.

As a Multi-Cycle Treasury program, all the CLASH data, including high-level science products—such as co-added images, source catalogs with photometric redshift data, and our models of the cluster mass distributions—are publicly available via the Mikulski Archive for Space Telescopes at **http://archive.stsci.edu/prepds/clash/**.

Acknowledgements

A complex survey like CLASH could not have been possible without the dedication and hard work of many people. Thanks to the entire CLASH science team and to all of those colleagues who contributed data to the project, as well as all the people at the Institute and Goddard Space Flight Center who help

Continued page 56

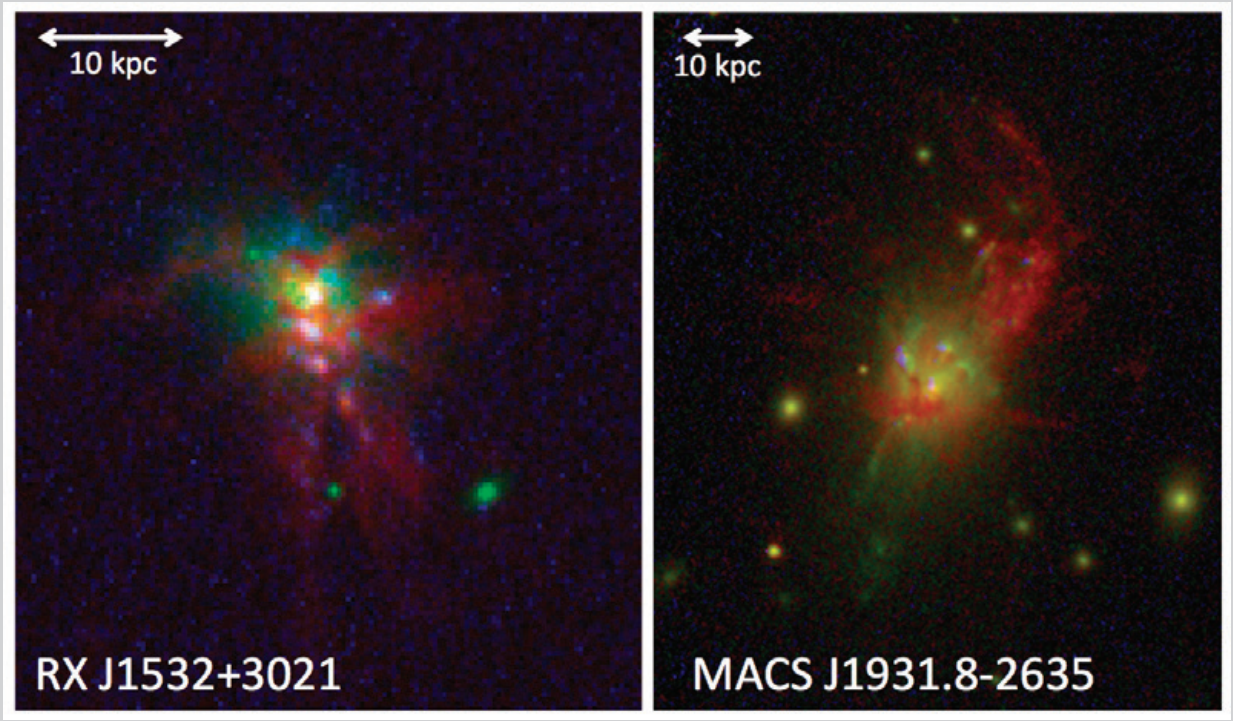

Figure 9: Two BCGs in CLASH, which host significant amounts of star-formation activity. Both galaxies are at intermediate redshift ($z \sim 0.35$). The red channel is dominated by H-alpha emission. It was constructed by differencing images obtained through a filter containing the redshifted H-alpha line and adjacent off-band images. The blue channel shows UV-bright regions. The green channel is continuum starlight. A 10 kpc scale is shown for reference. At least 5 of the 25 CLASH BCG show extended gaseous filaments and/or star-forming knots.

schedule and execute observations, process the data, and ensure that the telescope and its scientific instruments perform so well.

References

Bhattacharya, S., et al. 2013, ApJ, 766, 32
Coe, D., et al. 2012, ApJ, 757, 22
Coe, D., et al. 2013, ApJ, 762, 32
Faber, T., & Visser, M. 2006, MNRAS, 372, 136
Graur, O., et al. 2014, in prep.
Jouvel, S., et al. 2013, A&A, submitted
Merten, J., et al. 2014, in prep.
Postman, M., et al. 2012, ApJS, 199, 25
Rodney, S., et al. 2014, in prep.
Sartoris, B., et al. 2013, in prep.
Zheng, W., et al. 2012, Nature, 489, 406
Zitrin, A., et al. 2012a, ApJ, 749, 97
Zitrin, A., et al. 2012b, ApJ, 747, L9

The Many Lives of Data: New Science from the *Hubble* Archive

Rachel Osten, *osten@stsci.edu*

A good astronomical archive is like a well-stocked wine cellar: the datasets age like fine wines. Far from being relegated to a dusty electronic retirement after fulfilling their primary purpose, archival data can often be repurposed to accomplish different science, which brings new life to the data. As the holdings at the Barbara A. Mikulski Archive for Space Telescopes have grown, such opportunities have increased. These days, the science that can be done with archival data is limited only by the creativity of the astronomer. In many cases, the new science might not have been fully justified in its own right if it had been proposed earlier. Now, however, each new application adds value to both the dataset and the archive. One recent paper, Osten (2012), illustrates the expanding research opportunities with archival datasets. In this example, the original observations were a week-long stare at the Galactic Bulge, intended to discover transiting extrasolar planets. The new use is to study magnetic activity in old stars.

With a large haystack, there are many needles

The Advanced Camera for Surveys (ACS) on board the *Hubble Space Telescope* has a Wide Field Channel (WFC) with a large field of view (202 × 202 arcsec). With a full complement of filters, ACS/WFC was primarily designed for imaging surveys. The high stability of the instrument further enables precise relative photometry. Coupled with *Hubble*'s high spatial resolution, these performance factors led Kailash Sahu to devise a proposal for Cycle 12 to use ACS/WFC to search for transits of extrasolar planets in the old stellar population of the Galactic Bulge. The program searched for periodically dimming sources in a sample of 180,000 stars brighter than $V = 27$. The observations continued for a week, interrupted only by Earth occultations of the spacecraft. The exposures used two broadband filters, corresponding roughly to *V* and *I* bands. The exposures lasted about five minutes, six per *Hubble* orbit, and the typical spacing between exposures was about eight minutes.

For planet hunting, Sahu and colleagues formed photometric time series from subtracted images, and they searched them for evidence of transiting planets with orbital periods in the range 0.42–4.2 days. Because the sightline toward the Bulge lies in the constellation Sagittarius, they named this dataset SWEEPS, for "Sagittarius Window Eclipsing Extrasolar Planet Search." Sahu et al. (2006) detailed the initial results: the discovery of 16 planetary candidates, about half of which they thought were genuine.

Only two of the host stars were bright enough to follow up with the ground-based spectroscopy needed to estimate the stellar mass and place limits on the planetary mass.

Sahu's team found a population of ultra-short-period planets (periods of less than one day), which occur preferentially around lower-mass stars (less than about 0.9 M_{sun}). The absence of this type of planets around higher-mass stars could be due to irradiated evaporation on timescales less than 10 GY, the assumed age of the Bulge stars in the field. The frequency of planets around stars in the Bulge appears to be similar to that in the solar neighborhood, implying similar mechanisms of planetary formation and migration. The Sahu study also provides an important constraint on the frequency of exoplanets in a second Galactic region—the Bulge—which is quite different from the solar neighborhood.

From early on, other astronomers recognized that the SWEEPS dataset was ripe for spinoff science. The stellar field is rich, containing approximately 245,000 stars brighter than $V = 30$, with a broad distribution of metallicity. The crowded field facilitates the study of systematic effects due to increased stellar density. Also, the short exposure times, coupled with the relatively long duration of the observations, opens up a wide range of parameter space for time-domain science on the stars themselves. Indeed, the abstract of the original proposal (GO 9750) suggests "a variety of spinoff projects, including a census of variable stars and of hot white dwarfs in the bulge, and the metallicity distribution of bulge dwarfs." In addition, the SWEEPS dataset enables searches for interesting and rare objects. With such a large haystack, there must be many scientific "needles."

An immediate offshoot of the SWEEPS dataset was a poster by Sahu at the American Astronomical Society (AAS) meeting in 2006. It described the identification and study of 165 short-period eclipsing binaries with periods in the range 0.2–5 days.

Later, Gilliland (2008) used the data to study photometric variations in a sample of several hundred red-giant stars in the Bulge with luminosities in the range 30–350 L_{sun}. Most of these stars exhibit variations that can be interpreted as stellar oscillations. Even though the SWEEPS time resolution was not sufficient for asteroseismic analyses, the results established the near ubiquity of oscillations in evolved stars, and they were a harbinger of the rich asteroseismic results to come from the *Kepler* mission.

Continued page 58

Archive
from page 57

Sahu also used the SWEEPS dataset to search for microlensing events, which involve planetary-mass objects. During a star-star lensing event—which is due to a distant source star in the Bulge coincidentally passing behind and apparently near a lens star at intermediate distance—a planetary companion of the lens star can cause a major perturbation of the source-star brightness if the apparent position of the planet comes close to the Einstein ring. The typical timescale of a microlensing event is from hours to days, which is a good match to the SWEEPS dataset. As described in a poster from the 2009 AAS meeting, Sahu found no such events in the SWEEPS data. This result implies that planetary-mass objects from one Earth mass to 10 Jupiter masses make only a small contribution to the total mass budget.

A second epoch of observations of the SWEEPS field occurred roughly two years after the first. Although much shallower—only 2 *Hubble* orbits compared to 105 orbits in the 2004 program—the short baseline of the new observations, coupled with the high precision of the first-epoch data, nevertheless constrained the proper motions of thousands of stars in the Bulge. Clarkson et al. (2008) presented these results and used them to separate Bulge stars from the disk populations, and to investigate the dynamics of Bulge stars. Later, Clarkson et al. (2011) used the same dataset, together with the proper-motion constraints, to provide the first detection of blue straggler stars in the Bulge. Blue straggler stars are old, hydrogen-burning stars, which have temperatures and luminosities resembling younger stars. They are thought to result from accretion or stellar mergers. Previously, blue stragglers had been seen in a range of older stellar populations, and thus they were expected to occur in the Bulge as well. Before Clarkson et al. (2008), however, the absence of a precise and accurate method to separate Bulge stars from younger disk stars in the field had prevented a firm conclusion. Even so, the new discoveries—at least 18 genuine blue stragglers in a sample of 42 potential blue stragglers—appear to be discrepant from findings in stellar clusters (Clarkson et al. 2011).

Blips, not dips: stellar activity at old ages

Members of the original SWEEPS team led the early follow-on studies of the data. The beauty of the open archive is that, after the initial proprietary period for the data has elapsed, a wider audience can access and utilize the data, and expand the scientific applications even further. As an example, Osten et al. (2012) used the densely time-sampled data to study transient events caused by stellar flares, in a program called "Deep, Rapid Archival Flare Transient Search in the Galactic Bulge" (DRAFTS).

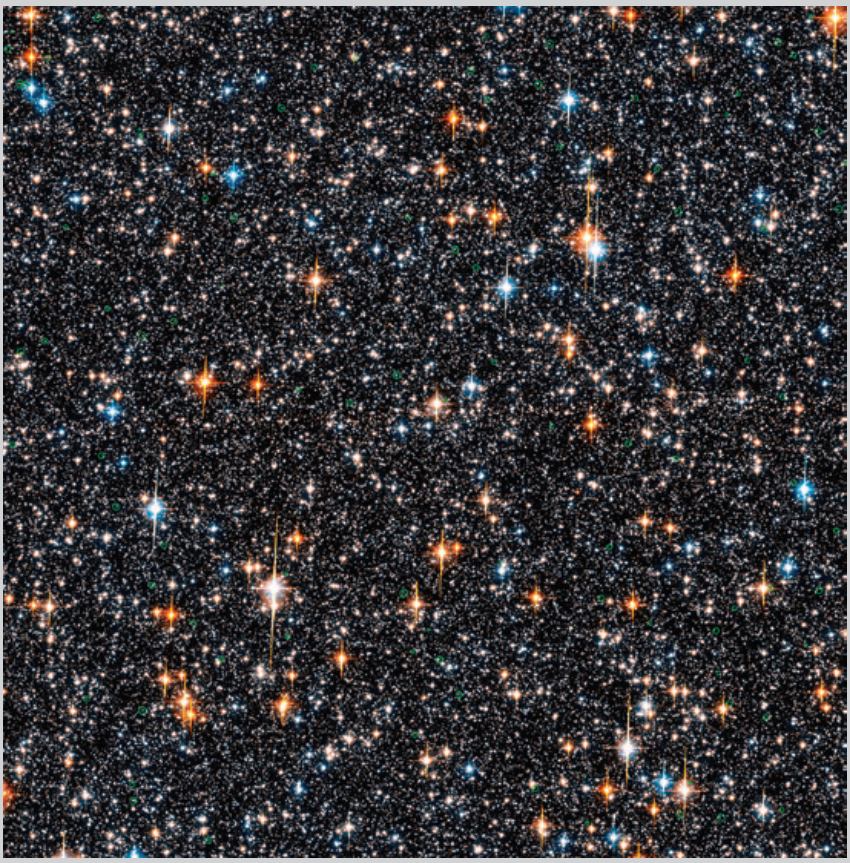

Figure 1: The SWEEPS star field, which is the basis for the DRAFTS archival project. Green circles: 105 flaring stars identified by DRAFTS as old, magnetically active stars.

Stellar flares are transient increases in the luminosity of a star, usually of short duration, with timescales ranging from a few minutes to several hours. Flares occur as the result of changing magnetic configurations above the stellar surface, where starlight originates. For stars with convective outer envelopes, flares are the most dramatic example of variability observed during residency on the main sequence. Flares occur on many types of cool stars, but appear more frequently in young stars, because their enhanced magnetic activity is driven by the interplay of rapid rotation and other factors of stellar youth.

While stellar flaring is expected to occur primarily in young stars, flares do arise in older stars, too (witness our middle-aged sun's flare events). Young M dwarfs can flare many times per day, a factor that facilitates further studies using pointed observations. Meanwhile, little is known about flaring in older stars, partly because it is more difficult to observe. The decline in stellar activity at ages greater than 1 GY means that short exposures of single stars will generally not find flaring activity. The SWEEPS dataset nicely fills this gap in parameter space with a huge sample of stars.

The signatures of stellar flares are found across most of the electromagnetic spectrum, from radio wavelengths to high-energy photons. They are observed in the widest range of stellar types at high energies, due to the increasing contrast between the coronal emission from flares and the non-flaring coronal emission from stars at increasingly shorter wavelengths. For this reason, at optical wavelengths, the typically blue flares are most readily observed in M dwarfs, which are intrinsically red.

Studies of stellar flares can contribute to several lines of research. They can help us better understand observations of magnetic reconnection in stellar atmospheres. They can constrain the rate of stellar flares expected in searches for optical transients caused by rare phenomena, such as gamma-ray bursts and stellar disruptions by black holes. Such research also has applications to space weather, as solar physicists seek to understand the implications of severe flaring for space travel, the habitability of extrasolar planets, and even life on Earth. For such studies, we no longer have just one object to investigate—the Sun—but a sample of many solar-type stars displaying the same phenomena.

Figure 1 shows the SWEEPS star field that forms the basis of the DRAFTS archival project.

The starting point for the DRAFTS data analysis was the suite of light curves of relative flux that already existed from the original SWEEPS data analysis. Only stars fainter than $V = 20$ were selected, in order to focus on stars on or near the main sequence of the Bulge stellar population. Because stellar flares show a larger signal at shorter wavelengths, the DRAFTS analysis concentrated on the time series obtained with the V606W filter.

Some light curves showed large-scale photometric modulation, which must be removed before searching for flares. These modulations were of the same magnitude as the flares, but on a different timescale. Our team identified flares by searching for statistically significant, correlated, positive excursions in

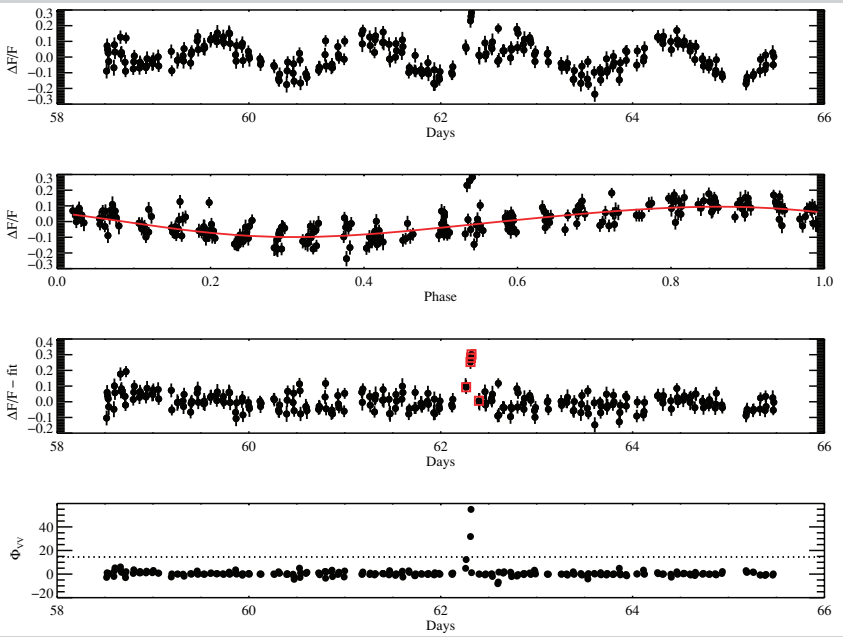

Figure 2: Flare detection in the DRAFTS study (Osten et al. 2012). *Top*: typical, original light curve of relative-flux measurements over the course of the seven-day SWEEPS observation. *Second from top*: the data folded over the sinusoid that best fit the large-scale photometric modulations; red line shows the fit. *Third from top*: the light curve after removing the sinusoid; red squares indicate the points belonging to a flare event. *Bottom*: the statistic used to identify flare peaks; horizontal line shows the threshold of significance.

Continued page 60

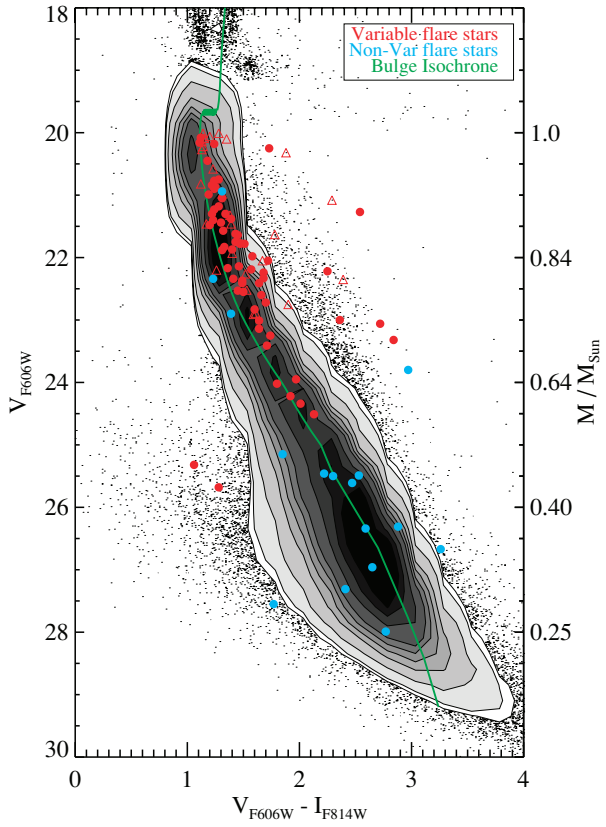

Figure 3: Color-magnitude diagram of all stars in the SWEEPS field (gray contours), with the location of stars determined to be flaring by the DRAFTS study (Osten et al. 2012). Green curve: the isochrone appropriate for the Bulge stars. Red and blue points: flaring stars with and without underlying large-scale photometric modulations, respectively. Filled red circles and open red triangles: flaring stars showing periodic or aperiodic large-scale photometric modulations, respectively. The results are limited by photon statistics at the faint end of stars. The brighter flaring stars are located slightly to the right of the best-fit isochrone, which suggests they may be binaries.

the light curve (see Fig. 2). For the brighter stars in the sample, the photon statistics were good enough to detect flare-like increases of a few percent of the underlying stellar light. For the faintest stars, the increases were of order unity. In total, we found 122 flares from 105 stars, out of 216,136 stars suitable for analysis.

Once the flares were identified, we could determine some properties. We integrated under the light curve to estimate the radiated energy, which was only a lower limit, due to the limitations of the time sampling and observing cadence. Because these stars are so far away (the mean Bulge distance is about 7.24 kpc), we expected to see larger flare energies than on the Sun, where the largest flares in white light release about 10^{32} erg, and the peak amplitude in integrated solar light is about 270 parts per million. Instead, the minimum flare energies inferred for the brighter-flaring stars in the DRAFTS sample are only about a factor of 4–160 sixty times larger than the largest solar-flare energy.

We also determined ensemble properties of the flares. We found that the distribution of flare frequency with energy roughly follows a power-law distribution, similar to that exhibited by flares on the well-studied M dwarfs. We found that the average energy-loss rate due to flares is a strong function of the underlying bolometric luminosity of the star. The loss rate increases with luminosity in a trend similar to that determined for flare stars that are M dwarfs.

Beauty marks and a fountain of youth?

Assuming the DRAFTS flare stars are at the distance and age of the Galactic Bulge, the analysis of Osten et al. (2012) suggests that stars are capable of maintaining elevated levels of flaring and magnetic activity longer than stellar spin-down timescales.

Most of the stars have proper motion measurements from the second epoch of observations, and thus are confirmed to be Bulge members with an age near 10 GY.

The location of these stars on the color-magnitude diagram shows that, if they are single stars, they span a range of masses from one solar mass down to about 0.25 solar masses, where the stellar interior is expected to become fully convective (see Fig. 3).

One surprising result was that, for most flaring stars exhibiting underlying photometric modulations, the modulations were periodic, with periods in the range of a few days. Periodicity is expected if the modulations were due to blemishes—so-called stellar "beauty marks"—on the rotating surface of a star. In that case, we would expect the period of modulation to be the same as the rotational period. However, we don't expect rotational periods as short as a few days in old, single stars, because such fast rotation is an established hallmark of stellar youth.

The flare rate for variable stars is far greater than the corresponding rate for non-variable stars in the DRAFTS sample. The flare characteristics of these stars indicate enhanced magnetic activity and implied youth, while the proper motion constraints suggest that they are old stars. Paradoxically, then, these stars are kinematically old but magnetically young. Binarity is one possible resolution of this apparent contradiction: tidally locked stars in binary systems can maintain fast rotation at old ages due to the coupling of spin and orbital angular momenta. They are thus able to maintain enhanced levels of magnetic activity over longer timescales than single stars, evidencing an astrophysical "fountain of youth." If we attribute the majority of stellar flaring to binarity, it implies that the space density of binary systems in the Galactic Bulge is enhanced by a factor of roughly 20 compared to the local value.

All good things must come to an end, and even tidally locked binaries will experience orbital and rotational evolution. Unlike single stars, which slow down with age, binaries will spin up as their orbits shrink. At some point the two stars will merge. Such binary coalescence has been suggested as the formation mechanism for a different type of magnetically active star—the active, evolved, but apparently single stars known as FK Com stars.

A characterization of the brightest flaring stars using spectroscopy will test the binary hypothesis. The results of this test will constrain the timescale of angular-momentum loss by cool stellar binaries in an old stellar population—an unanticipated outcome of the flare analysis, and even more remote from the original intent of the SWEEPS dataset.

In conclusion, DRAFTS shows that flares can be identified in a wide range of stellar types, not

just the M-dwarf flare stars typically observed at optical wavelengths. These flares imply that some stars—perhaps because of their unique evolutionary status—maintain enhanced magnetic activity into old age. Further study will probe this mystery and teach us more about the flaring process itself.

References

Clarkson, W., Sahu, K., Anderson, J., Smith, T. E., Brown, T., Rich, R. M., Casertano, S., Bond, H. E., Livio, M., Minniti, D., Panagia, N., Renzini, A., Valenti, J., Zoccali, M. 2008, ApJ, 684, 1110

Clarkson, W., Sahu, K., Anderson, J. Rich, R. M., Smith, T. E., Brown, T., Bond, H. E., Livio, M., Minniti, D., Renzini, A., Zoccali, M. 2011, ApJ, 735, 37

Gilliland, R. 2008, ApJ, 136, 566

Osten, R., Kowalski, A., Sahu, K., Hawley, S. 2012, ApJ, 754, 4

Sahu, K., Casertano, S., Bond, H. E., Valenti, J., Smith, T. E., Minniti, D., Zoccali, M., Livio, M., Panagia, N., Piskunov, N., Brown, T., Brown, T., Renzini, A., Rich, R. M., Clarkson, W., Lubow, S. 2006, Nature, 443, 534

A View of the Earth

Michael J. Massimino, *michael.j.massimino@nasa.gov*

In 1984 I was a senior in college, and I went to see the movie *The Right Stuff*. And a couple of things really struck me in that movie. The first was the view out the window of John Glenn's spaceship—the view of the Earth, how beautiful it was on the big screen. I wanted to see that view. And secondly, the camaraderie between the original seven astronauts depicted in that movie—how they were good friends, how they stuck up for each other, how they would never let each other down. I wanted to be part of an organization like that.

And it rekindled a boyhood dream that had gone dormant over the years. That dream was to grow up to be an astronaut. And I just could not ignore this dream. I had to pursue it. So I decided I wanted to go to graduate school, and I was lucky enough to get accepted to MIT.

While I was at MIT, I started applying to NASA to become an astronaut. I filled out my application, and I received a letter that said they weren't quite interested. So I waited a couple years, and I sent in another application. They sent me back pretty much the same letter. So I applied a third time, and this time I got an interview, so they got to know who I was. And then they told me no.

Figure 1: Mike Massimino is peering through a window on the aft flight deck of the Space Shuttle *Atlantis* as it orbits Earth. Astronaut Michael Good is in the background continuing repairs to *Hubble*.

So I applied a fourth time. And on April 22, 1996, I knew the call was coming, good or bad. I picked up the phone, and it was Dave Leestma, the head of flight crew operations at the Johnson Space Center in Houston.

He said, "Hey, Mike. This is Dave Leestma. How you doing this morning?"

And I said, "I really don't know, Dave. You're gonna have to tell me."

And he said, "Well, I think you're gonna be pretty good after this phone call, 'cause we wanna make you an astronaut."

Thirteen years after that, it's May 17, 2009, and I'm on space shuttle *Atlantis*, about to go out and do a spacewalk on the *Hubble Space Telescope*. And our task that day was to repair an instrument that had failed. Scientists used this instrument to detect the atmospheres of far-off planets. Planets in other solar systems could be analyzed using this spectrograph to see if we might find a planet that was Earth-like, or a planet that could support life. And just when they got good at doing this, the power supply on this instrument failed. It blew. So the instrument could no longer be used.

And there was no way really to replace this unit or to repair the instrument, because when they launched this thing, and they got it ready for space flight, they really buttoned it up. They didn't want anybody to screw with this thing. It was buttoned up with an access panel that blocked the power supply that had failed. This access panel had 117 small screws with washers, and just to play it safe,

Continued page 62

View from page 61

they put glue on the screw threads so they would never come apart. You know, it could withstand a space launch, and there was no way we could get in to fix this thing.

But we really wanted the *Hubble*'s capability back, so we started working. And for five years, we designed a spacewalk. We designed over one hundred new space tools to be used—at great taxpayers' expense, millions of dollars, thousands of people worked on this. And my buddy Mike Good (who we call Bueno)—he and I were gonna go out to do this spacewalk. I was gonna be the guy actually doing the repair.

And inside was Drew Feustel, one of my best friends. He was gonna read me the checklist. And we had practiced for years and years for this. They built us our own practice instrument and gave us our own set of tools so we could practice in our office, in our free time, during lunch, after work, on the weekends. We became like one mind. He would say it, I would do it. We had our own language. And now was the day to go out and do this task.

The thing I was most worried about when leaving the airlock that day was my path to get to the telescope, because it was along the side of the space shuttle. And if you look over the edge of the shuttle, it's like looking over a cliff, with 350 miles to go down to the planet. And there are no good handrails.

When we're spacewalking, we like to grab on to things with our space gloves and be nice and steady. But I got to this one area along the side of the shuttle, and there was nothing good to grab. I had to grab a wire or a hose or a knob or a screw. And I'm kind of a big goon. And when there's no gravity, you can get a lot of momentum built up, and I could go spinning off into space. I knew I had a safety tether that would probably hold, but I also had a heart that I wasn't so sure about. I knew they would get me back, I just wasn't sure what they would get back on the end of the tether when they reeled me in. So I was really concerned about this. I took my time, and I got through the treacherous path and out to the telescope.

The first thing I had to do was to remove a handrail from the telescope that was blocking the access panel. There were two screws on the top, and they came off easily. And there was one screw on the bottom right and that came out easily. The fourth screw is not moving. My tool is moving, but the screw is not. I look close and it's stripped. And I realize that that handrail's not coming off, which means I can't get to the access panel with these 117 screws that I've been worrying about for five years, which means I can't get to the power supply that failed, which means we're not gonna be able to fix this instrument today, which means all these smart scientists can't find life on other planets.

And I'm to blame for this.

And I could see what they would be saying in the science books of the future. This was gonna be my legacy. My children and my grandchildren would read in their classrooms: *We would know if there was life on other planets but Gabby and Daniel's dad broke the* Hubble Space Telescope*, and we'll never know.*

And through this nightmare that had just begun, I looked at my buddy Bueno, next to me in his space suit, and he was there to assist in the repair but could not take over my role. He had his own responsibilities, and I was the one trained to do the now broken part of the repair. It was my job to fix this thing. I turned and looked into the cabin where my five crewmates were, and I realized nobody in there had a space suit on. They couldn't come out here and help me. And then I actually looked at the Earth; I looked at our planet, and I thought, *There are billions of people down there, but there's no way I'm gonna get a house call on this one. No one can help me.*

I felt this deep loneliness. And it wasn't just a Saturday-afternoon-with-a-book alone. I felt detached from the Earth. I felt that I was by myself, and everything that I knew and loved and that made me feel comfortable was far away. And then it started getting dark and cold.

Because we travel 17,500 miles an hour, ninety minutes is one lap around the Earth. So it's 45 minutes of sunlight and 45 minutes of darkness. And when you enter the darkness, it is not just darkness. It's the darkest black I have ever experienced. It's the complete absence of light. It gets cold, and I could feel that coldness, and I could sense the darkness coming. And it just added to my loneliness.

For the next hour or so, we tried all kinds of things. I was going up and down the space shuttle, trying to figure out where I needed to go to get the next tool to try to fix this problem, and nothing was working. And then they called up, after about an hour and fifteen minutes of this, and said they wanted me to go to the front of the shuttle to a toolbox and get vise grips and tape. I thought to myself, *We are running out of ideas. I didn't even know we had tape on board. I'm gonna be the first astronaut to use tape in space during a spacewalk.*

But I followed directions. I got to the front of the space shuttle, and I opened up the toolbox and there was the tape. At that point I was very close to the front of the orbiter, right by the cabin window, and I knew that my best pal was in there, trying to help me out. And I could not even stand to think of looking at him, because I felt so bad about the way this day was going, with all the work he and I had put in.

But through the corner of my eye, through my helmet, you know, just the side there, I can kinda see that he's trying to get my attention. And I look up at him, and he's just cracking up, smiling and giving me the okay sign. And I'm like, *Is there another spacewalk going on out here?* I really can't talk to him, because if I say anything, the ground will hear. You know, Houston. The control center. So I'm kinda

like playing charades with him. I'm like, *What are you, nuts?* And I didn't wanna look before, because I thought he was gonna give me the finger because he's gonna go down in the history books with me. But he's saying, *No, we're okay. You just hang in there a little bit longer. We're gonna make it through this. We're in this together. You're doing great. Just hang in there.*

And if there was ever a time in my life that I needed a friend, it was at that moment. And there was my buddy, just like I saw in that movie, the camaraderie of those guys sticking together. I didn't believe him at all. I figured that we were outta luck. But I thought, *At least if I'm going down, I'm going down with my best pal.*

And as I turned to make my way back over the treacherous path one more time, Houston called up and told us what they had in mind. They wanted me to use that tape to tape the bottom of the handrail and then see if I could yank it off the telescope. They said it was gonna take about sixty pounds of force for me to do that.

And Drew answers the call, and he goes, "Sixty pounds of force?"

He goes, "Mass, I think you got that in you. What do you think?"

And I'm like, "You bet, Drew. Let's go get this thing."

I get back to the telescope, and I put my hand on that handrail, and the ground calls again, and they go, "Well, Drew, you know, you guys are okay to do this, but right now we don't have any downlink from Mike's helmet camera." I've got these cameras mounted on my helmet, so they can see everything I'm doing. It's kinda like your mom looking over your shoulder when you're doing your homework, you know?

And they go, "We don't have any downlink for another three minutes, but we know we're running late on time here, so if you have to . . ." And I'm thinking, *Let's do it now while they can't watch!* Because the reason I'm taping this thing is if any debris gets loose, they're gonna get all worried, and it's gonna be another hour, and we'll never fix this thing. We've been through enough already.

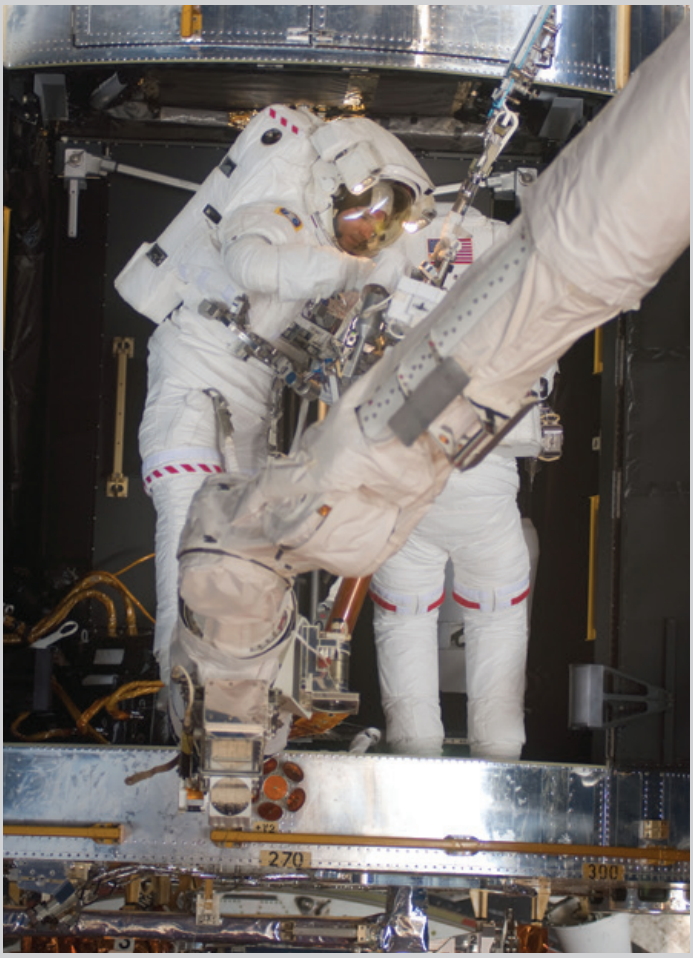

Figure 2: Astronauts Michael Good (*left*) and Mike Massimino (*right*) are repairing the Space Telescope Imaging Spectrograph (STIS) that will extend the *Hubble*'s life into the next decade.

So I'm like, *Let's do it now, while Mom and Dad aren't home. Let's have the party.*

So I say, "Drew, I think we should do it now." And Drew's like, "Go!" And *bam!* That thing comes right off. I pull out my power tool, and now I've got that access panel with those 117 little bitty screws with their washers and glue, and I'm ready to get each one of them. And I pull the trigger on my power tool and nothing happens, and I look, and I see that the battery is dead. And I turn my head to look at Bueno, who's in his space suit, again looking at me like, *What else can happen today?*

And I said, "Drew, the battery's dead in this thing. I'm gonna go back to the air lock, and we're gonna swap out the battery, and I'm gonna recharge my oxygen tank." Because I was getting low on oxygen; I needed to get a refill.

And he said, "Go." And I was going back over that shuttle, and I noticed two things. One was that that treacherous path that I was so scaredy-cat-sissy-pants about going over—it wasn't scary anymore. That in the course of those couple hours of fighting this problem, I had gone up and down that thing about twenty times, and my fear had gone away, because there was no time to be a scaredy-cat, it was time to get the job done. And what we were doing was more important than me being worried, and it was actually kinda fun going across that little jungle gym, back and forth over the shuttle.

The other thing I noticed was that I could feel the warmth of the sun. We were about to come into a day pass. And the light in space, when you're in the sunlight, is the brightest, whitest, purest light I have ever experienced, and it brings with it warmth. I could feel that coming, and I actually started feeling optimistic.

Sure enough, the rest of the spacewalk went well. We got all those screws out, a new power supply in, buttoned it up. They tried it; turned it on from the ground. The power supply was working. The instrument had come back to life. And at the end of that spacewalk, after about eight hours, I'm inside the air lock getting things ready for Bueno and me to come back inside, but my commander says, "Hey, Mass, you know, you've got about fifteen minutes before Bueno's gonna be ready to come in.

Continued page 64

View
from page 63

Why don't you go outside of the air lock and enjoy the view?"

So I go outside, and I take my tether, and I clip it on a handrail, and I let go, and I just look. And the Earth—from our altitude at *Hubble*, we're 350 miles up. We can see the curvature. We can see the roundness of our home, our home planet. And it's the most magnificent thing I've ever seen. It's like looking into heaven. It's paradise.

And I thought to myself, *This is the view that I imagined in that movie theater all those years ago*. And as I looked at the Earth, I also noticed that I could turn my head, and I could see the moon and the stars and the Milky Way galaxy. I could see our universe. And I could turn back, and I could see our beautiful planet.

And that moment changed my relationship with the Earth. Because for me the Earth had always been a kind of a safe haven, you know, where I could go to work or be in my home or take my kids to school. But I realized it really wasn't that. It really is its own spaceship. And I had always been a space traveler. All of us here today, even tonight, we're on this spaceship Earth, amongst all the chaos of the universe, whipping around the sun and around the Milky Way galaxy.

A few days later, we get back. Our families come to meet us at the airfield. And I'm driving home to my house with my wife, my kids in the backseat. And she starts telling me about what she was going through that Sunday that I was spacewalking, and how she could tell, listening, watching the NASA television channel, how sad I was. That she detected a sadness in my voice that she had never heard from me before, and it worried her.

I wish I would've known that when I was up there, 'cause this loneliness that I felt—really, Carol was thinking about me the whole time. And we turned the corner to come down our block, and I could see my neighbors were outside. They had decorated my house, and there were American flags everywhere. And my neighbor across the street was holding a pepperoni pizza and a six-pack of beer, two things that unfortunately we still cannot get in space.

And I got out of the car, and they were all hugging me. I was still in my blue flight suit, and they were saying how happy they were to have me back and how great everything turned out. I realized my friends, man, they were thinking about me the whole time. They were with me too.

The next day we had our return ceremony; we made speeches. The engineers who had worked all these years with us, our trainers, the people that worked in the control center, they started telling me how they were running around like crazy while I was up there in my little nightmare, all alone. How they got the solution from the Goddard Space Flight Center in Maryland, and how the team that was working on that Sunday figured out what to do, and they checked it out, and they radioed it up to us.

I realized that at the time when I felt so lonely, when I felt detached from everyone else—literally, like I was away from the planet—that really I never was alone, that my family and my friends and the people I worked with, the people that I loved and the people that cared about me, they were with me every step of the way.

Figure 3: Mike Massimino practices unscrewing the STIS panel with his bulky spacesuit gloves on.

The Institute's Educational Programs

Hussein Jirdeh, *jirdeh@stsci.edu*, **Bonnie Eisenhamer,** *bonnie@stsci.edu*, **and Denise Smith,** *dsmith@stsci.edu*

Two decades ago, the leaders of the Space Telescope Science Institute and NASA posed a question to themselves: could a small group of scientists and educators transform the breathtaking discoveries from the *Hubble Space Telescope* into meaningful and measurable educational products for America's schools, potentially reaching millions of youths at a time? In asking this question, we recognized that *Hubble*'s discoveries offer unprecedented opportunities to inspire, engage, and educate students of all ages and backgrounds in the fundamental concepts of science, technology, engineering, and mathematics (STEM). We embraced the potential as we saw it, and committed the Institute to making it a reality. Since then, the scope of our efforts has grown to include the wealth of compelling narratives associated with the *James Webb Space Telescope*. Over the years, we have learned much about the practical links between basic education and advanced scientific research, and we have made substantial contributions to national STEM goals. Today, more than half the state departments of education in the U.S. have integrated the Institute's educational materials into their programs. What makes this program such a success is that educator-scientist partnerships are central to producing all educational material—from design to implementation.

STEM education as a national priority

The year 2013 presented both a challenge and an opportunity for the Institute to examine the role of its educational programs in supporting a national STEM agenda. The President's fiscal year 2014 budget request proposed a reorganization of all federally funded STEM education programs in order to improve the delivery, impact, and visibility of their efforts. In addition, the reorganization sought to align the programs with national goals that primarily focus on STEM workforce development and STEM literacy. We, at the Institute, contribute to these goals and provide a range of opportunities that allow unique NASA science and products to play a significant role in these national priorities.

Institute programs

Federal agencies, which depend upon the cultivation of a talented and well-trained twenty-first century workforce, play a critical role in preparing the next generation of STEM workers. NASA, with the support of partners like the Institute, is well positioned for engaging young people and motivating them toward STEM careers. By providing expertise and content, serving as role models, and exposing students to real-world learning opportunities, our scientists and engineers help to inspire and educate future generations of innovators and explorers.

This broader discussion of federal priorities provides an opportunity to reflect upon the impact of STEM educational programs undertaken by national science projects like *Hubble* and *Webb*, both in terms of what has been accomplished and what it represents in the larger picture.

At its heart, a space telescope is a wellspring of new ideas and information—new knowledge, including scientific discoveries, technological advances, engineering solutions, and mathematical frameworks. A space telescope project has "STEM" written all over it. Nevertheless, the beneficial connections between forefront research and basic teaching and learning are not completely obvious and therefore must be thoughtfully developed.

Because of the Institute's science charter, our education and public outreach efforts naturally focus on the "S," for science. Under the heading "news," we collaborate with research scientists to produce press releases and science briefings that disseminate new knowledge worldwide through media channels. Under both "outreach" and "informal education," we develop resources—notably *HubbleSite* (**www.hubblesite.org**) and the *ViewSpace* multimedia exhibit, which reach 2.2 million users per month and nearly 9 million viewers per year, respectively. Finally, our *formal* educational programs—training teachers and developing and distributing education resources—are the direct contributions from *Hubble* and *Webb* to the totality of federal investments in formal STEM education.

Participants test Office of Public Outreach materials at a pre-service teacher conference in Alexandria, Virginia.

Students participate in a tactile astronomy lesson.

Students learn about light and spectra during an astronomy club session.

Institute staff explain the science behind *Hubble* images during the Johns Hopkins Physics Fair.

The keywords for the Institute's formal educational program are "partnerships," "middle school," "master teachers," "rigorous evaluation," and "leveraged distribution."

At the Institute, the creative process of curriculum support material development involves a purposeful partnership of scientists, engineers, and educators. We bring together active practitioners from each field to ensure that the scientific and technical content of our products is current and accurate, and that products meet pedagogical standards. This commitment to partnering scientists and educators to communicate cutting-edge mission science effectively with educators, students, and the public has become so deeply engrained in the *Hubble–Webb* culture, that many feel it epitomizes NASA's social contract with the nation.

Our partnerships with educators and the education industry allow us to reach new audiences and to integrate new techniques into our programs without duplicating effort. We enter into such partnerships selectively, according to criteria, such as sustainability, service to underserved/underrepresented populations, and the willingness to collect and share follow-up data based on summative evaluations—estimates of actual learning after a unit is taught.

The Institute's focus in formal education is on middle schools, where many students lose interest in science, technology, and math. Because of that, the middle-school years are a critical turning point in the STEM pipeline. Our approach builds on the natural appeal that astronomy has always held for children. To retain the interest of middle-school students, we create interactive educational materials using real data, keeping pupils engaged and providing them an opportunity to visualize themselves as real scientists.

The Institute's path to success

The Institute organizes and implements professional development workshops for master teachers, where we teach them how to use our educational materials. They bring this knowledge back to their schools. After training, each master teacher in our program agrees to teach at least two classes of middle-school science teachers. In this way, the ~1,100 master teachers who participated in our professional development workshops last year are expected to teach more than ~55,000 teachers, thereby reaching ~1.7 million students.

We conduct or commission evaluations of our educational products and programs to ensure they achieve their intended outcomes. To learn how, where, and why our materials are being utilized, we collect data from a sample of more than 1,400 venues, including colleges, school districts, and informal science education centers. The most important indicator of the positive impact of the Institute's educational products is their widespread use and adoption by the formal educational community. Institute materials are now used in all 50 states, and to more than half of the state departments of education, Institute materials are a required or recommended element.

To achieve national distribution with limited resources, it is necessary to use leverage in distributing our products. Our partnerships with educators and the education industry provide such leverage. So do our websites, particularly *Amazing Space:* **www.amazing-space.stsci.edu**.

Because all work at the Institute involves computers and the internet, we were early adopters of information technologies to distribute our educational products. Our online *Amazing Space* education curriculum support materials provide educators and students with interactive, inquiry-based learning and allow students to self-test—strategies known to enhance student learning. Nearly half of our access to students comes through *Amazing Space*. The other half comes from the extensive distribution of hard-copy materials by partners. In total, we reach more than 6 million students each year.

The Institute has a successful track record transforming *Hubble* discoveries and *Webb* developments into effective educational products, which reach millions of students nationwide. By targeting those students most vulnerable to missing out on STEM careers—middle school students—we are taking a concrete step toward advancing the President's goal of 1 million new STEM graduates within a decade.

More information is available at: **http://outreachoffice.stsci.edu.**

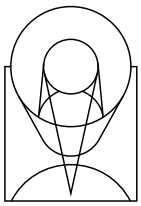

Contact STScI:

The Institute's website is: **http://www.stsci.edu**
Assistance is available at *help@stsci.edu* or 800-544-8125.
International callers can use 1-410-338-1082.
For current *Hubble* users, program information is available at:
http://www.stsci.edu/hst/scheduling/program_information.

The current members of the Space Telescope Users Committee (STUC) are:

Annette Ferguson (chair), University of Edinburgh, *ferguson@roe.ec.uk*
Brian Siana (deputy chair), University of California - Riverside, *brian.siana@ucr.edu*

Marc Buie, Southwest Research Institute
Adam Burgasser, University of California - San Diego
Jane Charlton, Penn State University
You-Hua Chu, University of Illinois Urbana
J. Christopher Howk, University of Notre Dame
Giampaolo Piotto, Universita di Padova
Andrea Prestwich, Smithsonian Astrophysical Observatory
David Sing, University of Exeter
Ann Zabludoff, University of Arizona, Steward Observatory

The Space Telescope Science Institute Newsletter is edited by Robert Brown, *rbrown@stsci.edu*, who invites comments and suggestions.
Contents Manager: Sharon Toolan, *toolan@stsci.edu*
Design: Pam Jeffries, *jeffries@stsci.edu*
To record a change of address or to request receipt of the Newsletter, please send a message to *address-change@stsci.edu*.

Contents:

Hubble Cycle 21 Proposal Selection 1

Staying Sharp: Keeping *Hubble* and *Webb* Seeing Clearly 20

Webb Update 26

Wide-Field Slitless Spectroscopy with *Webb*'s NIRISS 28

Observing Galaxy Assembly with the *James Webb Space Telescope* 31

Webb: The Stiffest Backbone in Space 35

Barbara A. Mikulski Archive for Space Telescopes 37

The CANDELS Multi-Cycle Treasury Program 45

Cluster Lensing And Supernovae Survey with *Hubble* (CLASH) 50

The Many Lives of Data: New Science from the *Hubble* Archive 57

A View of the Earth 61

The Institute's Educational Programs 67

Calendar

SWG meeting	2–4 December 2013
NASA Advisory Council meeting	11–12 December 2013
AURA Workforce & Diversity Committee (STScI)	12–13 December 2013
AAS meeting (Washington, DC)	5–9 January 2014
Future of the Workplace Committee meeting	23–24 January 2014
STIC meeting	February/March 2014
Hubble Fellows Symposium	10–12 March 2014
AAAS meeting (Chicago)	13–17 February 2014
Conference "Science with the *Hubble Space Telescope* IV," (Accademia dei Lincei, Rome) **http://www.stsci.edu/institute/conference/hst4**	17–20 March 2014
Workshop "The Cosmic Distance Scale" (STScI)	31 March–2 April 2014
NASA Advisory Council meeting	16–17 April 2014
AURA Annual meeting	23–27 April 2014
Spring Symposium (STScI) Habitable Worlds Across Time and Space **http://www.stsci.edu/institute/conference/habitable-worlds/**	28 April–1 May 2014
Pan-STARRS consortium/workshop (STScI)	23–27 June 2014

SPACE TELESCOPE SCIENCE INSTITUTE
3700 San Martin Drive
Baltimore, Maryland 21218

www.nasa.gov

NON PROFIT
U.S. POSTAGE
PAID
PERMIT NO. 8928
BALTIMORE, MD

NP-2013-11-076-GSFC